

**AN EVALUATION OF HORIZONTAL SUB-DRAINAGE SYSTEMS MITIGATING  
LANDSLIDE HAZARD IN SHIKURUWE VILLAGE, BUDUDA DISTRICT**

**CYNTHIA MAMFA MAYALA**

**S21B32/040**

**A FINAL YEAR RESEARCH AND DESIGN PROJECT REPORT SUBMITTED TO THE  
FACULTY OF ENGINEERING, DESIGN AND TECHNOLOGY, IN PARTIAL FULFILLMENT  
OF THE REQUIREMENTS FOR THE AWARD OF A DEGREE OF BACHELOR OF SCIENCE  
IN CIVIL AND ENVIRONMENTAL ENGINEERING OF UGANDA CHRISTIAN UNIVERSITY**

**April, 2025**



**UGANDA CHRISTIAN  
UNIVERSITY**

*A Centre of Excellence in the Heart of Africa*

## **ABSTRACT**

Rainfall-induced landslides pose a significant threat in BUDUDA district in Eastern Uganda, due to intense precipitation, geological instability, and increasing population density. This study assessed the suitability of horizontal sub-drainage systems to mitigate landslide risk in SHIKURUWE village. The research involved site characterization, a hydrological study, and the design of a horizontal sub-drainage system. Key findings revealed that moderately steep slopes, low permeability, and fine-grained soils contributed to water stagnation in the soil profile. High rainfall patterns were found to be influenced by global meteorological phenomenon such as the El Niño. Further, land use and soil properties significantly influenced water losses in the watershed. Finally, the introduction of a horizontal sub-drainage system down slope was observed to improve drainage in both steady state and transient conditions, hence reducing the pore water pressure, and increasing the factor of safety of the slope.

## DECLARATION

I, MAMFA MAYALA Cynthia, declare that this report entitled ‘Reducing Landslide Risk in SHIKURUWE Village, BUDUDA District. An Evaluation Of Horizontal Sub-Drainage Systems’ is my own original work and all sources utilized in its preparation are fully acknowledged and referenced in the report. I declare that the research was conducted in an ethical manner in accordance, and has not been submitted to any other institution for any qualification or award.

Signature.....

Date.....

MAMFA MAYALA Cynthia

## APPROVAL

This is to certify that this research and design project by MAMFA MAYALA Cynthia has been conducted under my supervision and has been approved for submission to the university.

Signature.....

Date.....

Dr. Eng. Morris OLENG

ACADEMIC SUPERVISOR

## **DEDICATION**

To my beloved parents MAMFA OBUDI Didier and MAYALA BANTEA Claudine who have been of great support throughout my academic journey. I am grateful for the unconditional love, encouragements and prayers for the success bestowed upon me. This project is dedicated to both of you, and I am certain to have made you proud.

## ACKNOWLEDGMENT

I am first of all grateful to the Almighty Lord for His infinite goodness and mercy to have enable me to come to the completion of this research and design experience. I am grateful for the gift of life and wisdom, and the unconditional love and protection.

My most sincere appreciation goes to the NGANGI Fund Goma-DRC for awarding me a full scholarship and financially supporting my academic journey.

Special thanks to the faculty of Engineering, Design and Technology, in particular the Head of Department, Mr. Tom Mwanje More, and the Project Coordinator, Mr. Tayebwa Rodgers for their guidance throughout the Research and Design Project.

I would like to express my sincere gratitude to my project supervisor Dr. Eng. Morris OLENG for his unconditional support, guidance, and encouragement throughout this project. His insights and expertise were invaluable in shaping the direction of the project.

I would like to thank the Uganda Ministry of Water and Environment through the Department of Hydrology Luzira, together with the Uganda Meteorological Center Luzira for providing the necessary hydrological data required in the research.

I would like to also thank the Geotechnical Engineering and Technology Laboratory (GETLAB) Kasangati for providing the necessary equipment and facilities to conduct different tests on the soil samples.

# TABLE OF CONTENTS

ABSTRACT .....	II
DECLARATION.....	III
APPROVAL.....	IV
DEDICATION .....	V
ACKNOWLEDGMENT .....	VI
TABLE OF CONTENTS.....	VII
LIST OF TABLES.....	IX
LIST OF FIGURES .....	X
LIST OF EQUATIONS.....	XII
LIST OF ABBREVIATIONS.....	XIII
CHAPTER ONE: INTRODUCTION .....	1
1.1 BACKGROUND .....	1
1.2 INTRODUCTION .....	2
1.3 PROBLEM STATEMENT .....	3
1.4 OBJECTIVES .....	4
1.4.1 Main objective .....	4
1.4.2 Specific objectives .....	4
1.5 RESEARCH QUESTIONS .....	5
1.6 SIGNIFICANCE .....	5
1.7 JUSTIFICATION .....	6
1.8 SCOPE .....	6
1.8.1 Geographical scope .....	6
1.8.2 Content scope .....	7
CHAPTER TWO: LITERATURE REVIEW .....	9

2.1 GENERALITIES .....	9
2.2 LANDSLIDE HISTORY IN BUDUDA DISTRICT .....	13
2.3 MITIGATION MEASURES IN PLACE .....	15
2.4 CHALLENGES FACED IN LANDSLIDE MITIGATION .....	17
2.5 SUB SURFACE DRAINAGE SYSTEMS .....	18
2.6 MATERIAL .....	24
2.7 APPLICATION OF SUB DRAINAGE SYTEMS .....	26
CHAPTER THREE: METHODOLOGY .....	30
3.1 OVERVIEW AND RESEARCH DESIGN .....	30
3.2 SITE CHARACTERIZATION .....	31
3.3 STUDY OF THE HYDROLOGY .....	57
3.4 DESIGN OF THE HORIZONTAL SUB DRAINAGE SYSTEM .....	74
CHAPTER FOUR: RESULTS AND DISCUSSION .....	89
4.1 SITE CHARACTERIZATION .....	89
4.2 STUDY OF THE HYDROLOGY .....	98
4.3 DESIGN OF THE HORIZONTAL SUB DRAINAGE SYSTEM .....	106
CHAPTER 5: CONCLUSIONS AND RECOMMENDATIONS .....	121
5.1 CONCLUSIONS .....	121
5.2 RECOMMENDATIONS .....	123
REFERENCES .....	125
APPENDICES .....	130
APPENDIX A: Secondary data of BUDUDA Rainfall (2000_2025) .....	130
APPENDIX B: Secondary data of BUDUDA borehole .....	158
APPENDIX C: Slope stability analysis_slip surfaces tables .....	169
APPENDIX C: Pictures .....	181

## LIST OF TABLES

<i>Table 1 . Summary of the Objectives and Proposed Methodology used to achieve them</i>	30
<i>Table 2 . Average monthly rainfall values</i> .....	59
<i>Table 3 . Yearly intensity, Average daily rainfall intensity on rainy days, and maximum daily rainfall intensity.</i> .....	60
<i>Table 4 . Rainfall return period computation</i> .....	61
<i>Table 5 . Characteristics of the different sub-catchments</i> .....	66
<i>Table 6 . Land cover and Interception storage values</i> .....	67
<i>Table 7 . Slope and Surface storage values</i> .....	68
<i>Table 8 . Key parameters for Unit Clark transformation method</i> .....	72
<i>Table 9 . Values for time of concentration and storage coefficient</i> .....	72
<i>Table 10 . Slope classification</i> .....	90
<i>Table 11 . Atterberg limits values</i> .....	91
<i>Table 12 . Key parameters for soil classification</i> .....	93
<i>Table 13 . Characteristics of sub catchments</i> .....	98
<i>Table 14 . Water losses in the watershed.</i> .....	105
<i>Table 15 . Factor of safety ranges</i> .....	117

## LIST OF FIGURES

<i>Figure 1 . 2016 landslide scar in SHIKURUWE village. ....</i>	<i>4</i>
<i>Figure 2 . Geographical scope .....</i>	<i>7</i>
<i>Figure 3 . Co-seismic and rainfall induced susceptibility map of Uganda. ....</i>	<i>14</i>
<i>Figure 4 . Landslide monitoring scheme. ....</i>	<i>17</i>
<i>Figure 5 . Types of sub drains. ....</i>	<i>18</i>
<i>Figure 6 . Drain configuration. ....</i>	<i>23</i>
<i>Figure 7 . Natural dewatering of the gully the bank with installed sub-drains. ....</i>	<i>28</i>
<i>Figure 8 . (a) Handy GPS interface; (b) sample preservation ....</i>	<i>34</i>
<i>Figure 9 . Atterberg limit graph .....</i>	<i>35</i>
<i>Figure 10 . Testing specimen for triaxial test.....</i>	<i>51</i>
<i>Figure 11 . Daily rainfall data for 25 years. ....</i>	<i>58</i>
<i>Figure 12 . System diagram of the runoff process at local scale .....</i>	<i>64</i>
<i>Figure 13 . HEC-HMS Model grid for the watershed. ....</i>	<i>66</i>
<i>Figure 14 . Topography of site .....</i>	<i>76</i>
<i>Figure 15 . Model domain. ....</i>	<i>80</i>
<i>Figure 16 . Plan view of drain configuration. ....</i>	<i>81</i>
<i>Figure 17 . Slope analysis with piezometric line assumed to be at the groundsurface. ....</i>	<i>83</i>
<i>Figure 18 . Particle size distribution of the soil sample. ....</i>	<i>85</i>
<i>Figure 19 . Dimensionless curves of maximum water table height with respect to time for slopes of slopes. ....</i>	<i>88</i>
<i>Figure 20 . Elevation map.....</i>	<i>89</i>
<i>Figure 21 . Angle map.....</i>	<i>90</i>
<i>Figure 22 . Atterberg limit graph .....</i>	<i>93</i>
<i>Figure 23 . Infiltration rate graph.....</i>	<i>96</i>
<i>Figure 24 . Watershed delineation map.....</i>	<i>98</i>

<i>Figure 25 . Monthly rainfall pattern</i> .....	100
<i>Figure 26 . Yearly rainfall intensity</i> .....	101
<i>Figure 27 . Maximum daily rainfall intensity chart</i> .....	102
<i>Figure 28 . Average daily rainfall intensity on rainy days</i> .....	103
<i>Figure 29 . Return period graph</i> .....	103
<i>Figure 30 . Infiltration rate graph for sub basin 3</i> .....	106
<i>Figure 31 . Influence of Kx on the groundwater flow.</i> .....	107
<i>Figure 32 . Plan view for steady state conditions.</i> .....	109
<i>Figure 33 . Piezometric line for steady state conditions.</i> .....	110
<i>Figure 34 . Upper layer flooding (m AMSL) in stress period 23 of the 25 year 24-hour precipitation event.</i> .....	113
<i>Figure 35 . Improved drain configuration</i> .....	114
<i>Figure 36 . Steady state simulation for improved drain configuration</i> .....	115
<i>Figure 37 . Transient simulation for improved drained configuration</i> .....	116

## LIST OF EQUATIONS

<i>Equation 1 . Moisture content for Liquid Limit</i> .....	37
<i>Equation 2 . Moisture Content for plastic limit</i> .....	39
<i>Equation 3 . Plastic index</i> .....	39
<i>Equation 4 . Linear Shrinkage</i> .....	41
<i>Equation 5 . Initial moisture content for particle size distribution</i> .....	41
<i>Equation 6 . Determination of the mass that passed the 75<math>\mu</math>m sieve</i> .....	42
<i>Equation 7 . Determination of the dry mass sample</i> .....	43
<i>Equation 8 . Determination of the soil density</i> .....	44
<i>Equation 9 . Calculation for discharge in falling head permeability test</i> .....	48
<i>Equation 10 . Determination of the coefficient of permeability</i> .....	49
<i>Equation 11 . Linear interpolation for maximum surface storage</i> .....	69
<i>Equation 12 . Maximum infiltration rate</i> .....	70
<i>Equation 13 . Maximum soil storage</i> .....	70
<i>Equation 14 . Tension storage</i> .....	71
<i>Equation 15 . Time of concentration and Storage coefficient</i> .....	72
<i>Equation 16 . Governing groundwater flow equation used in MODFLOW</i> .....	75
<i>Equation 17 . Recharge flow rate estimation in ModelMuse</i> .....	79
<i>Equation 18 . Saturated unit weight</i> .....	82
<i>Equation 19 . Shrinkage limit</i> .....	91
<i>Equation 20 . Initial volume of soil for linear shrinkage</i> .....	92
<i>Equation 21 . Bulk unit weight</i> .....	95

## LIST OF ABBREVIATIONS

AMSL: Above Mean Sea Level

ADRIRD: Average Daily Rainfall Intensity on Rainy Days

cm: centimeter

CD: Consolidated and Drained

DEM: Digital Elevation Model

HEC-HMS: Hydrologic Engineering Center-Hydrological Modelling System

LS: Linear Shrinkage

LL: Liquid Limit

m: meter

mm: millimeter

PI: Plastic Index

PL: Plastic Limit

UU: Unconsolidated and Undrained

Wc/ Mc: Moisture Content

WGS84: World Geodetic System 1984

YRI: Yearly Rainfall Intensity

# CHAPTER ONE: INTRODUCTION

## 1.1 BACKGROUND

BUDUDA District in eastern Uganda, is one of the regions most prone to rainfall-induced landslides. This vulnerability is largely due to its location within the Mount Elgon region, an extinct volcanic shield with a maximum elevation of 4,321 meters above sea level. Landslides in the area are naturally triggered by the combination of high elevation, intense precipitation, and the weathering processes typical of such geological formations (Oleng, Ozdemir and Pilakoutas, 2024). BUDUDA has an estimated land area of approximately 274 square kilometres, with Mount Elgon Park occupying about 40% of this area. It is densely populated, as any other district in the Mount Elgon region, with settlements spreading across hills, slopes, and valleys. According to preliminary results from the 2024 Uganda census, the total population of BUDUDA is estimated to be 277,475, compared to only 211683 in the 2014 census (Census, 2024). The growing population is drawn to the region due to its fertile lands and relatively reliable climate, which support intensive agriculture, its main economic activity. The district primarily cultivates Arabica coffee and bananas, which constitute the major crops (Metroeconomica and Baastel, 2015).

Climate change has significantly contributed to the increase in landslide events in the district by causing intense rainfall events. For instance, the occurrence of several major landslides recorded during 2010\_2019 decade,

such as the NAMETSI and BUKALASI landslides in 2010, the BUWALUKANI landslide in 2012, and the MAROBO landslide in 2017 among others, align with the climate projections for the Lake KYOGA basin of which Mount Elgon is situated in the northern cattle corridor, where rising temperatures and increased precipitation have been observed during the same period (Obubu *et al.*, 2021).

## 1.2 INTRODUCTION

Landslides pose a significant concern in BUDUDA district. A comprehensive statistical analysis conducted over more than eight decades indicates that landslide hazards account for 95 percent of deaths (2,275), 60 percent of serious damage to property (352 homes), and have directly and indirectly impacted 94 percent of the population (UNDRR DesInventar Sendai, 2020). On this regard, the 2010 Uganda National Policy for Preparedness and Management outlines several essential policy actions. These include prohibiting the settlement and resettlement of individuals living in high-risk areas, promoting afforestation, and encouraging appropriate land use practices (Directorate of Relief, 2010). Despite the presence of these guidelines and several studies offering the most up-to-date landslide susceptibility maps, many residents remain hesitant to abandon the fertile lands upon which they rely for livelihood (Namuenge *et al.*, 2024).

Horizontal sub-drainage systems have a wide range of applications. They are used in civil engineering for road and highway construction, in agriculture and irrigation for optimizing crop yields, and in mining. Additionally, these

systems play a crucial role in disaster control, including landslide prevention and stabilization, as well as flood management and storm-lantern control (Tantri et al., 2023). The purpose of this project was therefore, to design a Horizontal Sub surface Drainage System with the ability of significantly draining the infiltrated water.

### 1.3 PROBLEM STATEMENT

SHIKURUWE village is situated in NAPOSHI parish in BUSHIKA Sub County, in the western part of the district. The sub county has a total population of 27,259, and a density of 1,401 people per kilometre square (Uganda Water Supply ATLAS, 2024). The sub county has known several landslides, most of which happened in 1997, provided that more than 60% of the land is located on slopes greater than 15 degrees, which is critical for accelerated mass movement. SHIKURUWE village has a couple of landslide records, of which the most recent and documented happened in 2016. The landslide scar of coordinates ( $x=649,193$  and  $y=117,456$ ) is located at an altitude of 1468 meters above sea level, on a slope of 28.26%. The scar is 86 meters long and 332 meters wide, 6.3 meters deep as seen in **FIG 1.1**. The slope is considered abandoned as the relocation process was conducted, although agriculture is still taking place (Nantumbwe, Bob R. Nakileza et al. 2017).

A study on ground displacement in the district indicated that mitigation measures could be applied to slopes with a medium displacement rate to enhance their stability. In general, when unstable layers are washed away during a landslide, a relatively stable ground remains, and it takes time for

the remaining soil to become unstable again (Makabayi, Musinguzi and Otukei, 2021a). Hence, his study aimed to design a horizontal subsurface drainage system, and to assess its effectiveness in reducing fluctuations in water levels within the soil profile.

**Figure 1** depicts the 2016 landslide scar in SHIKURUWE village, as captured by Google Earth pro in late January 2025. The red line outlines the boundary of the scar.

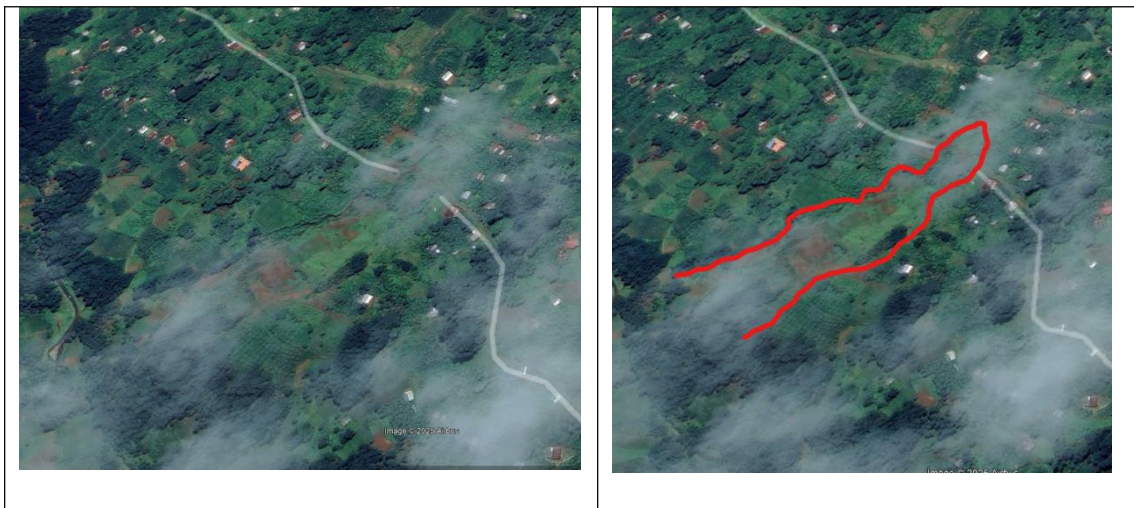


*Figure 1. 2016 landslide scar in SHIKURUWE village.*

## **1.4 OBJECTIVES**

### ***1.4.1 Main objective***

The main objective was to assess the suitability of horizontal sub drainage system approach in the mitigation of landslide risks.

### ***1.4.2 Specific objectives***

The specific objectives were:

- i. To perform a site characterizations;
- ii. To conduct a hydrologic study;
- iii. To design the horizontal sub drainage system.

## **1.5 RESEARCH QUESTIONS**

- i. What are the key soil properties to look into to obtain a better understanding of the landslide mechanism?
- ii. What are the watershed characteristics, and how do they influence landslide occurrence?
- iii. What are the key parameters that will guide the design of the horizontal sub drainage system, and how can the design be optimized?

## **1.6 SIGNIFICANCE**

Provided the increased occurrence of rainfall-induced landslides in the district that result into significant loss of life and damage to property, there is a need for effective and sustainable mitigation measures to protect the growing population and their assets. Horizontal sub-drainage systems have the potential to reduce the risk of landslides by managing subsurface water, a key contributing factor to slope instability (Tantri *et al.*, 2023). By designing and evaluating the suitability of such a system, this study provides an insight and recommendations that can inform future landslide mitigation efforts, contributing to the safety of communities in the landslide prone areas.

## 1.7 JUSTIFICATION

Landslides are a frequent natural hazard in BUDUDA District, resulting in significant loss of life, displacement of people, and economic hardship. Over the years, these landslides have caused extensive damage to infrastructure, including roads, bridges, and buildings, which disrupts economic activity (World Bank, 2019). The region is particularly vulnerable to rainfall-induced landslides because the soil structure that promotes a high water retention. For instance, these soils have a clay content of about 30%, exhibit low drainage rates, and field capacity. This leads to stagnation when seepage water interacts with the clay layer (Makabayi, Musinguzi and Otukeyi, 2021b).

Sub surface drainage systems are an effective approach to mitigate slope failures linked to seepage. Taking into considerations the intensity and duration of rainfall event, the hydraulic conductivity of the soil, the positioning and spacing of the drains in relation to the depth of the groundwater level, and the soil profile among other factors, it has been demonstrated that the horizontal subsurface drainage can significantly enhance the factor of safety of a slope up to 25 percent (Tantri *et al.*, 2023).

## 1.8 SCOPE

### 1.8.1 Geographical scope

**Figure 2** shows the geographical scope of the project (black dot). The research was conducted in SHIKURUWE village of coordinates (x= 649187, y= 117488) in BUSHIKA sub county, BUDUDA district.



the rainfall patterns, and to evaluate infiltration and water losses within the study area.

### **3. Design of sub-drainage system**

A horizontal sub-drainage system was finally designed based on findings of the site characterization and the hydrological study. The aim was to determine the appropriate design parameters, and to assess the system's potential impact on groundwater levels, and slope stability.

## CHAPTER TWO: LITERATURE REVIEW

### 2.1 GENERALITIES

BUDUDA district in western UGANDA lies at the foot of the South-Western slopes of the Mount Elgon Volcano, between latitude  $2^{\circ} 49'N$  and  $2^{\circ} 55'N$ , longitude  $34^{\circ} 15'E$  and  $34^{\circ} 34'E$  (Poesen and Deckers, 2009).

#### 1. GEOMORPHOLOGY

The geomorphology of the area is greatly controlled by the volcanism and doming of the country rock.

##### *a. Geology*

In general, BUDUDA is covered by three major rock formations (Badru *et al.*, 2022). These include:

- i. Volcanic rocks and associated sediments covering more than half of the district area ( $229\text{Km}^2$ ) in the northern and central parts;
- ii. Undifferentiated gneisses including elements of P(B) and, in the north, granulite facies rocks (covering  $84\text{Km}^2$ );
- iii. A small portion of southern ( $4\text{Km}^2$ ) covered with Undifferentiated gneisses including elements of P(B) and, in the north, granulite facies rocks.

##### *b. Slope geometry*

Slope geometry is dependant on the height and the slope angle. The critical height of slope is a function of the shear strength, density and bearing capacity of the slope foundation. Slope stability decreases with the

increase of the height, also inducing a shear stress within the toe of the slope from the added weight. On the other hand an increase in the slope angle induces a tangential stress, reducing stability (Poesen and Deckers, 2009).

### ***c. Soil properties and geological discontinuities***

#### ***i. Soil properties***

Seven types of soils are identified in BUDUDA district, for instance, Humose red sandy clay, Loams, Black and Grey clay often calcareous soil, Black humose sandy clay loam, Red clay loams and sandy clay Loams, Red sandy - sandy clay loams, and Red sandy clay loams occasionally lateralized (Badru *et al.*, 2022). These soil types are spread in the district as follows:

- Yellowish brown sandy clay loams with Black humose sandy clay loam is found in the northern part of the district in the forest reserve at the mountain;
- Humose red sandy clay loams covers the biggest percentage(41.7%) of the district;
- Black and grey clays often calcareous and Red sandy - sandy clay loams cover a small portion (0.01%) of the south west part of the district.

BUDUDA district has three major geological formations, which are explained by *Poesen and Deckers (2009)* as follows:

- Soils on carbonatite dome

The soils on the carbonatite dome in Bukigai are clay-rich, containing over 30% clay with a uniform color profile. There is less than 20% variation in clay content over a depth of at least 12 cm in the top 2 meters, while sand and

silt content decreases with depth. The top horizons have a reddish hue, and the B horizon features shiny ped faces.

These soils are permeable to water and plant roots up to 200 cm and experience minimal run-off erosion, unless on unprotected slopes exceeding 15%. Classified as Rhodic Nitisols, they are stable and resistant to landslides. Drilling shows that these soils extend to about 40 meters and are derived from iron-rich minerals like magnetite and haematite, giving them their distinctive red colour. Their stability is likely due to the high cohesion from cementing minerals such as calcium carbonate.

- Soils in the western zone

In the western zone, specifically along the BUDUDA and BUSHIKA transects west of the carbonatite dome, the main soil types are Cambisols, Nitisols, Acrisols, and Lixisols.

- Soils in the eastern zone

The eastern zone experienced the highest number of landslides in 1997, which were generally shallow compared to the ones observed in the western zone. In this region, the higher incidence of landslides could be associated to factors such as terraces, slope concavity, slope gradient, and high infiltration rates of top layers of the soil with high clay content in the downer layers leading to water stagnation, increasing a landslide risk.

ii. Geological discontinuities

A geological discontinuity is a plane or surface that marks a change in physical or chemical characteristics in a soil or rock mass. A discontinuity

can have different forms such as a bedding plane, schistosity, foliation, joint, cleavage, fracture, fissure, crack, or fault plane (Poesen and Deckers, 2009). This discontinuity controls the type of failure which may occur in a rock slope. The properties of discontinuities such as orientation, persistence, roughness and infilling are play important role in the stability of jointed rock slope. Discontinuities may occur multiple times with broadly the same mechanical characteristics in a discontinuity set, or may be a single discontinuity. This makes a soil or rock mass anisotropic.

## **2. HYDROLOGY**

### ***a. Climate and precipitation***

BUDUDA District has a tropical climate characterized by distinct wet and dry seasons. The wet seasons occur from March to May and from September to November, bringing heavy rainfall that averages around 1,500 mm annually. This intense precipitation, particularly during prolonged rainstorms, significantly increases the risk of landslides. The dry seasons, which last from December to February and from June to August, experience reduced rainfall, yet still present challenges due to the region's topography (Kitutu et al, 2010).

### ***b. Surface water***

Surface water in BUDUDA consists of rivers, streams, and wetlands that are essential for the local ecosystem and the communities that inhabit the area. Among the primary water bodies are the MANAFWA River and the SIPI River, which provide water for domestic use, irrigation, and livestock. These rivers

originate from Mount Elgon and flow through the valleys, supporting both natural habitats and human activities (Nantumbwe, Bob R. Nakileza et al. 2017).

## **2.2 LANDSLIDE HISTORY IN BUDUDA DISTRICT**

Landslides are a widespread issue around the world. In the highlands of East Africa, for example, they are primarily caused by weathering processes, various tectonic activities related to the East African Rift Valley, and the wet climates typical of tropical mountainous areas. The favorable conditions in these mountains, for instance the climate and fertile soils, have attracted populations for the culture of crops like Arabica coffee, bananas, and potatoes. Consequently, recent decades have seen a demographic boom in these mountainous areas, leading to an intensive agriculture and poor land management (Namuenge *et al.*, 2024). This has increased pressure on the naturally fragile slopes, resulting in a higher frequency of landslide events.

Landslide causes have been categorized into two main types: co-seismic and rainfall-induced, along with human activities. The combination of co-seismic and rainfall-induced landslides is more prevalent in the western part of the East African Rift Valley, particularly in the eastern part of the Democratic Republic of Congo and the western regions of Rwanda and Uganda (specifically in the KASESE and KISORO districts), while the rainfall induced landslides is more prevailing as moving away from the rift valley (Olung, Ozdemir and Pilakoutas, 2024).

**Figure 3** depicts the landslide co-seismic and rainfall-induced susceptibility map of Uganda by Oleng, Ozdemir and Pilakoutas (2024). The combination of co-seismic and rainfall-induced landslide is more prevalent in the western part of the country, while rainfall-induced landslides occur in the eastern part.

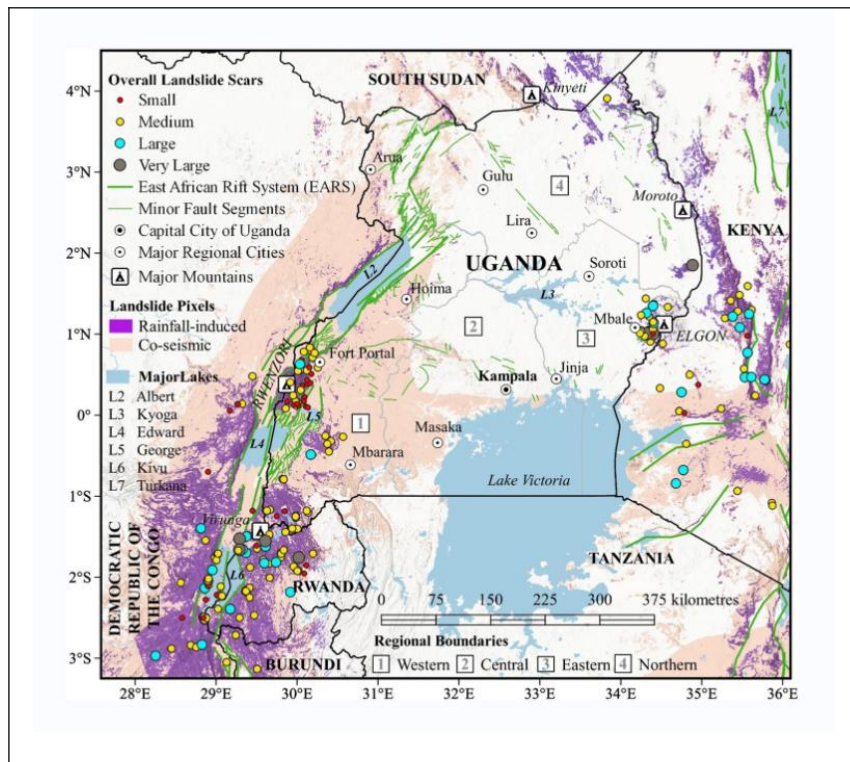


**Figure 3. Co-seismic and rainfall induced susceptibility map of Uganda.**

**Source: (Oleng, Ozdemir and Pilakoutas, 2024)**

In Uganda, landslides occur predominantly in the Western and Eastern regions, with a higher frequency observed in the Eastern part, particularly in the Mount Elgon region, due to its geological formation. The volcanic soils in this area exhibit a high infiltration rate, making them more susceptible to rainfall-induced landslides (Oleng, Ozdemir and Pilakoutas, 2024). Hence districts such as BULAMBULI, SIRONKO, MANAFWA, and BUDUDA which are located in that region have experienced significant life, environmental,

economic, and infrastructure losses over the decades. In BUDUDA district, climate change, poor land management practices, intensive agriculture, along with rising population pressure have increased the slope susceptibility to landslides (Nema, 2020).

## 2.3 MITIGATION MEASURES IN PLACE

1. Ugandan policies once prioritized disaster response and recovery, but in 2010, a new National Policy for Disaster Preparedness and Management shifted the focus to pre-disaster mitigation. This led to the creation of a Disaster Preparedness department within the Office of the Prime Minister, along with a national Disaster Risk Reduction Platform and Disaster Management Committees at district and sub-county levels. (Gorokhovich *et al.*, 2013).
2. A relocation project of the victims and people exposed to danger of looming landslides was implemented by the government and development partners such as Red Cross and Oxfam in close collaboration with sub county authorities (C Namuenge, J E. Ssenku, 2024).
3. In addition to that, local populations were encouraged to actively monitor early warning signs of landslides, particularly from May to June and August to November, which are the months most prone to landslides. Signs to look for included crack formation, the sudden appearance of water during rainfall events, and small soil slips along the roads. Residents were also advised to avoid areas where water collects, known

as moisture zones, and to steer clear of steep dykes that are frequently affected by landslides ('Landslides in Uganda', no date).

4. A widespread mitigation measure at community and household level consisted of digging and constructing trenches and terrace barriers that involved using sacks filled with sand. This was conducted along with afforestation. Afforestation consisted in planting trees, especially those that can bear fruits (mangoes, avocado, oranges and lemon). This had the advantage of both address landslides and generate income at the same time by household heads and local leaders (C Namuenge, J E. Ssenku, 2024).
5. Gorokhovich *et al* (2013) proposed a cost effective scheme for MURWARWA village that involved placing vertical bars (metal or wooden) in rows along the slope, above and below the scarp. The required equipment included an optical theodolite and a surveying rod, with a benchmark bar for positioning. Regular mapping (bi-weekly or monthly) was to help detect any movements, particularly during the rainy season. In this system, an increase in movement speed was a sign to trigger evacuation warnings for the local population. Additionally, the setting up of three rain gauges monitored by local schoolchildren under teacher supervision were recommended. This data, combined with slope movement measurements, was expected to improve warnings about impending landslides (Gorokhovich *et al.*, 2013).

**Figure 4** shows the proposed cost effective scheme for MURWARWA village by Gorokhovich *et al* (2013).

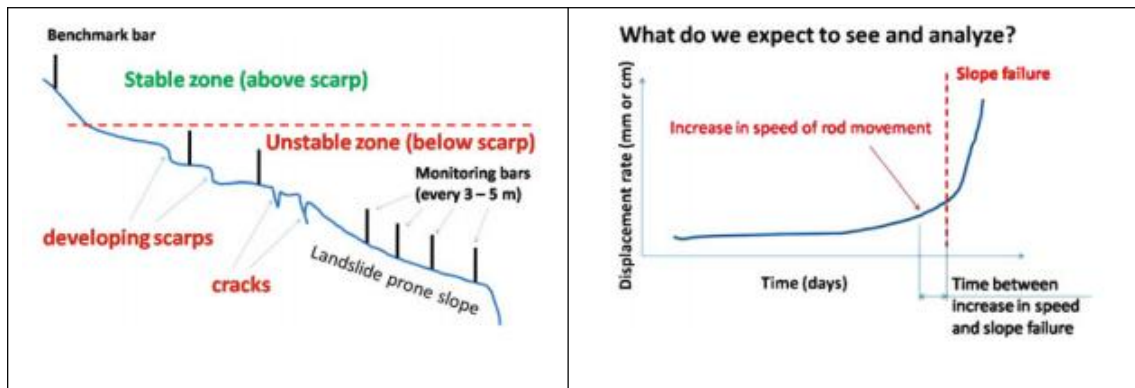


Figure 4. Landslide monitoring scheme.

Source : (Gorokhovich et al., 2013). (b) Expected landslide behavior derived from monitoring data. Source: (Gorokhovich et al., 2013)

## 2.4 CHALLENGES FACED IN LANDSLIDE MITIGATION

1. A delayed support from government agencies such as the office of the prime minister was observed. This made some interventions ineffective despite the fact that they could have made a considerable impact if executed in time. Furthermore, there is a limited scope of sensitization where most of the high-risk areas do not receive the service due to various challenges (C Namuenge, J E. Ssenku, 2024).
2. Poor timing, poor coordination between government, the disaster management teams, and humanitarian agencies to effectively support the landslide victims and duplication; along with proper sensitization: negligence; no clear information, no community understanding of the information. These challenges made the early warning system created in 2018 (Namono et al., 2019)

## 2.5 SUB SURFACE DRAINAGE SYSTEMS

### 2.5.1 TYPES OF SUB SURFACE DRAINAGE SYSTEMS

According to H. Rahardjo, V. A. Santoso (2012), there are three main types of sub surface drainage systems, namely:

1. **Horizontal Drains**: these are installed parallel to the ground surface to lower the groundwater table and reduce pore-water pressure. They are often used in slope stabilization.
2. **Vertical Drains**: these systems consist of pipes or wells that extend downward to intercept groundwater, commonly used in soft soil areas to accelerate consolidation.
3. **French Drains** : A French drain is a trench filled with gravel or rock containing a perforated pipe that redirects surface and groundwater away from an area.

**Figure 5** depicts the types of sub-drainage systems. (a) shows the Horizontal and Vertical drains, while (b) shows the cross-section of a French drain installation.

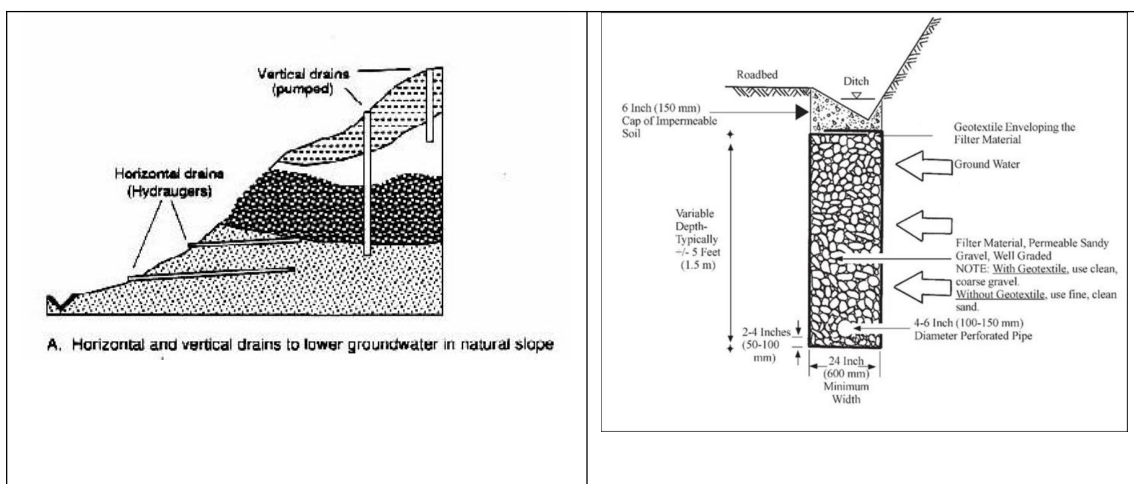


Figure 5. Types of sub drains.

*(a) Horizontal and vertical drains for sub surface drainage control. Source: (California Coastal Commission, no date). (b) French drain cross section. Source: (Rolt et al., 2020)*

## 2.5.2 DESIGN CONSIDERATIONS OF THE HORIZONTAL SUB-SURFACE DRAINAGE SYSTEMS

Water affects the slope stability in various ways including: introduction of seepage forces, increase in the weight of the slide mass, development of excess water pressure, and decrease in shear strengths (Cook, Santi and Higgins, 2008).

The design considerations of the horizontal sub surface drainage system are explained by Cook, Santi and Higgins (2008), and entail the following points:

### 1. Slot size and filtering mechanism

#### a. Slot size

Slots, also known as pipe perforations, allow water from the slope to enter the horizontal drain pipe, which then carries the water away. These slots are arranged in two longitudinal rows that are spaced 120° apart around the circumference of the pipe. They generally come in widths of 0.25 mm, 0.5 mm, or 1.3 mm. The wider slots are designed for use in coarse sand or gravel and can accommodate fine sand and silt without clogging. However, the narrower slots are more prone to plugging and may require regular cleaning, but they allow fewer particles to enter, making them suitable for fine-grained materials. The medium-width slots are the most commonly used.

#### b. Filtering mechanism

The filtering mechanism can either consist of a soil media or a geotextile

membrane.

i. Soil media

The filter requirements are given by:

- **Slot width** =  $\frac{D_{85} \text{ of soil}}{2}$
- Though not common as slots, circular slots can be used to perforate the pipe, and the filter requirement for a pipe with circular holes is given by:  
Diameter hole <  $D_{85}$  of soil

ii. Filter membrane media:

This is a geotextile material that surrounds the pipe. The geotextile material is further explained under point 2.5.

## 2. Drain spacing

The spacing of drains is generally determined during installation. In practice, this process often involves a considerable amount of trial and error, and depends on site layout and accessibility (Crenshaw and Santi, 2004). Some researchers have attempted to develop quantitative methods for estimating drain spacing, however these methods either do not offer the most economical and efficient solutions, or still require some trial and error to achieve the desired phreatic draw-down. Consequently, the conventional approach to determining drain spacing relies largely on general guidelines and engineering experience, which can be summarized as follows:

- i. For parallel drains in high-permeability soils, initial drains should be spaced at 8-15-m intervals;
- ii. For parallel drains in fine-grained soils, initial drains should be installed at 1-8-m intervals;
- iii. Additional drains may be necessary depending on site conditions and to

tap zones that produce substantial amounts of water;

- iv. For fan configurations, enough drains should be installed to result in an average spacing equivalent to the guidelines given for parallel drains.

### **3. Drain length**

During their installation, drains should penetrate through the slip area to effectively remove water and enhance the stability of the slope. However, these drains should not extend more than 3 to 5 meters past the slip surface, as extending them further does not provide additional benefits beyond the point where the critical slip surface intersects the top of the slope.

### **4. Drain inclination**

Horizontal drains are designed to be inclined upward from the outlet to maintain a positive hydraulic gradient, promoting more effective water flow out of the slope. The inclination angle typically ranges from 2° to 10° from the horizontal, although angles of 25° or more can be used in certain installations. Nevertheless, lower angles are generally preferred because they result in lower elevations at the back ends of the drains, which enhances the potential for groundwater draw-down that the drains can achieve.

### **5. Drain configuration**

The drain configuration refers to how drains are installed within the slope profile. In general, drains are positioned at multiple levels to account for subsurface water access from various points, depending on the terrain's accessibility to those levels. This approach effectively drains perched zones and isolated water pockets. Additionally, the installation should be carried

out near the toe of the slope to help lower the groundwater table, which in turn reduces pore-water pressure (H. Rahardjo, V. A. Santoso, 2012).

The drain configuration can either be in parallel or in fan-shaped (array).

**a. Fan-shaped configuration**

The fan-shaped configuration (see FIG.5 (a)) exhibits several advantages among which:

- i. It is not selective of the location: suitable locations for drilling are rare on sloping terrain and have to be prepared ahead of time;
- ii. The installation process is faster because the time required for resetting the equipment after each drain installation is reduced;
- iii. Easy collection of water from several drains at once for conveyance off the slope;
- iv. High likelihood of intersecting previously unrecognized open discontinuities or perched layers of water is higher since the drains are installed at several different orientations within the slope

**b. Parallel configuration**

The advantages of parallel configuration (see FIG 5 (b)) are as follows:

- i. This configuration is used often on relatively linear features such as highways, canals, and rail-roads
- ii. They provide more confidence in measuring spacing of drains and in representing the slope with simplified models.

**Figure 6** shows the types of drain configuration. (a) is the plan view of a fan-shaped configuration, and (b) a side view of a parallel configuration.

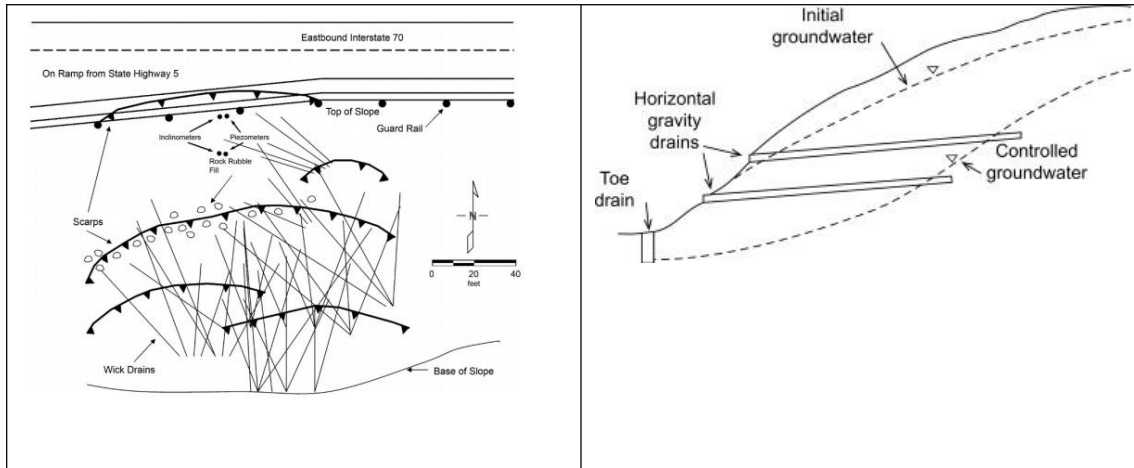


Figure 6. Drain configuration.

(a) *Drain in fan configuration* Source: Cook, D.I., Santi, P.M. and Higgins, J.D. (2008).

(b) *Drains in parallel configuration.* Source: Peter G. Nicholson (2015).

## 6. Drain Protection and Water Redirection

After the drain has been installed, a protective sleeve of galvanized pipe is usually installed and grouted in place to protect the lower 1.5-6 m from invasion by tree roots and to prevent soil erosion at the outlet. The sleeve also protects the pipe from impact by straying vehicles, or rockfall events. A collector pipe may be attached to the sleeve to direct water to a designated discharge point off the slope. In extreme climates, drain outlets should be buried in sand or gravel to protect them from ice build-up or blockage.

## 7. Drain Markers and Location Records

Drain marking is the final step in the installation of a drain. This process involves recording the drain's location in relation to survey monuments or permanent landmarks. While drain marking is sometimes overlooked, it is a crucial step. The water discharged from a drain can often promote substantial vegetation growth, which may obscure the outlet locations. As a result, having clear drain markers and maintaining a record of drain

locations is essential for facilitating repairs and cleaning, as well as for evaluating slope stability.

## **2.6 MATERIAL**

This section briefly introduces the materials used in horizontal sub-drainage systems, for instance the pipe material and the geosynthetic material.

### **2.6.1 THE GEOSYNTHETIC**

Geotextile materials are fibrous materials that consist of elements such as individual fibers, filaments, and yarns among others. These constituents are long, small in cross section, and they are strong in tension. Geotechnical material are primarily characterized by their flexibility. This property is crucial as it allows good contact conditions and reduces the stress concentration in the fibers. In addition to this, they possess hydraulic functions that have a high void ration, for instance high permeability, due to the fibrous nature of the elements making it (H. Niroumand, A. Kassim, A. Ghafooripour et la; Septemner 2012). In slope stabilization, the geotextile material has the following functions:

#### **1. Drainage function or fluid transmission**

Here the geotextile material is placed in contact with the material of low permeability through which water is seeping slowly. Here the material gathers and conveys water within its own plane towards the outlet.

#### **2. Filtration**

The material acts as a filter, allowing water to pass normal to its own plane, while preventing soil particles from being carried away by the liquid current.

### **3. Separation**

Here the geotechnical material is placed between two materials which have the tendency to mix when they are squeezed together under applied loads. As a separator, the geotextile must retain the soil particles and must have sufficient strength to withstand the stresses induced by the applied loads.

### **4. Protection**

This is achieved as the geotextile material distributes the stresses and strains transmitted to protect the material. For example, the geotextile can be placed between two materials to preventing one material from damaging the other by exercising concentrated loads.

### **5. Tension membrane**

This is achieved when the geotextile is placed between two materials having different pressures to balance the pressure difference, hence, strengthening the structure.

### **6. Tensile member**

A geotextile acts as a tensile member when it provides tensile modulus and strength to a soil with which it is interacting through interface shear strength, for instance the interlocking, friction, cohesion and adhesion.

#### **2.6.2 PIPE**

The pipe material (pipe casing) consists of hard polyvinyl chloride pipes (PVC) or gas pipes with an internal diameter of over 40mm. The pipe can either be perforated over its whole length, or at the specific sections traversing the aquifer. Nevertheless, rigid pipes are not recommended for landslide or unstable areas considering their incapacity of accommodating

the landslide movement that is occurring in an area without separating at the joints (David L. Rpyster. No date).

## **2.7 APPLICATION OF SUB DRAINAGE SYTEMS**

### **2.7.1 ROAD PROJECTS**

Road slope stabilization involves stabilizing the slopes adjacent to roads to prevent landslides. Key triggers for landslides in road projects include intense rainfall, changes in water levels, and stream erosion. Other factors that contribute to slope instability are excessive slope angles or heights, inadequate drainage, weak foundations, the removal of vegetation that helps anchor the soil, increased loading on the slopes, environmental influences, poor handling of fill materials, high groundwater tables, unsuitable geological features, soil liquefaction, and wildfires (NCHRP, 2012).

Subsurface drains are designed to remove shallow groundwater located less than 15 feet (5 meters) beneath the ground surface (GSPW 2003). This includes water found within the road surface, base, and sub-grade materials. These drains, such as under-drains and French drains, serve three primary purposes: intercepting water before it reaches the road, lowering the water table, and removing excess free moisture. Additionally, subsurface drains collect seepage water from surface run-off, helping to prevent an increase in the groundwater table. (NCHRP, 2012).

## 2.7.2 SLOPE STABILIZATION

### 1. *Gully erosion control*

#### a. Definition

Gully erosion is one of the most damaging types of soil erosion, occurring on slopes or hillsides due to concentrated water flow. Failures of gullies and riverbanks, along with head-cut retreats, pose significant threats to agricultural land and infrastructure. Valley bottom gullies are commonly found in periodically saturated lowlands and contribute to the silting of rivers and reservoirs. Erosion from these gullies leads to irreversible changes in soil productivity, affecting food security. Controlling and rehabilitating gully erosion is a complex and costly process that requires a deep understanding of gully formation. (Zegeye *et al.*, 2021).

Bank erosion, as described by Simon *et al.* (1999), results from hydraulic forces at the bank toe causing undercutting and steepening, combined with gravitational forces acting on the bank mass. Rates of failure depend on bank height, angle, and soil shear strength, which is sensitive to changes in pore-water pressure (Zegeye *et al.*, 2020).

#### b. Case of Ethiopia

Gully erosion is a serious concern that raised in Ethiopian highlands after deforestation in the 1980s. These highlands such as the DEBRE MAWI watershed near Lake TANA in the upper Blue Nile Basin, are characterized by shallow, highly weathered, and fractured basalt overlain by dark brown compacted clay, followed by light brown wet and sticky clay soil and then

finally by black clay and organic-rich soil sequences (Zegeye et al., 2020). Previous attempts to stabilize gullies with gully plugs, vegetation, and reduced bank slopes have failed as vegetation does not work for gullies deeper than 3 meters. The gully plugs on the other hand, diverted water, creating new gullies (Zegeye et al., 2020).

c. Horizontal sub drainage approach

The study by Zegeye *et al.* (2021) showed that gully dewatering through the use of a horizontal subsurface system was both a economical and an effective solution. For instance, over a period of two years, the draining reduced the soil losses by about 70%, as a result of a reduction in the pore water pressure. increased the shear strength and the critical shear stress of the slope.

**Figure 7** depicts the natural dewatering of the gully after installation of the sub-drainage system.



**Figure 7.** Natural dewatering of the gully the bank with installed sub-drains.

**Source:** Zegeye *et al.*, 2021

## 2. Residual soil slopes

Residual soils are formed from rapid in situ chemical and mechanical weathering of rock masses, primarily due to the heavy rainfall and high temperatures characteristic of tropical regions. Rainfall-induced slope failures are common in tropical and subtropical areas where residual soil is underlain by a deep groundwater table. Intense, short-duration rainfall can increase pore-water pressure, leading to a decrease in the soil's shear strength and ultimately compromising slope stability. These failures typically manifest as shallow slides, frequently observed in South-east Asia (H. Rahardjo, V. A. Santoso, 2012). The effectiveness of a horizontal drainage system is influenced by several factors, including the type, location, number, length, and spacing of the drains (Tantri *et al.*, 2023).

## CHAPTER THREE: METHODOLOGY

### 3.1 OVERVIEW AND RESEARCH DESIGN

This chapter outlined the methodology that was utilized to achieve the research objectives. These included site characterization, study of the hydrology, and the design of the horizontal sub drainage system.

The present study was an applied research, and classified as correlational as it intended to determine the relationship between water fluctuation in the soil profile and the factor of safety (FOS), the relationship between the factor of safety and the occurrence of a landslide, and ultimately, the relationship between the sub drainage system and the fluctuation of water in the soil profile.

**Table 1** summarize the specific objectives of the research, and the proposed methodology to achieve them, including the corresponding guiding standard.

*Table 1. Summary of the Objectives and Proposed Methodology used to achieve them*

No	PROPOSED METHODOLOGY		STANDARD/SOFTWARE
	<b>Objective one: To characterize the site</b>		
<b>1</b>	Determination of the site geometry		
	i.	Contour map	QGIS
	ii.	Angle map	QGIS
<b>2</b>	Determination of the soil properties		
	i.	Atterberg limits	BS 1377-2:1990
	ii.	Soil classification	BS EN ISO 17892: Part 4: 2018
	iii.	Unit weight	BS EN ISO 17892-3-2018

	iv.	Coefficient of permeability	<b>BS EN ISO 17892-11: 2019</b>
	v.	Cohesion and angle of friction <ul style="list-style-type: none"> <li>● Unconsolidated and Undrained conditions;</li> <li>● Consolidated and drained conditions.</li> </ul>	<b>BS: 1377: 1990: Part 7: Clause 8</b>
			<b>BS 1377-7:1990</b>
<b>Objective two: To conduct a hydrological study</b>			
<b>1</b>	Delineation the watershed determination of its characteristics		<b>QGIS</b>
<b>2</b>	Analysis of the rainfall dataset		<b>WPS-EXEL</b>
<b>3</b>	Estimation of the water losses in the watershed		<b>HEC-HMS</b>
<b>Objective three: To design a horizontal subdrainage system</b>			
	Determination of the influence of the sub-drains on groundwater levels		<b>MODEL MUSE</b>
	Geotechnical analysis		<b>GeoStudio</b>
	Design of a drain section		<b>Analytical methods</b>

## 3.2 SITE CHARACTERIZATION

### 3.2.1 SITE GEOMETRY

The site geometry encompassed the delineation of the area of interest, along with the determination of elevation contours and the slope angle.

A **Digital Elevation Model (DEM)** is a 3D computer representation of the surface of a terrain, showing the elevation of different points on the ground.

These are commonly used in Geographic Information System (GIS), and are a

common basis for digitally produced maps. DEMs can be created from various sources such as satellite imagery, aerial photography, and ground-based surveys. They have a wide range of applications including creation of topographic maps, watershed modelling, and flood simulations (F. Hutchinson and C. Gallant.2000.). The resolution of a DEM refers to the size of the grid cells that make up the model. The higher the resolution, the more details it will contain.

A DEM of resolution 30 meters was obtained from the USGS platform, and was used to generate the topographic maps, and to delineate the watershed in the area of interest. During the site visit, the coordinates of a point in the area of interest were obtained with the Handy GPS application as seen in **FIG.8(a)**. The application has an accuracy of 1 meter, and it provides data in forms of '*Northings and Eastings*' (*MINNA CLARKE ELLIPSOID*). Care should be put on the specification of the coordinate reference system (CRS), which in this case was the commonly used '*World Geodetic System 1984 (WGS84)*'. This collected data was converted into degrees prior to its use in QGIS. A polygon shape file of the area of interest was finally generated in delineating the area over an open street-map. The acquired DEM was clipped in accordance with the area of interest extent, and the contour and slope maps were finally generated.

### **3.2.2 SOIL PROPERTIES**

This activity entailed the determination of all the key parameters related to the slope stability. These included the atterberg limits, the particle size distribution, the unit weight, the coefficient of permeability, and the

strength parameters.

## **SAMPLING PROCEDURE AND SAMPLE PRESERVATION**

The sampling procedure was conducted in SHIKURUWE village, on a slope with a 2016 landslide scar (Nantumbwe, Bob R. Nakileza et al. 2017). Sampling was performed in the mid-slope, on a 15 by 10 area. The procedure followed recommendations highlighted by (Budhu, no date). Soil samples were obtained from 3 trial pits of dimension 1\*1\*1 meter, two along the slope and 10 meters apart, and the third 15meters away in the horizontal direction. An equivalent of 20 kilograms were extracted from each pit, and preserved into three air-tight polythene bags. At the lab, the three samples were labeled 163, 164, and 165 respectively.

**Figure 8(a)** shows the Handy-GPS interface. The app shows the UTM coordinates (Easting: 649187, Northing: 117488) based on the WGS84 datum, with an accuracy of +/-1 meter. The reported altitude is 1455 meters.

**Figure 8(b)** shows a soil sample packed in layers of air-tight polythene bags to prevent excessive loss of moisture during transportation from the site to the laboratory.

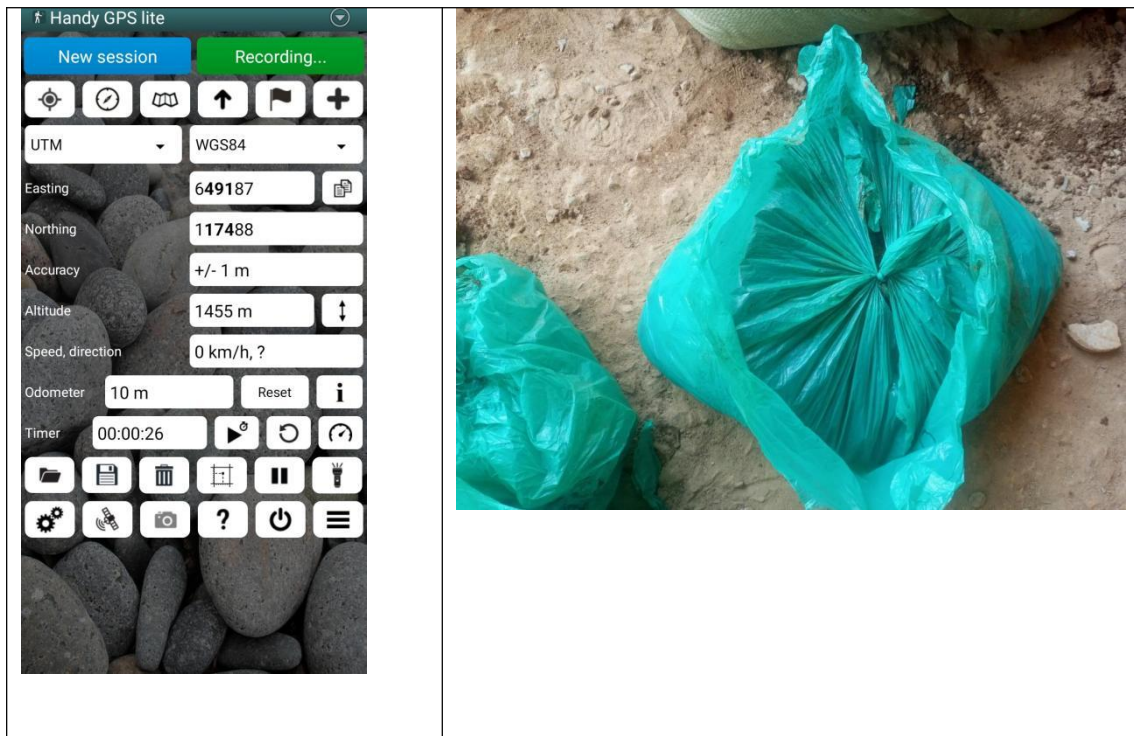


Figure 8. (a) Handy GPS interface; (b) sample preservation

## 1. ATTERBERG LIMIT

Atterberg limit tests was performed in accordance with the BS 1377-2:1990 standard. Atterberg limits are a set of tests performed to determine the physical properties of fine grained soils such as clay and silts (GEOTECHNICAL ENGINEERING BUREAU. 2015). They consist of three tests that measure the moisture content of a soil at different states.

- i. Liquid limit: this is the moisture content at which a soil changes from a liquid state to a plastic state.
- ii. Plastic limit: this is the moisture content at which a soil changes from a semi-solid state to a solid state. This is determined by measuring the moisture content at which soil can be molded into a ball.

iii. Shrinkage limit: this is the moisture content at which soil changes from a semi solid to a solid state. This is determined by measuring the moisture content at which a soil stops shrinking.

**Figure 9** depicts the Atterberg Limits graph, that illustrates the relationship between the soil moisture content ( $W_c$ ), and the total volume. Four distinct states of soil consistency are noticed as the water content increases: brittle (solid), semi-solid, plastic, and liquid.

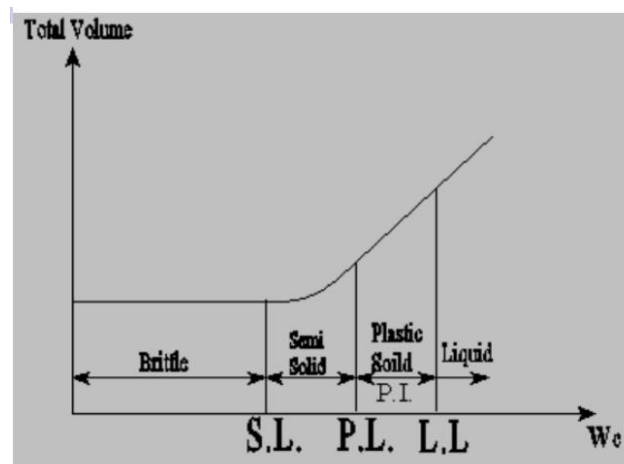


*Figure 9. Atterberg limit graph*

### Sample preparation

The sample was oven-dried at  $110^{\circ}$  for 24 hours. It was then crushed and particles retained at the 425mm sieve were removed. A specimen of about 400g was then transferred onto a glass plate and water was added to form a thick homogeneous paste using palette knives. The paste was placed in a airtight container for 24 hours to allow a thorough penetration of water into the specimen.

### *a. LIQUID LIMIT*

The liquid limit was determined by cone penetrometer method, which is based on the measurement of penetration into the soil of a standardized cone.

#### Apparatus

- A glass plate
- Palette knives
- Penetrometer
- A stainless steel cone, 35,mm long with a polished surface
- A damp cloth
- A wash bottle
- A metal cup of 55mm diameter and 40mm depth

#### Test procedure

- The 400g of damp specimen was placed on glass plate, and water was gradually added until sufficient to reach a first reading with the cone penetrometer reading about 15mm. The paste was mixed for about 8 minutes using the palette knives;
- A portion of the mixture was put into the metal cup with a palette knife and trimmed until a smooth level surface was achieved;
- The cone was lowered until it almost touched the soil surface in the metal cup, then it was released for a period of 5 seconds. The dial gauge was lowered to contact the cone shaft and the reading was taken slightly above 15mm for the samples.

- The cone was then lifted and cleaned carefully;
- Moisture content samples were picked from the area penetrated by the cone and weighed and taken into the oven for drying.
- For the readings less than 0.5mm, the soil was removed from the metal cup and remixed to achieve consistent results.
- The procedure was repeated for penetrometer readings of 18mm, 20mm, and 25mm. more water was added for each reading, such that the approximately a range of 15-25mm readings were covered.
- The metal cup was washed and dried for every addition of water.

### Calculation

**Equation 1** shows the obtention of moisture content of the soil specimen expressed in percentage, which was the ratio of the mass of water that was evaporated from the soil sample during the oven-drying process ( $m_2 - m_3$ ), over the mass of dry sample ( $m_3 - m_1$ ). Therefore,

$$M_c = \frac{m_2 - m_3}{m_3 - m_1} * 100$$

#### *Equation 1 Moisture content for Liquid Limit*

Where

$m_1$ : mass of the container in g

$m_2$ : mass of the container and the wet soil in g

$m_3$ : mass of the container and dry soil in g

#### **b. PLASTIC LIMIT**

The plastic limit test was done as a continuation of the liquid limit test. The specimen from the three test pits were prepared the same way as for liquid

limit.

### Apparatus

- A 3mm diameter rod
- Palette knives
- Glass plate
- Water

### Test procedure

- About 40g of paste was placed on a glass plate and allowed to dry partially until it became plastic enough to be shaped into a ball;
- The soil was then molded between the fingers and rolled between the palms of the hands until the soil dries sufficiently to be able to form cracks on its surface;
- The soil was divided into sub specimen of about 20g and then 3mm diameter threads were formed with forward and backward movement of the hands. These were measured by the rod to ensure that they were 3mm;
- The first crumbling point was the plastic limit. The crumbled threads were then gathered and transferred to labeled containers for moisture content determination.
- The procedure was repeated for the three samples from the three trial pits.

### Calculations

**Equation 2** shows the obtention of moisture content of the soil specimen

expressed in percentage, which is the ratio of the mass of water that was evaporated from the soil sample during the oven-drying process ( $m_2 - m_3$ ), over the mass of dry sample ( $m_3 - m_1$ ), therefore,

$$M_c = \frac{m_2 - m_3}{m_3 - m_1} * 100$$

*Equation 2. Moisture Content for plastic limit*

Where

$m_1$  : mass of the container in g

$m_2$ : mass of the container and the wet soil in g

$m_3$ : mass of the container and dry soil in g

The plastic index was finally obtained from the liquid limit and the plastic limit values.

**Equation 3** shows the formula for the Plastic Limit, calculated as the difference between the Liquid Limit and the Plastic Limit of the soil sample.

$$PI = LL - PL$$

*Equation 3. Plastic index*

Where

**PI**: plastic index

**LL**: liquid limit

**PL**: plastic limit

### **c. LINEAR SHRINKAGE**

The linear shrinkage test measures the total linear shrinkage from linear measurements on a bar of the soil that passed the 425mm sieve at the moisture content of the liquid limit. It is also done as a continuation of the

liquid limit and the plastic limit tests and the sample is prepared as part of the liquid limit test.

#### Apparatus

- Glass plate
- Palette knives
- Oven
- Clean water
- A linear shrinkage mold
- Grease
- Vernier calipers

#### Test procedure

- The mould was cleaned thoroughly and a light film of grease was applied to its inner face to prevent the soil from sticking to the surface of the mold;
- The paste for linear shrinkage was removed at the moisture content where the penetrometer reading was 20mm during the liquid limit test;
- The paste was then placed in the shrinkage mould and a palette knife was used to achieve a smooth level surface. The molds were left to air dry for a day and then were placed in the oven at 105<sup>0</sup>C;
- The mould was then cooled and the length of the bar was measured using the Vernier caliper.

#### Calculations

**Equation 4** shows the calculation for Linear Shrinkage expressed as a percentage reduction in length due to drying.

$$LS = \left(1 - \frac{L_D}{L_0}\right) * 100$$

*Equation 4. Linear Shrinkage*

Where

$L_0$ : initial length in mm

$L_D$ : length of the oven dried specimen in mm

## 2. SOIL CLASSIFICATION

The soil was classified by the particle size distribution test, in accordance with BS EN ISO 17892: Part 4: 2018.

### a. Moisture content

A mass of wet soil + tin was measured in labeled tins of known mass and then oven-dried at 110° for 24-hours. The mass of dry soil+ tin was then determined.

**Equation 5** shows the obtention of the initial moisture content of the specimen, which was the ratio of the mass of water that was evaporated from the soil sample during the oven-drying process ( $w_1 - w_2$ ), over the mass of dry sample ( $w_2$ ).

$$MC = \frac{w_1 - w_2}{w_2} * 100$$

*Equation 5. Initial moisture content for particle size distribution*

Where

$w_1$  : mass of the wet soil + the tin in g

$w_2$ : mass of the dry soil + the tin in g

This operation was repeated twice for every specimen in triplicate.

### b. Wet sieving

A dry specimen of about 1.5 kg was weighed and recorded as **A**, and then soaked in water for a minimum of 12-hours, to allow larger particles to soften prior to the wet sieving process .

The wet sieving procedure entailed washing thoroughly the soil specimen through a series of two sieves until water coming out of the sieves was relatively clean.

The finer sieve had a diameter of 75µm, meaning that only particles of diameter less than 75µm (silt) were allowed to pass through. The other sieve, also referred to as the ‘guard sieve’, had a diameter of 600µm. Its purpose was to prevent damaging the finer sieve if used alone. After sieving, the specimen was oven-dried at 110° for 24-hours.

This procedure was done in triplicate for every sample.

c. Dry sieving

The weight of the dry specimen was recorded as **B**, then the specimen was passed through a series of different sieve sizes as per standard , and the mass retained at each sieve recorded.

d. Determination of the mass that passed the 75µm sieve (Pan+C)

The soil particles that passed through the 75µm sieve are referred to as fine-grained, and they encompass silt and clay particles.

**Equation 6** shows the obtention of the mass of fine-grained particles, which was the sum of the mass retained on the pan after dry-sieving, and **C**, the difference in mass due to sample washing.

$$Mass_{fine-grained} = Pan + C$$

**Equation 6. Determination of the mass that passed the 75µm sieve**

Where

**Pan:** mass of soil retained on the pan after the dry sieving process

**C:** mass of dry sample (D) - dry mass after washing (B)

**Equation 7** shows the obtention of the mass of dry sample (D), using the initial dry mass before washing (A), over the moisture content  $M_c$  expressed in percentage.

$$D = \frac{\text{Dry mass before washing (A)} * 100}{100 + M_c}$$

*Equation 7. Determination of the dry mass sample*

### 3. UNIT WEIGHT

The bulk unit weight of the soil was indirectly determined by the specific gravity test in accordance with (BS EN ISO 17892-3-2018).

#### a. Sample preparation

The oven-dried sample was crushed and passed through a 2mm sieve, after which it was divided into three specimen of about 100g for the test in triplicate.

#### b. Aparatus used

- A weighing scale;
- Nine clean and dry pycnometers of capacity 250ml and a lid;
- A beaker of capacity 100ml.

#### c. Testing procedure

The label and the weight of the empty pycnometer with the lid was recorded. In a beaker, a 50mg of the specimen was measured, and then poured into the pycnometer. The mass of the pycnometer plus the sample plus the lid was then recorded.

Water was poured into the pycnometer up to a level slightly above the

level of the soil specimen, and then vigorously mixed until dissolution of the soil. The solution was allowed to settle for a minimum of 12-hours. After that period of time, the pycnometer was entirely filled with water, closed with the lid, and the solution briefly mixed to allow an even dispersal of particles in water. The weight of the pycnometer with the lid plus the solution (water+specimen) was recorded.

**Equation 8** shows the obtention of specific gravity (G) which is dimensionless, from the ratio of mass of dry soil ( $m_2 - m_1$ ) over the difference between the mass of water ( $m_4 - m_1$ ) and the mass of wet soil ( $m_3 - m_2$ ).

$$G = \frac{m_2 - m_1}{(m_4 - m_1) - (m_3 - m_2)} * 1000$$

*Equation 8. Determination of the soil density*

Where

$m_1$ : mass of pycnometer (g);

$m_2$  : mass of pycnometer and dry soil (g);

$m_3$ : mass of pycnometer, soil, and water (g);

$m_4$  : mass of pycnometer full of water only (g).

#### 4. COEFFICIENT OF PERMEABILITY

The permeability test is a test conducted to determine the coefficient of permeability (K), which is the rate of flow under laminar flow conditions

through a unit cross sectional area of porous medium under unit hydraulic gradient (B. Ahmed, August 2021). The falling head permeability test is commonly used in connection with the studies where the drainage and settlement of soft foundations are involved. This test can also serve as a check on the consolidation test results.

There are two types of permeability tests, for instance the constant head permeability test, and the falling head permeability test.

- The constant head permeability test is performed on coarse materials such as sand. Here water is forced by a known constant pressure through a soil sample of known dimensions, and the rate of flow is then determined. The type of sample used is undisturbed, and remolded prior to testing. During sample preparation, water is added to bring the sample slightly below the apparent optimum moisture content (OMC), or sufficient water to enable a good compaction using the 45.4 kg compaction method.
- The falling head permeability test on the other hand, is performed on fine-grained materials such as clay. Here water is forced by a falling head through a soil sample of known dimensions, and the rate of flow is determined. Undisturbed samples are required for this test, however, remolded specimens can also be used, though they cannot be as accurate as undisturbed samples.

The coefficient of permeability (K) was determined by the falling head permeability test in accordance with the BS EN ISO 17892-11: 2019 standard, since the soil sample was a clay type. The test was performed on remolded specimen, hence an adequate compaction was necessary prior to the test.

a. Sample preparation

i. **Apparatus used**

- Permeameter with its accessories;
- Weighing scale;
- 2 mm sieve
- Measuring jar
- Trimming knife
- Tins for moisture content test
- Oven
- Metallic rings of dimensions D6mm, h4mm
- Protective glass plates

ii. **Procedure**

- The soil sample is preferably dried and sieved to remove particles retained on the 2mm sieve. An alternative is to work at the moisture content of the sample which was previously determined in other tests. In this case, the specimen was ensured to be composed of fine particles by further crushing any larger particles, and an amount of 2.5 kg was taken;
- Water was gradually added to the specimen until the optimum moisture content was attained for compaction;
- The weight of the empty mould, as well as the one of two empty tins per specimen was recorded according to their respective label;
- The permeameter was assembled. The compaction method utilized was the 4.5 kg, which is suitable for soil particles up to medium particle size. This method entails compacting the specimen in 5 layers with 27 blows

each, with a 4.5 kg hammer in a 1 liter mould;

- After compaction, the mould was trimmed, and the weight of the mould plus the compacted specimen recorded. Some of the trimmed compacted soil was recovered to determine the moisture content. Hence, the mass of the tin plus the wet specimen was taken and recorded, and the specimen oven-dried at 110° for 24 hours ;
- The compacted specimen was mechanically recovered from the oiled mould;
- The weight of the empty ring was taken and recorded according to the respective label;
- The specimen was divided into two, and a half was kept as reserve. The metallic ring was ensured to be inserted evenly into the compacted soil, trimmed at both ends, and the weight of the ring plus the specimen recorded, then two glass plates were placed at both ends of the specimen to prevent a loss of moisture, finalizing the sample preparation process.

b. Apparatus used for the permeability test

- Thermometer
- Filter papers
- Rings
- Porous stone
- Stand pipe
- Measuring cylinder
- Water supply

### c. Test procedure

The apparatus was loaded, by placing a filter paper and then the ring, and another filter paper on top. The ring was then fastened to prevent any water from spilling out. The water head was measured at a known starting point.

Before starting the flow measurements, the soil sample was saturated and the stand pipes were filled with de-aired water to given level, (in this case it was 90ml).

The soil sample, a cylindrical core was placed in a test chamber with the water above it.

The test then started by allowing water to flow through the sample until the water in the stand pipe reached a lower limit. The reading was recorded when the difference in the level was about 20ml.

The starting time and the ending time were recorded for the three specimens, and then converted into seconds.

**Equation 9** shows the obtention of the discharge (Q) in cubic centimeter, which was the product of the cross-sectional area of the tube ( $\pi R^2$ ) and the head difference ( $h_0 - h_1$ ).

$$Q (cm^3) = \pi R^2(h_0 - h_1)$$

*Equation 9. Calculation for discharge in falling head permeability test*

Where

$h_0$  : initial height of water

$h_1$  : final height of water

$R$ : diameter of the tube

This was performed several times until a consistent value is reached for the value of  $k$  (m/s) in the table.

### Calculations

The information collected included the following:

- Initial water head ( $h_0$ ) in the stand pipe
- Final water head ( $h_1$ ) in the standpipe after a set time.
- Time ( $t$ ) it takes for the water level to fall from  $h_0$  to  $h_1$
- Length of the soil sample which is the same as the ring dimensions
- Cross sectional area of the stand pipe through which the water flows

**Equation 10** shows the obtention of the coefficient of permeability  $K$  from Darcy's law for falling head permeability test, which related the dimensions of the testing apparatus (area of burette, length of soil column, and area of soil column), and the change in water over time to quantify the ability of the soil to transmit water.

$$K = \frac{aL}{At} \ln \frac{h_0}{h_1}$$

*Equation 10. Determination of the coefficient of permeability*

where

$K$  :coefficient of permeability

$a$  :area of the burette

$L$  :length of the soil column

$A$  :area of the soil column

$h_0$  :initial height of water

$h_1$  :final height of water ( $h_0 - \Delta h$ )

$t$  :time required to get head drop

## 5. COHESION AND ANGLE OF FRICTION

Cohesion and angle of friction are fundamental soil parameters that describe the soil's resistance to forces that cause it to slide or deform, known as the shear strength. Cohesion represents the internal bond of the soil, stemming from the attraction of fine particles such as clay, while the angle of friction reflects the resistance to sliding due to the interlocking and friction between particles (ABG. No date). These soil parameters can be determined in either unconsolidated and undrained, or consolidated and drained conditions.

### *a. UNCONDOLIDATED AND UNDRAINED CONDITONS*

The Triaxial test provides undrained stress-strain response of a cylindrical soil specimen under triaxial compression loading without consolidating the specimen (Andrew Lees,2020). It also provides the undrained shear strength parameters by performing the tests on different confining pressures. Initially, a confining pressure ( $\sigma_3$ ) is applied through water around the specimen in triaxial cell. The drainage valve is closed throughout the test, which does not allow the consolidation of the specimen. The specimen is then subjected

to shearing by applying the constant rate of deformation under undrained compression loading conditions. The excess pore water pressure is not measured during shearing; hence the shear strength parameters are analyzed in total stress conditions only.

### Sample preparation

The testing specimen consisted into a reconstituted sample of 38.1mm in diameter and 76.2mm long ( $H = 2D$ ) .

**Figure 10** shows a typical testing specimen for triaxial test, which has a diameter of 38.1mm and a height of 76.2mm.



*Figure 10. Testing specimen for triaxial test*

#### i. Apparatus

- Loading frame capable of generating constant rate of movement;
- Proving ring (Capacity ranging from 1 kN to 50 kN);
- Bottom platen of required diameter made with Perspex glass (diameter of the plate is selected according to the diameter of the sample);
- Top cap of required diameter made with Perspex glass with a circular

groove to accommodate the plunger of triaxial cell;

- Dial gauge (0.01 mm accuracy);
- Hardened Steel ball;
- Triaxial cell, in which using water hydro-static pressure can be applied to the specimen and having a central plunger that can be connected to proving ring to measure the vertical load/pressure. The cell (made of Perspex) is usually designed with a non-ferrous metal top and base connected by tension rods;
- Bottom base plate with a pedestal of diameter similar to the diameter of specimen and valve arrangements to apply cell pressure;
- Air-water interface system (Cylinder filled with water and a balloon inside it which applies air pressure to the water filled in cylinder);
- Air Compressor;
- Constant pressure system with regulators, valves and pressure meter to control the cell pressure;
- De-aeration tank;
- Latex rubber membrane;
- Rubber O-rings;
- Membrane Stretcher (An open-ended cylindrical section former, required inside diameter fitted with a small rubber tube on its side).

ii. Test procedure

- The bottom plate was placed on the pedestal of base plate of triaxial

cell, then the specimen was placed on top of it;

- The top cap was placed on the specimen;
- The specimen arrangement was sealed properly with the latex rubber membrane and rubber O-rings using the membrane stretcher;
- The cell was placed such that properly set up and uniformly clamped down to prevent leakage of pressured water during the test;
- The plunger was moved down and set up on the circular groove of the top cap, and the ball was then placed on the top of plunger;
- The center-line of the specimen was adjusted such that the proving ring, the steel ball, plunger and specimen were in the same line;
- The cell was filled with water with bleed valve open, then closed when the cell was completely filled;
- The air water interface was then regulated using valves and regulator of constant pressure system, and the pressure was applied to water with the balloon in interface system;
- The valve connecting the pressure to the cell was opened to apply the required cell pressure (50 kPa, 100 kPa and 150 kPa...). The pressure gauge was monitored such that to make any necessary adjustment to keep the pressure constant during the test;
- A small deformation was applied to the system until the underside of the hemispherical seating of the proving ring, through which the loading was applied, just touched the steel ball on cell piston. This procedure is

called the *docking of triaxial system*;

- After docking a dial gauge was fixed to measure the vertical compression of the specimen;
- The position of the gear was adjusted on the load frame to give suitable rate of deformation;
- The load was applied, and the readings of the proving ring and compression dial for every 25 divisions in compression dial gauge were automatically recorded by the machine;

The loading continued until failure or 20% axial strain a picture of the failure pattern of the specimen was finally taken as illustrated by **FIG.3.5**.

#### ***b. CONSOLIDATED AND DRAINED CONDITIONS***

This test was used to determine the shear strength parameters of soil under consolidated drained conditions primarily the cohesion and the angle of internal friction. The soil sample was consolidated under a known normal stress and then sheared at a slow rate to ensure drainage and prevent pore pressure buildup. This test followed BS 1377-7:1990.

#### **Sample preparation**

Representative soil samples were taken that were large enough to meet the test's size dimensions. The sample was carefully trimmed into a shape that fit the shear box ensuring a smooth and uniform surface, the moisture content of the samples was determined by oven drying to obtain dry weigh,

which was needed for calculations.

i. Apparatus

- A shear box;
- Loading frame;
- Normal load application system linear displacement transducer;
- Sample cutting tools.

ii. Test procedure

- The trimmed sample was placed inside the shear box, ensuring the top and bottom surfaces were level;
- The sample was carefully paced between the halves of the shear box and were aligned properly for the test;
- A normal load ( $\sigma_3$ ) was applied to the top of the top sample by placing a known weight or load on the top of the shear box;
- The normal stress was applied to avoid sudden disturbance of the sample;
- The sample was allowed to consolidate under the applied normal load. During this phase, the pore pressure dissipated and the sample reached a state where volume change stopped that is full consolidation.
- The consolidation phase ensured that the sample was drained. For clay soils, consolidation may take several hours or days;

- The settlement of the sample was monitored to ensure proper drainage and consolidation;
- After the consolidation was complete, the shearing phase began. The top half of the shear box was displaced horizontally by the shear apparatus causing the soil sample to shear along a horizontal plane;
- A slow, controlled shear by moving the top part of the box at a constant rate. The shear force was applied gradually, ensuring that drainage of the pore water occurs;
- The shear force ( $\tau$ ) was recorded continuously throughout the test using a load cell attached to the shear box. The horizontal displacement (strain) was recorded using a displacement transducer;
- The test continued until failure was observed. This typically occurs when the shear force reaches a peak and then drops indicating failure;
- The test stopped once significant displacement occurred or when the shear stress started to level off;
- The test was repeated with different normal stresses for example 50 kpa, 100 kpa, 200 kpa. And a failure envelope was plotted from the results.

### *iii. Results*

The failure data from the test was used to plot the shear stress versus normal stress for the samples. From the data points, a Mohr-Coulomb failure envelope was generated providing the cohesion and the angle of friction of the soil. The intercept of the Mohr-Coulomb failure envelope gives the

cohesion ( $c$ ). The slope of the failure envelope gives the angle of internal friction ( $\varphi$ ).

### **3.3 STUDY OF THE HYDROLOGY**

A spatial analysis was conducted using QGIS, utilizing a DEM to examine the topography, land use, and land cover. Subsequently, a hydrological analysis was carried out with the Hydrologic Modelling System (HEC-HMS). The aim of this objective was to determine the distribution of water in the various elements of the watershed.

#### **1. WATERSHED DELINEATION**

Watershed delineation entailed the identification of the river network that drains the study area, along with the specific drainage basin. The largest river in the area being TSUTSU river, the information about its catchment area was extracted from the DEM previously acquired using, QGIS. The large catchment was then divided into four sub catchments, and the outlet of the respective sub-catchment determined.

#### **2. RAINFALL**

A twenty five-years daily rainfall dataset was acquired from a weather station in BUDUDA district (coordinates  $x= 34.33$  and  $y=1.017$ ), and plotted. In the context of risk aversion, the design had to account for the worst case scenario of inflow, which in this case corresponded to the highest daily

rainfall value in the dataset (UNISDR, 2017). In addition to this, further statistical analysis were performed to determine the monthly rainfall frequency pattern, the yearly rainfall intensity, as well as the rainfall return time.

**Figure 11** shows the plotted graph of the 25-years daily rainfall dataset. The precipitation was recorded in inches, then converted to millimeters for a easier analysis. The orange arrow points at the highest rainfall value (1330.96mm) that was recorded on July 7<sup>th</sup>, 2007.

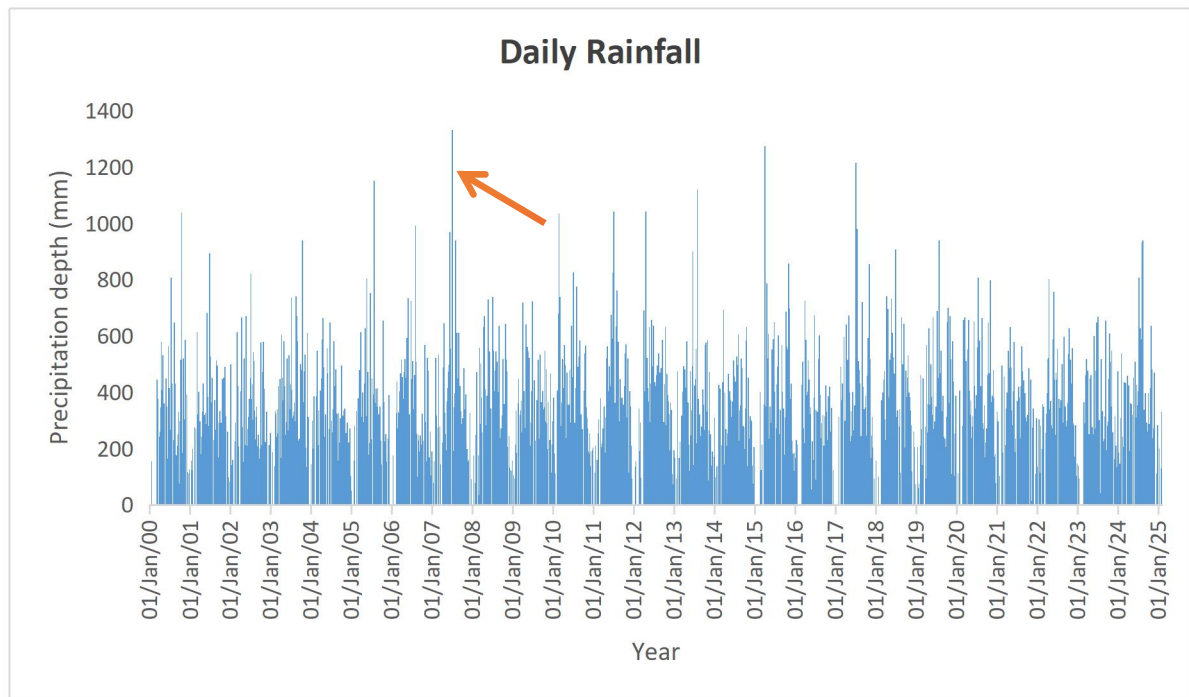


**Figure 11.** Daily rainfall data for 25 years.

### a. MONTHLY RAINFALL PATTERN

The monthly rainfall pattern corresponds to the average monthly rainfall throughout the data set.

**Table 2** shows the derivation of the average monthly rainfall data from

statistical analysis in WPS-EXCEL.

*Table 2. Average monthly rainfall values*

Month	Rainfall depth (mm)
January	20695.92
February	43995.34
March	76928.98
April	124452.38
May	123134.12
June	107579.16
July	121699.02
August	125168.66
September	93685.36
October	125364.24
November	85450.68
December	31193.74
<b>Grand Total</b>	<b>1079347.6</b>

#### **b. YEARLY RAINFALL INTENSITY**

**Table 3** shows the yearly rainfall intensity (YRI), along with the average daily rainfall intensity on rainy days (ADRIRD), and maximum daily rainfall intensity were generated from statistics in WPS-EXCEL.

**Table 3. Yearly intensity, Average daily rainfall intensity on rainy days, and maximum daily rainfall intensity.**

Year	Yearly rainy day count	Yearly rainfall	YRI	ADRIRD	Max daily intensity
2000	169	39695.12	108.7537534	234.8823669	1038.86
2001	187	40152.32	110.0063562	214.7182888	894.08
2002	189	38336.22	105.0307397	202.8371429	820.42
2003	200	43395.9	118.8928767	216.9795	939.8
2004	173	37467.54	102.6507945	216.5753757	662.94
2005	172	39235.38	107.4941918	228.1126744	1150.62
2006	199	43157.14	118.2387397	216.8700503	993.14
2007	204	43883.58	120.2289863	215.1155882	1330.96
2008	209	44932.6	123.1030137	214.9885167	739.14
2009	178	39921.18	109.3730959	224.2762921	723.9
2010	227	48541.94	132.9916164	213.8411454	1036.32
2011	216	51833.78	142.0103562	239.9712037	1041.4
2012	202	46075.6	126.2345205	228.0970297	1041.4
2013	209	45156.12	123.7153973	216.0579904	1120.14
2014	219	42418	116.2136986	193.6894977	693.42
2015	189	43461.94	119.0738082	229.9573545	1275.08
2016	169	35689.54	97.77956164	211.1807101	726.44

2017	194	45605.7	124.9471233	235.0809278	1216.66
2018	184	43883.58	120.2289863	238.4977174	906.78
2019	214	44820.84	122.7968219	209.4431776	939.8
2020	203	47073.82	128.9693699	231.8907389	807.72
2021	185	40576.5	111.1684932	219.3324324	632.46
2022	217	46814.74	128.2595616	215.736129	802.64
2023	194	41541.7	113.8128767	214.1324742	668.02
2024	218	44800.52	122.7411507	205.5069725	939.8

### c. RAINFALL RETURN PERIOD

The rainfall return period refers to the probability that a particular rainfall event will occur again in a near future, and it is mostly considered in the modelling process when design for the worst case scenario (M. Amoakowaash, L. Kofiste, A. Omari-sasu et al. 2021). The exceedance probability on the other hand, refers to the probability that a given rainfall magnitude will be exceeded in any given year. Rainfall events with a high return time depict a lower exceedance probability, while the ones with a low return time have a higher exceedance probability.

**Table 4** shows the maximum rainfall, the return period, and the Exceedance probability generated through statistical analyses in WPS-EXCEL.

*Table 4. Rainfall return period computation*

Year	Maximum rainfall (mm)	Rank	Return period (years)	Exceedance probability
2007	1330.96	1	26	0.038461538
2015	1275.08	2	13	0.076923077
2017	1216.66	3	8.666666667	0.115384615
2005	1150.62	4	6.5	0.153846154
2013	1120.14	5	5.2	0.192307692
2011	1041.4	6	4.333333333	0.230769231
2012	1041.4	7	3.714285714	0.269230769
2000	1038.86	8	3.25	0.307692308
2010	1036.32	9	2.888888889	0.346153846
2006	993.14	10	2.6	0.384615385
2003	939.8	11	2.363636364	0.423076923
2019	939.8	12	2.166666667	0.461538462
2024	939.8	13	2	0.5
2018	906.78	14	1.857142857	0.538461538
2001	894.08	15	1.733333333	0.576923077
2002	820.42	16	1.625	0.615384615
2020	807.72	17	1.529411765	0.653846154
2022	802.64	18	1.444444444	0.692307692
2008	739.14	19	1.368421053	0.730769231

2016	726.44	20	1.3	0.769230769
2009	723.9	21	1.238095238	0.807692308
2014	693.42	22	1.181818182	0.846153846
2023	668.02	23	1.130434783	0.884615385
2004	662.94	24	1.083333333	0.923076923
2021	632.46	25	1.04	0.961538462

### 3. HYDROLOGICAL MODEL

The purpose of the hydrological model was to understand the movement of water in the watershed.

Hydrological Modelling System (HEC-HMS) 4.12 program is a product developed by the US Army Corps of research and development program, and produced by the Hydrologic Engineering Center (HEC) (Feldman, 2000). The program works on the principle of watershed run-off process which begins with the precipitation falling onto the vegetation, land surface and water bodies, only to be returned to the atmosphere in the form of evaporate-transpiration. A portion of the precipitation on the vegetation falls onto the land surface, joining the precipitation that had already fallen onto the surface. On the surface, a portion infiltrates the ground, while the rest joins the stream. The precipitation that infiltrated the ground is stored in the upper or saturated soil layer. This either further gets carried to the surface by capillary action, or flows horizontally as inter-flow, or further percolates

vertically to join the aquifers as groundwater. All of the water previously mentioned eventually flow towards the stream (Vijayaprakash, M. 2020).

**Figure 12** depicts the principle of watershed run-off process used by HEC-HMS, how water precipitation enters the watershed, how it moves through the different elements of the watershed, and how it returns back to the atmosphere.

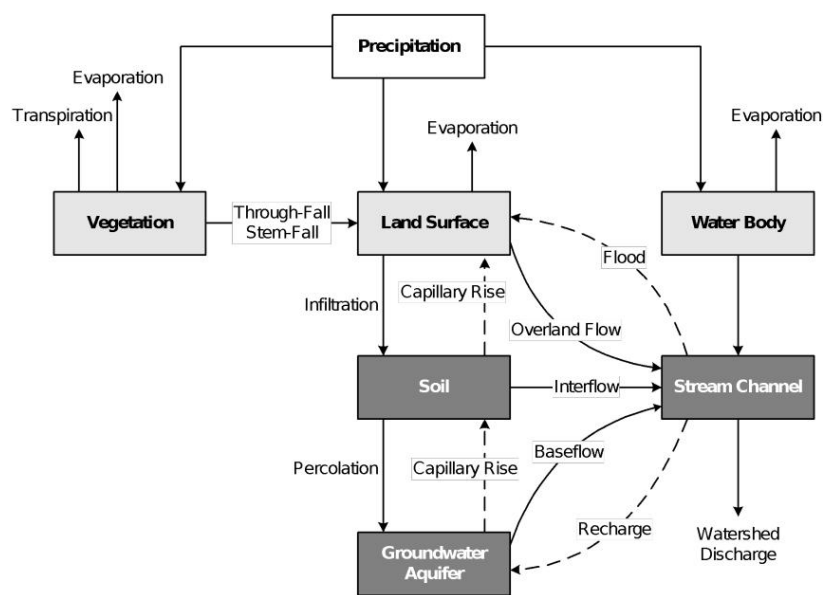


*Figure 12. System diagram of the runoff process at local scale*

*(Source: Ward, 1975)*

#### a. MODEL DOMAIN AND CONCEPTUAL MODEL

The model domain shown in **FIG 12**, had HEC-HMS grid cells equivalent to the DEM resolution (30m by 30m). The previously delineated watershed was divided into three sub-catchments of which the characteristics are displayed in **Table 5**.

i. The basin model consisted of three sub-basins (where the slope of

interest was located in sub-basin 3), two reaches, and three junctions (where the junction 3 is the outlet of the watershed). Every sub-basin accounted for the canopy interception, the surface, and the soil moisture, and was assumed to have a linear reservoir;

- ii. The meteorologic model considered the specified hydrograph and an annual evaporation for all the sub-basins;
- iii. The model had a control specification with a starting and ending dates corresponding to the ones in the time-series data, together with a time interval which was taken as an hour;
- iv. In the time-series data, the precipitation gage was a 24-hours data set corresponding to the peak rainfall value of the 25-years rainfall data.

**Figure 13** depicts the model developed with HEC-HMS. The active cells in color scale of assigned land surface elevations, with dimension 30 m by 30 m. The watershed was divided into 3 sub-basins, and different icons represent the sub-basins, the reaches, and the junctions respectively.

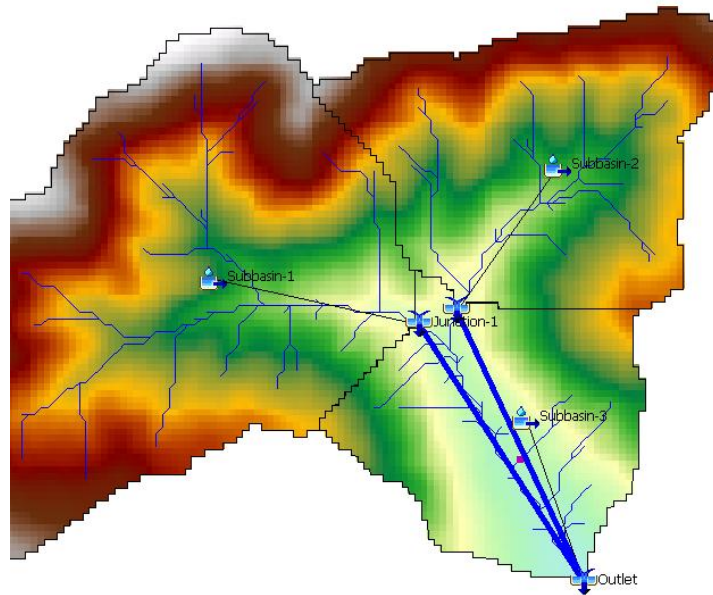


*Figure 13. HEC-HMS Model grid for the watershed.*

**Table 5** shows the characteristics for every sub catchment of the watershed, for instance the surface area, the longest river path, and the slope.

*Table 5. Characteristics of the different sub-catchments*

Sub-catch	Surface (Km <sup>2</sup> )	Longest river path (Km)	Slope $\frac{m}{m}$
1	3.3	3999.615	0.093
2	1.9	3410.236	0.1
3	1.5	1611	0.33

## b. BASIN MODEL

This encompassed the identification of the basin constituents (sub basins, outlets here referred to as junctions, and reaches), linking them from upstream to downstream, and defining their respective parameters. Hence, our basin model flow was as follow:

Sub basin1 → junction1 → reach1 → outlet

Sub basin2 → junction2 → reach2 → outlet

Sub basin 3 → outlet

## BASIN CONSTITUENT PARAMETERS

### i. SUB BASIN

The sub basin comprised the watershed area, the vegetation, the slope, the water loss type, and the transformation method.

- ***Vegetation: Simple canopy method***

Simple canopy method requires an initial, and a maximum storage value to be assigned to the sub-basin.

The initial storage was assumed to be 40%, provided that it rained the day before the considered simulation day. The maximum storage value on the other hand, is dependant on the type of vegetation.

**Table 6** explains estimation of the maximum storage value in relation to the vegetation type, according to Buchhorn et al (2019).

**Table 6. Land cover and Interception storage values**

<b><i>Vegetation type</i></b>	<b><i>Max storage</i></b>
Herbaceous vegetation	2.0
Cropland	2.0
Urban area	0.5
Water bodies	0.0

Evergreen needle leaf	2.0
Deciduous broad leaf forest	2.0
Mixed forest	3.0

Considering that the vegetation type of the area is primarily herbaceous vegetation (banana plantations) and cropland (coffee and cassava), the maximum storage was taken as 2.0.

- ***Surface: simple surface method***

The simple surface method also requires the user to define the initial, and maximum storage value.

The initial storage value was assumed to be 60% for the same reasons stated before. The maximum storage value is dependent on the slope of the terrain. The slope of the terrain was previously extracted from the DEM under site characterization, where the maximum value was 28.26%.

**Table 7** gives an insight of the maximum storage values estimation based on the type of surface slope (Vijayaprakash, M. 2020).

**Table 7. Slope and Surface storage values**

<b><i>Category</i></b>	<b><i>Type of surface Slope (%)</i></b>	<b><i>Surface Storage (mm)</i></b>
Paved Impervious	NA	3.18-6.35
Flat, Furrowed	0-5	50.8
Moderate to Gentle Slopes	5-30	6.35-12.70
Steep, Smooth Slopes	>30	1.02

From the table, the slope of 28.26% fell under the category of ‘Moderate to Gentle slopes’. A linear interpolation was applied to determine the maximum storage corresponding to the slope of interest.

**Equation 11** is an application of linear interpolation, considering the value above ( $S_{30}$ ), and below ( $S_5$ ) the one for the slope ( $S_x$ ).

$$\frac{S_{30} - S_x}{S_{30} - S_5} = \frac{\text{Slope}_{30} - \text{Slope}_x}{\text{Slope}_{30} - \text{Slope}_5}$$

**Equation 11. Linear interpolation for maximum surface storage**

$$\frac{12.70 - S_x}{12.70 - 6.35} = \frac{30 - 28.26}{30 - 5}$$

$$12.70 - S_x = 0.44196$$

$$S_x \text{ (mm)} = 12.258$$

- **Loss: SMA method**

Provided our interest in the effects of rain on the soil, the selected loss method was the Soil Moisture Accounting (SMA). This method requires several parameters to calculate the loss from three layers (soil, GW1, and GW2).

1. Initial storage condition

Based on the rule, the soil layer was assigned 50%, groundwater layer 1 as 20 % and groundwater layer 2 as 30% (Vijayaprakash, M. 2020).

2. Infiltration rate

The infiltration rate only pertains only to the top soil, which consists of a clay layer.

**Equation 12** shows the obtention of the maximum infiltration rate, which

was the average of the infiltration rate values obtained from the falling head permeability test for the three trial pits.

$$\text{Max IR (mm/hr)} = \frac{IR_1 + IR_2 + IR_3}{3}$$

*Equation 12. Maximum infiltration rate*

Therefore,

$$\text{Max IR (mm/hr)} = \frac{9.39 + 367.1 + 444.67}{3} = 273.68$$

### 3. Soil storage condition

This included the calculation of soil storage, tension storage and soil percolation.

#### i. Soil maximum storage

**Equation 13** shows the obtention of the soil maximum storage, which was the product of the soil depth and the porosity, where the porosity was obtained from the bulk density and the specific gravity. The soil depth was taken to be 1 meter, with respect to the depth of sampling excavation.

$$\text{Max soil storage (mm)} = \text{soil depth} * \text{porosity (\%)}$$

*Equation 13. Maximum soil storage*

Where

$$\begin{aligned} \text{Porosity (n)} &= 1 - \frac{\rho_{\text{bulk}} * 100}{2.7} \\ &= 1 - \frac{1.933 * 9.81}{2.7} * 100 = 28.40\% \end{aligned}$$

Therefore,

$$\text{Max soil storage (mm)} = 1000 * \frac{28.40}{100} = 284$$

#### ii. Tension storage

**Equation 14** shows the obtention of the tension storage, which was the product of the soil depth, and the field capacity, where the field capacity was taken as 40% for clay soils (Vijayaprakash, M. 2020).

$$\mathbf{Tension\ (mm) = soil\ depth * field\ capacity\ (\%)}$$

**Equation 14. Tension storage**

Therefore,

$$\mathbf{Tension\ (mm) = 1000 * \frac{0.4}{100} = 40}$$

iii. Percolation

The percolation in the soil layer was taken to be 40% of the infiltration rate, and 10% for GW1 and GW2 respectively (Vijayaprakash, M. 2020). Hence,

$$\mathbf{Soil\ percolation\ (mm/hr) = 273.68 * \frac{40}{100} = 109.472}$$

$$\mathbf{GW1/GW2\ percolation\ (mm/hr) = 273.68 * \frac{10}{100} = 27.368}$$

- **Transformation: Unit Clark transform method**

The time of concentration (Tc) and storage coefficient (R) are the essential parameters for this method. Tc represents the time required to travel from the farthest point of the watershed to the outlet, while R represents the amount of water stored within the watershed during runoff. These parameters are dependent on the characteristics of the watershed (Timothy Melching, Charles S Kocher et al. 2000).

**Table 8** summarizes the characteristics of the watershed used in the computation of the time of concentration, and the storage coefficient, for

instance the longest river path, and the slope.

**Table 8. Key parameters for Unit Clark transformation method**

<i>Sub-basin</i>	<i>Longest flow length (Km)</i>	<i>Slope (<math>\frac{m}{Km}</math>)</i>
1	3.99	92.6
2	3.4	100
3	1.6	33.33

**Equation 15** shows the obtention of  $T_c$  and  $R$  when the longest flow path and the slope are known (Timothy Melching, Charles S Kocher et al. 2000).

$$T_c = 1.54 * L^{0.875} * S^{-0.181}$$

$$R = 16.4 * L^{0.342} * S^{-0.790}$$

**Equation 15. Time of concentration and Storage coefficient**

where

**L:** longest flow length in kilometers;

**S:** main-channel slope determined from elevations at points that represent 10 and 85 percent of the distance along in meters per kilometer.

**Table 9** summarizes the different values of  $T_c$  and  $R$  for the different sub basins.

**Table 9. Values for time of concentration and storage coefficient**

<i>Sub basin</i>	<i><math>T_c</math> (hr)</i>	<i><math>R</math> (hr)</i>
1	2.28	0.74
2	1.95	0.66

3	1.23	1.21
---	------	------

ii. **JUNCTION**

The junctions are the sub basin outlets determined when delineating the watershed. They should be linked to the other basin components, specifying the downstream element immediately following it.

iii. **REACH**

Reaches are related to the rivers of the system. The flow routing selected was the Muskingum model, for which the main parameters are K (hr) and X. A number of sub reaches was also determined, which were dependent on K and the running time-frame.

**c. METEOROLOGICAL COMPONENT**

The distribution of precipitation over the basin was performed using specified hydrograph method, and the evapo-transpiration method taken as ‘annual evapo-transpiration’, where the rate was taken as 4mm/day.

**d. TIME SERIES**

The time series component contains the precipitation gages. A precipitation gage consists of a time series gage where the data source, unit, and time interval are specified, a time window to specify the start day and start hour, as well as the end date and end hour. Finally it has a table allowing to enter

the rainfall data corresponding to the time window specifications, and graph to visualize the plotted graph for the entered data.

Daily rainfall was acquired for 25 years (Jan 1<sup>st</sup> 2000- Feb 5<sup>th</sup> 2025), and plotted to determine the peak rainfall. The peak daily rainfall has a value of 1330.96mm, and was considered as the design time frame in the context of risk aversion.

#### e. **CONTROL**

The principle is to control the simulation run. This is done by specifying time to start and stop the simulation, along with the time interval. The start date/time and the end date/time is specified in the time window. This runs both for event and continuous simulation.

The conceptual model model was set to run for 24 hours (03 Jul. 2007 00:00- 03 Jul. 2007 23:00), with a time interval of an hour.

### **3.4 DESIGN OF THE HORIZONTAL SUB DRAINAGE SYSTEM**

Two software were simultaneously utilized to understand the effect of drains on the slope stability: MODEL MUSE enabled the groundwater modelling, and the determination of the groundwater levels with and without sub-drains, while GeoStudio 2024 2.4 used the piezometric line previously obtained together with geotechnical parameters of the slope to determine the factor of safety, which is the indicator of the slope stability.

## i. MODEL MUSE

MODFLOW-6 program in MODEL MUSE is a widely accepted, finite-difference, public domain groundwater flow model produced by the United States Geologic Survey (USGS).

Equation 16 shows the basic governing equation for transient groundwater flow in a saturated anisotropic porous medium. The sum of rate of change of change of flow in the x ( $\frac{\delta}{\delta x} (K_x \frac{\delta h}{\delta x})$ ), y ( $\frac{\delta}{\delta y} (K_y \frac{\delta h}{\delta y})$ ), and z ( $\frac{\delta}{\delta z} (K_z \frac{\delta h}{\delta z})$ ) directions is equal to rate of change of storage within the porous medium ( $S_s \frac{\delta h}{\delta t}$ ) (R. Carrol, T. Badger. 2013).

$$\frac{\delta}{\delta x} (K_x \frac{\delta h}{\delta x}) + \frac{\delta}{\delta y} (K_y \frac{\delta h}{\delta y}) + \frac{\delta}{\delta z} (K_z \frac{\delta h}{\delta z}) = S_s \frac{\delta h}{\delta t}$$

*Equation 16. Governing groundwater flow equation used in MODFLOW*

Where

$K_x, K_y, K_z$ : hydraulic conductivity in the x, y, and z direction respectively;

$\frac{\delta h}{\delta x}, \frac{\delta h}{\delta y}, \frac{\delta h}{\delta z}$ : hydraulic gradient in the x, y, and z directions respectively;

$S_s$ : specific storage

$\frac{\delta h}{\delta t}$ : the rate of change of hydraulic head with respect to time.

## ii. GeoStudio

GeoStudio is an integrated geotechnical analysis software suite for analyzing slope stability, groundwater flow, and heat and mass in soil and rock. Its strength is in limit equilibrium slope stability analysis for civil and mining engineering projects, hence making it a powerful toll in solving slope stability, groundwater flow, and environmental challenges (GeoStudio

official website, 2021).

### 3.4.1 INFLUENCE OF THE SUB-DRAINS SYSTEM ON GROUNDWATER LEVEL

#### 1. SITE DESCRIPTION

The slope of the topography for which the system is being designed is relatively uniform from the slope crest to the base of the slope at approximately 27.73% (15.5°). The subsurface conditions are assumed to consist of a single layer reaching up to 275 meters in thickness. This is the sub-catchment 2 earlier delineated under section section 3.3(1). However, it was previously merged with sub-catchment 1 provided its small extent.

**Figure 14** shows the topography of model for groundwater modelling. The grid cells of the watershed equal to the resolution of the DEM (30m by 30m), and they are coloured with respect with the assigned values for elevation.

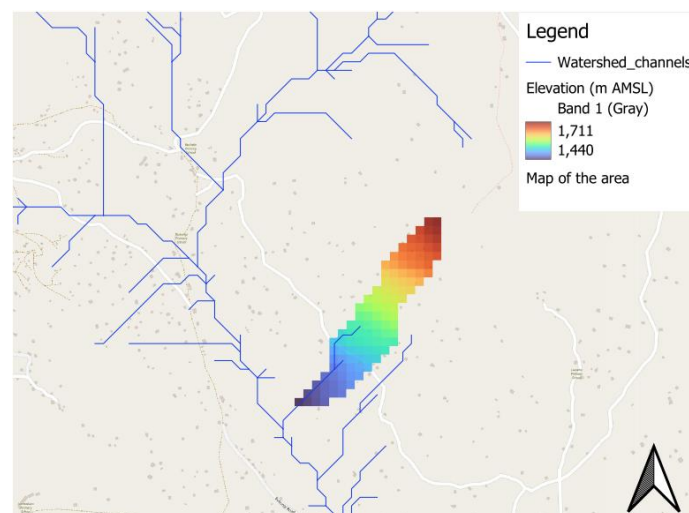


**Figure 14.** Topography of site

## 2. MODEL DOMAIN AND CONCEPTUAL MODEL

### a. MODEL DOMAIN

The model domain is defined in FIG. 14 with MODFLOW cells 5 m by 5 m in the x-y direction, which is rotated ( $-33^\circ$ ) so that the grid is parallel to the slope.

### b. CONCEPTUAL MODEL

#### i. Hydrologic parameters

The hydrologic parameters include specifying the coefficient of permeability in the x, y, and z directions ( $K_x$ ,  $K_y$ , and  $K_z$ ), along with the specific yield ( $S_y$ ) and the initial head of the system.

- $K_y$  and  $K_z$  were assumed to be equal to  $K_x$  (isotropic condition, VKA=1),

where  $K_x$  was obtained from:

$$K_x = K \frac{m}{s} / \frac{1}{3600 * 24} \frac{m}{day}$$
$$K_x = 1.545 * 10^{-7} * 3600 * 24 \frac{m}{day}$$
$$K_x = 0.0133 \frac{m}{day}$$

- The specific yield  $S_y$  was taken as 0.01 for clay soils (A. I. Joghanson. 1967).
- The initial head of the each grid cell was considered to be equal to its top elevation.

#### ii. Layer definition

This is a single layer model where the maximum thickness is 275 meters at the highest elevation (1711m AMSL) and minimum thickness is 6 meters at

the lowest elevation (1440m AMSL). The bottom of the modeled layer is at 1436 meters above mean sea level.

iii. Boundary conditions

- **Specified head boundary condition (CHD)**

The specified head boundary conditions are typically applied to the cells for which MODFLOW does not need to solve heads. Specified head cells are assigned a head value for a specific period of time for which head does not change. These conditions anchor the solution, and they represent features such as lakes, rivers, or distant observed heads. However, they should be positioned at a region sufficiently far from the region to be investigated as they can sometimes introduce inaccuracies. For most slope stability problems, the specified head boundary is likely assigned to the up and down-gradient model boundary locations (R. Carrol, T. Badger. 2013).

Considering the fact that there was no data about the ground water of the slope, the model domain comprised the whole watershed to avoid the need to designate water flux across the boundary conditions. This means that water was assumed to only enter the system from precipitation, with all water flowing towards the watershed outlet at lower elevation.

- **Specified flux (RCH)**

Specified flux boundary conditions are utilized in the event that the discharge is known. In this case, MODFLOW still solves for head where this flux is specified. There are several types of flux conditions among which no

flow, inter-basin flow, pumping/injection flow, and groundwater recharge, which was our interest.

**Equation 17** shows the principle of application of the recharge flow rate to the cell in Model muse, which is function of the recharge flux and the area of the cell.

$$Qr_{i,j} = R_{i,j}\Delta r_j\Delta c_i$$

*Equation 17. Recharge flow rate estimation in ModelMuse*

Where

$Qr_{i,j}$  is the recharge flow rate applied to cell i,j (L<sup>3</sup>/T)

$R_{i,j}$  is the recharge flux (L/T) input by the user

$\Delta r_j\Delta c_i$  is the area of the cell (L<sup>2</sup>)

The recharge was set to be uniformly distributed across the domain.

**Figure 15** show the model domain. (a) Plan view showing the modeled grid , the active cells in color scale of assigned land surface elevations. The cell dimension is 5m by 5m. (b)The cross section B-B' depicts a single layer model (maximum thickness 275m and minimum thickness 6m), as well as no flow cells, specified boundary (green vertical line) condition and recharge (black vertical lines) which is applied uniformly across the domain.

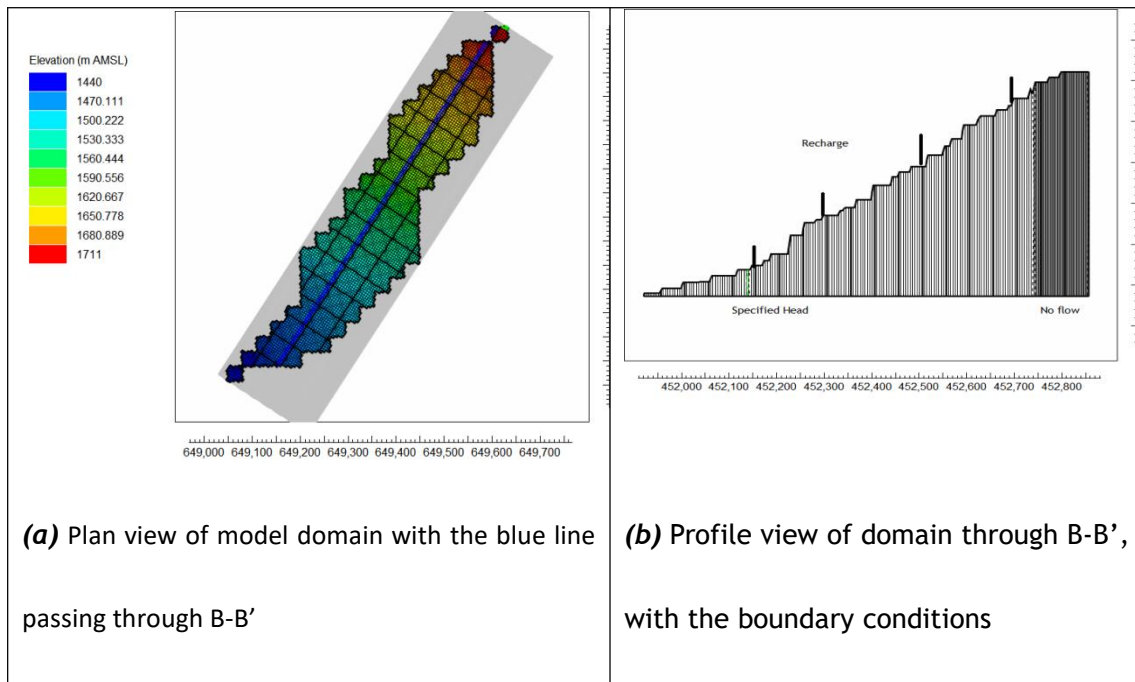


Figure 15. Model domain.

### 3. DRAIN CONFIGURATION

Drains are also assigned to the cells of the domain through a boundary condition (DRN).

In MODFLOW, drains are designed to remove water from the aquifer based on the difference between head in the aquifer, and the drain's elevation. This implies that flow into the drain and out of the aquifer only occurs when the levels in the aquifer are higher than the drain, and drop to zero when heads drop below the drain elevation (R. Carrol, T. Badger. 2013).

Two drain arrays in a fan-shaped configuration were considered. Drain array 1 consisted of 8 drains drilled at an angle of approximately  $6^\circ$  from each other, with a length of 100 meters, and at lower elevation of 1469m AMSL. Drain array 2 on the other hand, consisted of 4 drains drilled at an angle of

approximately 12° from each other, with a length of about 200 meters, and at lower elevation of 1469m AMSL.

Ideally, drains should have been positioned below the lowest elevation (1440m AMSL), however, the shape of the domain was such that it would not permit a proper positioning of the drains to spread effectively. Therefore, the outlet of the watershed was raised to 1470m AMSL, and the drains at 1469m AMSL.

**Figure 16** depicts plan view of the drain configuration on the domain. The model cells are 5m by 5m, and colored with the elevation DEM. Red lines represent the drain placement. (a) shows the drain array 1, and (b) the drain array 2.

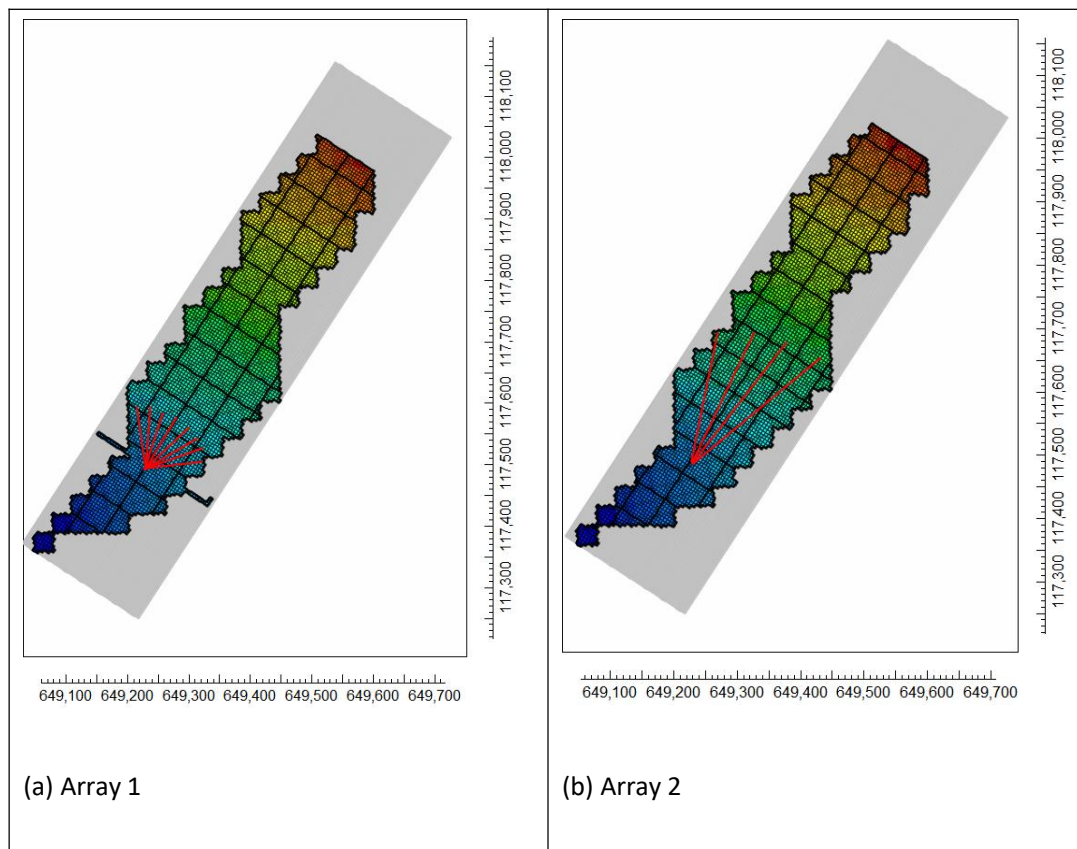


**Figure 16. Plan view of drain configuration.**

### 3.4.2 GEOTECHNICAL ANALYSIS OF THE SLOPE

A prior slope stability analysis was performed in GeoStudio, assuming that the piezometric line was located at the ground surface (total saturation), with strength parameters of both unconsolidated undrained conditions and consolidated and drained conditions. In the UU conditions, the material had a bulk unit weight of 18.97 KN/m<sup>3</sup>, cohesion of 37.03 Kpa, and an angle of friction of 14.07°. In CD conditions, the material had a saturated unit weight of 21.75 KN/m<sup>3</sup> obtained from the calculation below, a cohesion of 4 Kpa, and an angle of friction of 34.2°.

The saturated unit weight was obtained from the porosity (n= 0.284 as calculated for soil storage under section 3.3). First, the void ratio was calculated as:

$$e = \frac{n}{1 - n} = \frac{0.284}{1 - 0.284} = 0.3966$$

**Equation 18** shows the obtention of the saturated unit weight for the slope analysis in consolidated and drained conditions. The saturated unit weight can be calculated when knowing the specific gravity, the unit weight, and the void ration. Thus,

$$\gamma_{sat} = \frac{G_s + e}{1 + e} * \gamma_w$$

**Equation 18. Saturated unit weight**

Where  $G_s$  was the specific gravity taken as 2.7, and  $\gamma_w$  was the unit weight of water equal to 9.81 KN/m<sup>3</sup>. Therefore,

$$\gamma_{sat} = \frac{2.7 + 0.3966}{1 + 3966} * 9.81 = 21.75 \text{KN/m}^3$$

Figure 17 depicts the slip surfaces for both scenarios when assuming that the slope was fully saturated (piezometric line at ground surface). (a) slip surfaces in UU conditions where the factor of safety was 0.351, (b) slip surfaces in CD conditions where the factor of safety was 0.897.

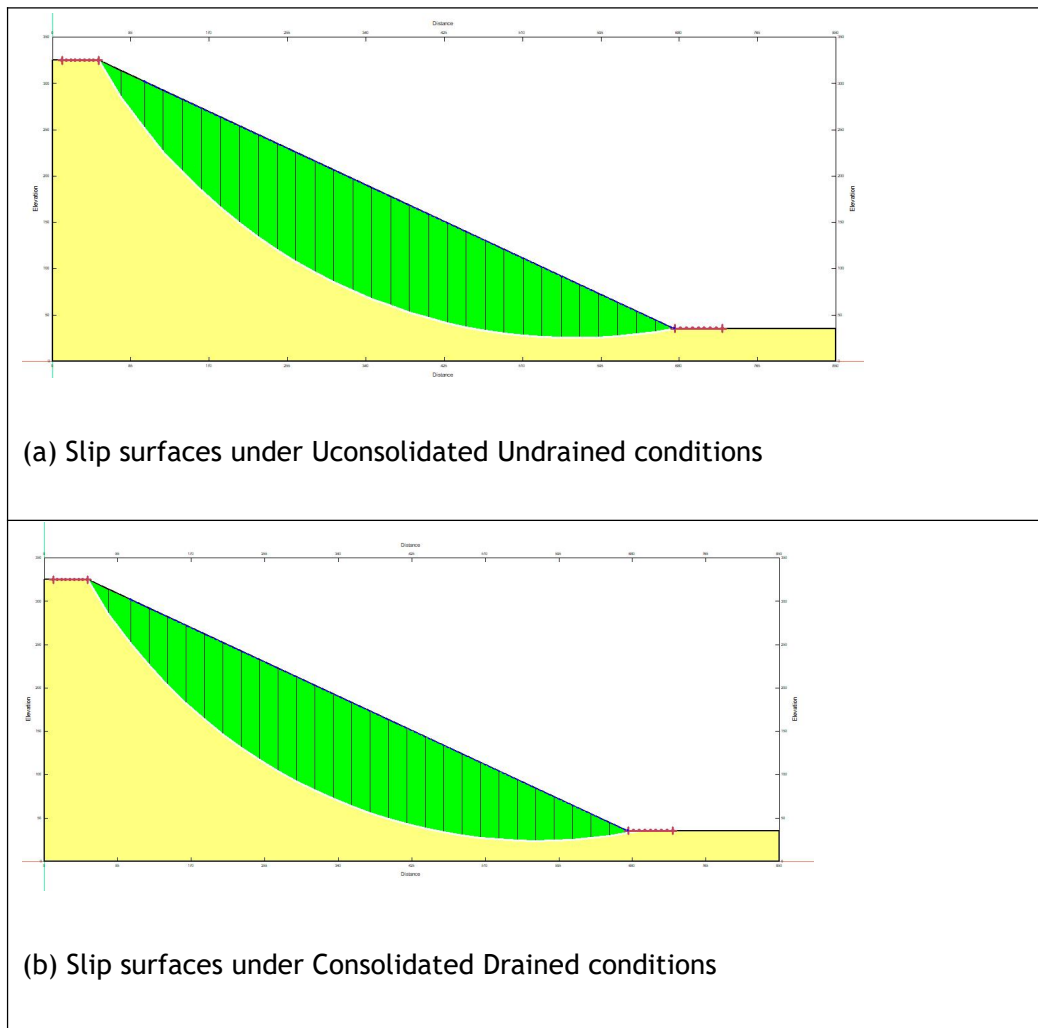


Figure 17. Slope analysis with piezometric line assumed to be at the ground surface.

The slope stability analysis showed that the slope was more prone to failure under unconsolidated and undrained conditions than under consolidated and drained. The following analyses in steady state and transient conditions are discussed in results and discussion.

### 3.4.3 DESIGN OF A DRAIN SECTION

The design of the drains encompasses the determination of the drain dimensions (slot size, drain length and diameter), and spacing, elevation, and the angle of drilling. The drain length and diameter, along with the elevation and angle of drilling, were estimated during the groundwater modelling in MODEL MUSE.

#### 1. SLOT SIZE

As seen in the design considerations in section 2.5, slot sizes are perforations of width ranging from 0.25 to 1.3mm that allow water from the slope to enter the horizontal drain pipe (Cook, D.I., Santi, P.M. and Higgins, J.D. 2008). They are arranged in two longitudinal rows that are spaced 120° apart around the circumference of the pipe. Considering circular slots, the filter requirements were given by:

$$\text{Slot diameter} < D_{85\text{soil}}$$

From the particle size distribution performed in objective one,  $D_{85\text{soil}}$  is the sieve size at which 85 percent of the material passed.

**Figure 18** shows the particle size distribution of the soil, which is observed to be fine-grained. About 87.2% of the total mass passed the 75µm sieve. Therefore the slot size was taken to be the lower limit of the slot range (0.25mm), with care on the geotextile material to prevent clogging.

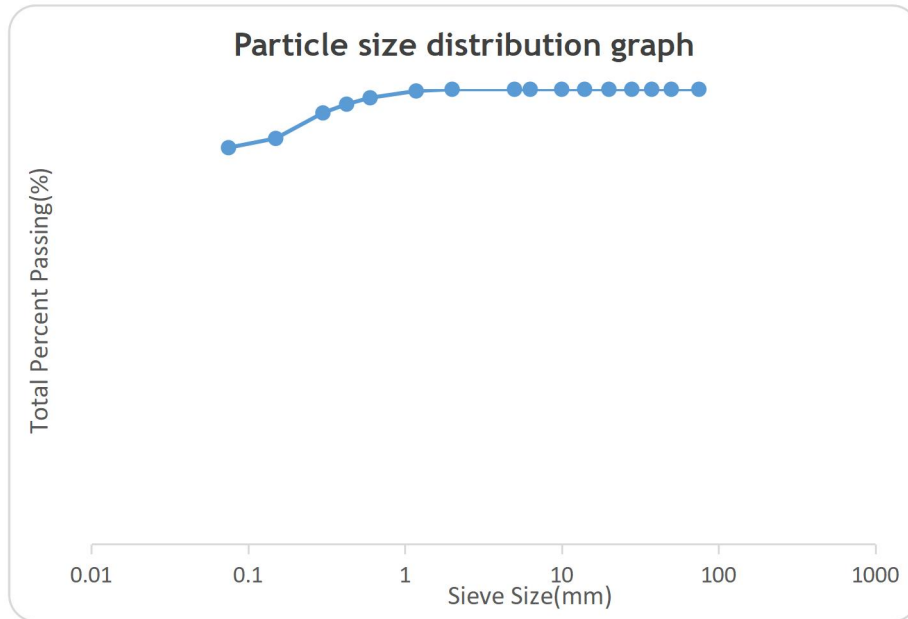


Figure 18. Particle size distribution of the soil sample.

## 2. DRAIN SPACING

The drain spacing was determined from analytical methods, discusses by R. Carrol, T. Badger. 2013. They outline the following steps in order to solve the drain spacing  $L_d$ :

1. Assume the drain depth with respect to peak water level  $H_m^0$ ;
2. Calculate the ratio  $m = \frac{H_m^0}{D}$ , where D is the maximum water table elevation above the impermeable surface;
3. Calculate the y-axis  $\frac{h_m}{H_m^0}$  such that  $h_m$  is the maximum height of water table for which stability of slope is maintained;
4. Find intersection of the calculated  $\frac{h_m}{H_m^0}$  and curve choice m, and trace back to the x-axis to obtain the value of  $\frac{K \cdot D \cdot t}{S_y L_d^2}$ ;
5. Solve for drain spacing  $L_d$  for given value of x-axis  $\frac{K \cdot D \cdot t}{S_y L_d^2}$ .

### Initial assumptions

- i. The time required to sufficiently lower the water table during a large storm was 0.75 days;
- ii. The design storm would force the water table to flood the system such that water rises above the land surface;
- iii. During the storm, water raised at a height of 0.5m above the surface;
- iv. Drains were located at elevation 1440m AMSL;
- v. The impervious surface is at 1436m AMSL.

### Calculations

The hydraulic conductivity and the specific yield were 0.0133 m/day and 0.01 respectively

1.  $D$  was the maximum water table elevation above the impermeable surface. Considering a point at elevation 1445m AMSL. As water raised at a height of 0.5 meters above the surface,  $D$  was obtained as  $[(1445 - 1436) + 0.5]$ , hence 9.5m;
2.  $H_m^0$ : the drains were located at elevation 1440m AMSL, meaning  $[9.5 - (1440 - 1436)]$ , hence 5.5m below the peak water level;
3.  $m = \frac{H_m^0}{D}$  was therefore obtained as 0.57;

4. The maximum water height for which stability of slope is maintained ( $h_m$ ) was considered to be the same as the elevation of the drains (1440m AMSL), hence  $1440 - 1436 = 4$  meters.
5. The value on the y-axis  $\frac{h_m}{H_m^0}$  was therefore obtained as 0.727.
6. The slope had an angle of  $15.5^\circ$ , equivalent to 28.26%. Therefore, graph b was used. From the graph,  $\frac{K*D*t}{S_y L_d^2}$  in the x-axis was obtained as 0.084;
7. Finally,  $L_d$  was solved as  $\sqrt{\frac{K*D*t}{0.084*S_y}} = \sqrt{\frac{0.0133*9.5*0.75}{0.084*0.01}} = \mathbf{10.61m}$ .

**Figure 19** shows the dimensionless curves of maximum water table height with respect to time for slopes of slopes. (a) 10%, (b) 30%, (c) 50%, and (d) 70%. Source: Carrol, T. Badger. 2013. Design Guidelines for Horizontal Drains used for Slope Stabilization.

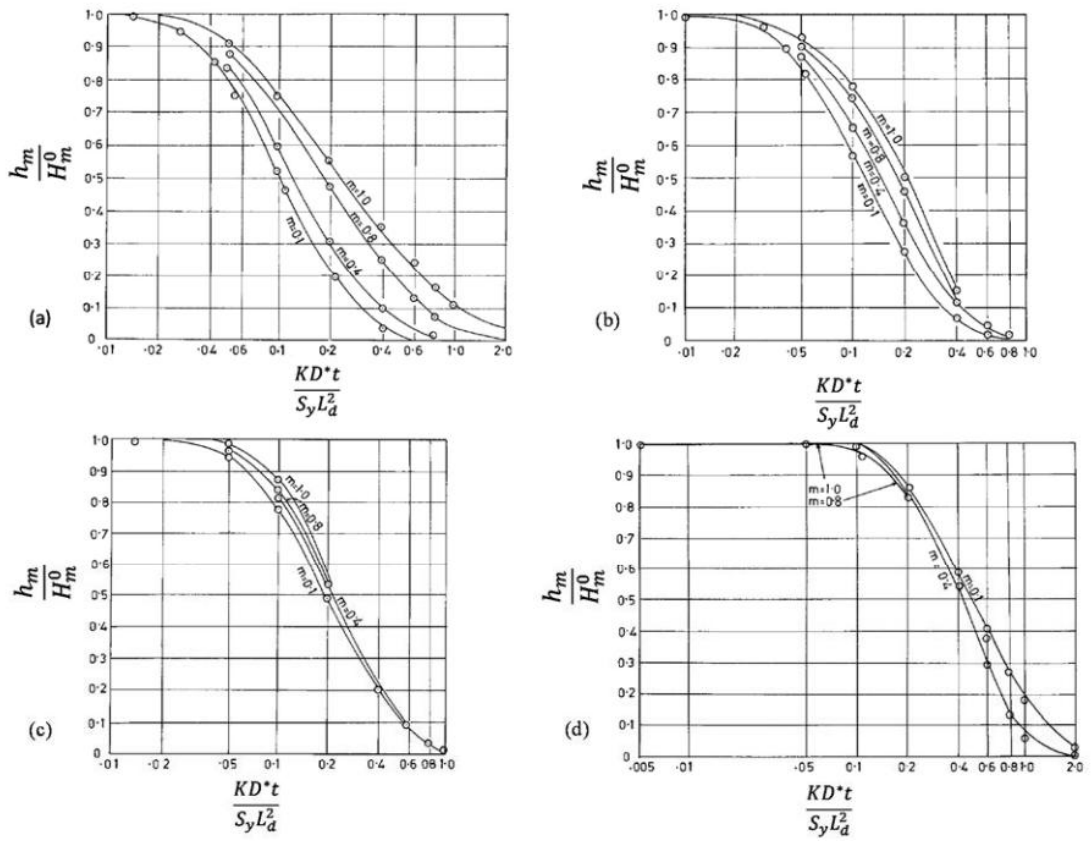


Figure 19. Dimensionless curves of maximum water table height with respect to time for slopes of slopes.

# CHAPTER FOUR: RESULTS AND DISCUSSION

## 4.1 SITE CHARACTERIZATION

### 4.1.1 SITE GEOMETRY

#### 1. ELEVATION

Figure 20 depicts the elevation map of the area of interest. Altitudes were observed to range between 1400 and 1722 meters AMSL.

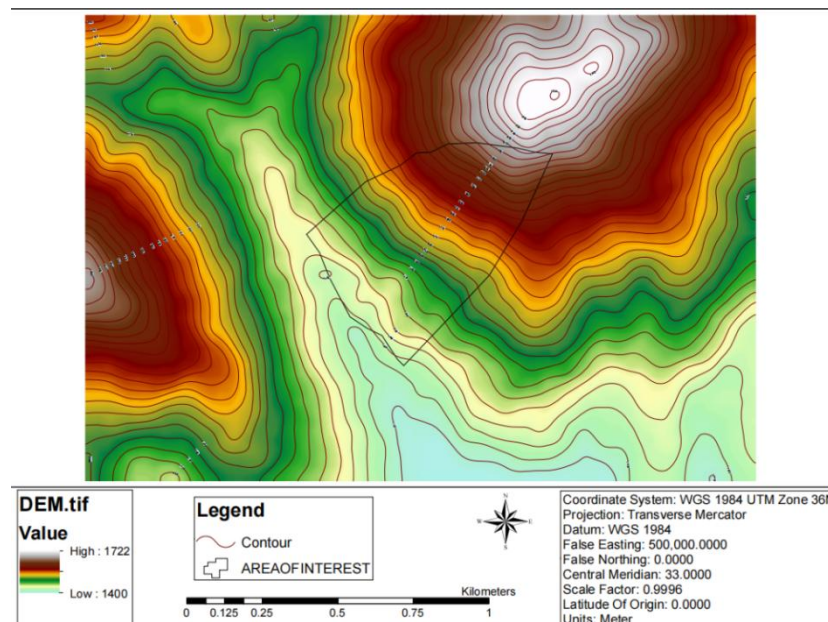
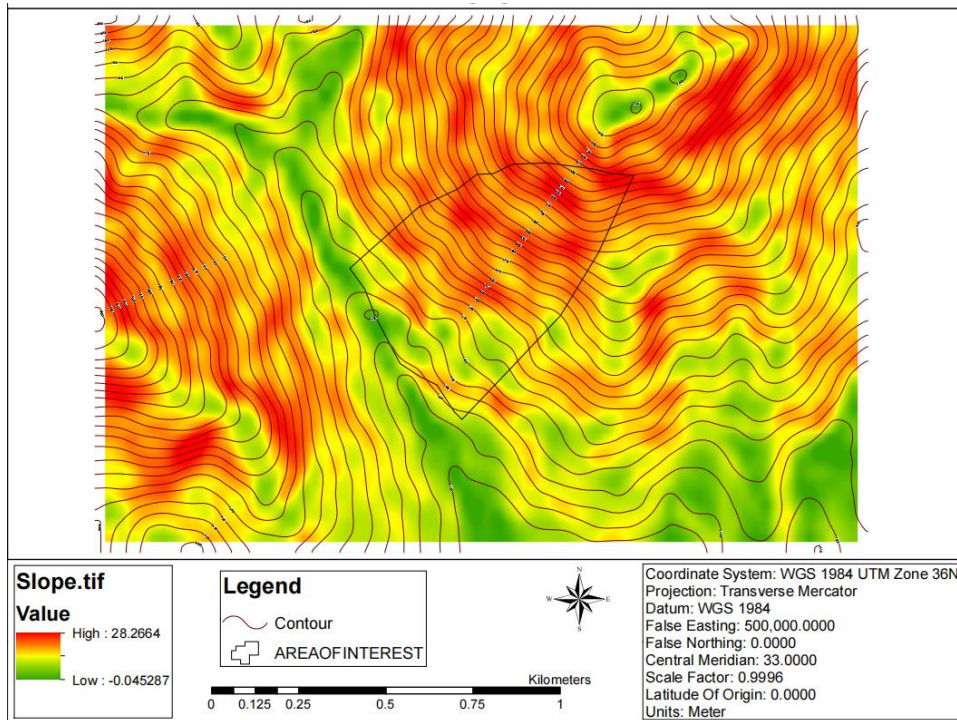


Figure 20. Elevation map

#### 2. ANGLE

In general, the slopes of BUDUDA range between  $14^\circ$  and  $41^\circ$  ( Knapen et. al, 2006).

Figure 21 depicts the angle map. The slopes in the area had a maximum angle value of 28.26%, or  $15.78^\circ$ .



**Figure 21. Angle map**

Sikdar, P K Chakraborty, et al (2004) classify the types of slope according to the slope angle. The slopes were therefore classified as moderate to moderately steep.

**Table 10** shows the slope classification based on the slope angle (°).

**Table 10. Slope classification**

<i>Class</i>	<i>Symbol</i>	<i>Description</i>
0 - 5°	A	Very gentle
5° - 10°	B	Gentle
10° - 15°	C	Moderate
15° - 25°	D	Moderately steep

25° -35°	E	Steep
>35°	F	Very steep

#### 4.1.2 SOIL PROPERTIES

##### 1. ATTERBERG LIMITS

###### a. Atterberg limits values

Atterberg limits depict the behaviour of soils in relation to the water content.

Equation 19 shows the obtention of the shrinkage limit, which is dependant on the Liquid Limit and the Plastic Index.

$$SL = 46.4 * \left( \frac{LL + 45.5}{PI + 46.4} \right) - 43.5$$

*Equation 19. Shrinkage limit*

Where

LL: liquid limit

PI: plastic index

Table.11 summarizes the values obtained for the different Atterberg limits for the sample, where the shrinkage limit was obtained from equation 19.

*Table 11. Atterberg limits values*

PI	PL	LL	SL
19.09	28.98	48.07	22.79

**b. Atterberg limits graph**

Equation 20 shows the obtention of the initial volume of soil, considering the dimensions of the mold for linear shrinkage test, L= 140.2mm and R= 12.5mm.

$$V_{initial} = \frac{1}{2} \pi * R^2 * L$$

*Equation 20. Initial volume of soil for linear shrinkage*

$$V_{initial} = \left(\frac{1}{8} * \pi * 12.5^2 * 140.2\right) = 34410.257 \text{mm}^3$$

i. The volume of soil at shrinkage limit (22.79%) was obtained from

$$V_{SL} = 0.5\pi(12.5)^2(140.2)[1 - 0.228] = 26564.72 \text{ mm}^3$$

Considering the linear relationship between the water content and the volume of soil, the volume at plastic limit and liquid limit was obtained as follows:

ii. The volume at plastic limit (soil + water)

$$V_{PL} = \frac{[100\% + (28.98 - 22.79)\%] \times 26564.72}{100\%} = 28185.17 \text{mm}^3$$

iii. The volume at liquid limit (soil + water)

$$V_{LL} = \frac{[100\% + (48.07 - 22.79)\%] \times 26564.72}{100\%} = 33285.60 \text{mm}^3$$

**Figure 22** depicts the Atterberg Limits graph which volumes at the different limits were obtained from the calculation above.

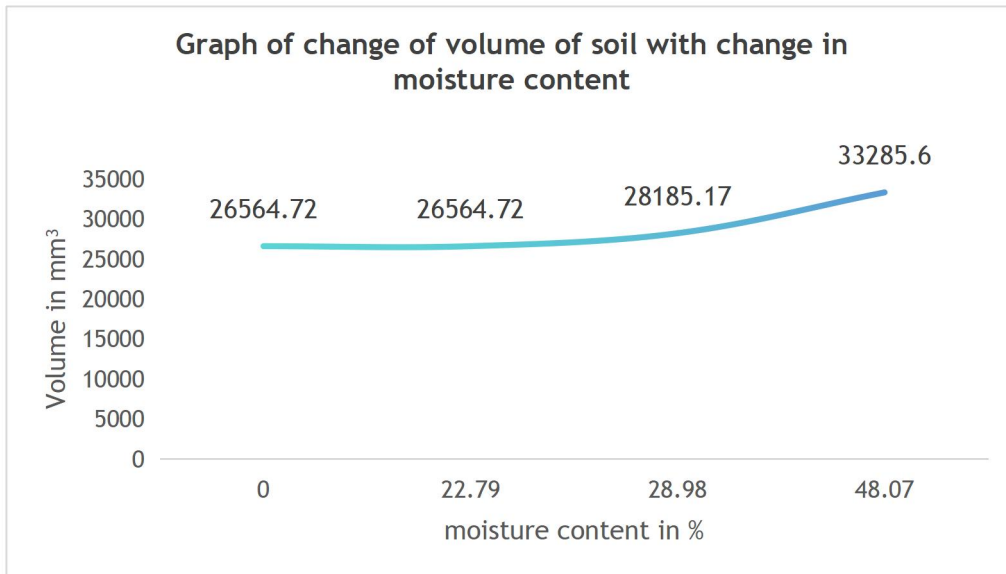


**Figure 22. Atterberg limit graph**

## 2. SOIL CLASSIFICATION

The soil classification followed the Unified Soil Classification Standard (USCS), which classifies the soil according to a prefix and a suffix. For this, the total mass sieved, along with the mass retained at the 75µm and the Atterberg limits should be known.

**Table 12** shows the results of the key parameters for the USCS classification.

**Table 12. Key parameters for soil classification**

Total mass sieved	Mass retained at 75µm sieve	PI	LL
143.11	15.11	19.09	48.07

### a. PREFIX

The prefix is relative to the texture of the soil sample, which can be coarse grained, fine grained, or organic soils. This is determined by the amount of

particles retained at the 75µm sieve. In this case, less than 50% was retained on the sieve of interest for the three samples, hence the soil is considered to be fine grained.

Fine grained soils can either be classified as inorganic clay, or silt\organic clay. In this case, the average plastic index (PI) was as high as 19.09, which was above the A line and greater than 7. The soil was considered as inorganic clay, hence the prefix C.

#### **b. SUFFIX**

For fine grained soils, the suffix is relative to the plasticity, which can be considered as low if the liquid limit is less than 50%, or high if it is greater than 50%. In this case, the average liquid limit was as high as 48.07, which was relatively high, hence the extensive use of the suffix H.

#### **c. OVERALL CLASSIFICATION**

The soil was classified as CH, which is consistent with the study by Poesen and Deckers, 2009, who classified the soil in the same region as CH, with the prevalence of Nistisols in the western zone of the district. Nistisols are characterized by a high clay content, significant shrink-swell capacity, and a poor drainage.

### 3. UNIT WEIGHT

1. The bulk unit weight was obtained from the bulk density test performed in the sample preparation of the falling head permeability test, with an average value of  $1.934 \text{ gcm}^{-3}$ .

**Equation 21** shows the obtention of the bulk unit weight from the bulk density ( $\rho$ ) and the gravity ( $g$ ).

$$\gamma = \rho * \frac{g}{100}$$

*Equation 21. Bulk unit weight*

Where

$$\rho (\text{kgm}^{-3}) = 1.934 \text{ gcm}^{-3} * 1000$$

$$g = 9.81 \text{ ms}^{-2}$$

$$\gamma = 1.934 * 1000 * \frac{9.81}{1000} = \mathbf{18.97 \text{ kNm}^{-3}}$$

The unit weight of  $18.97 \text{ kNm}^{-3}$  is within the range of clay soil which is between 16 and  $22 \text{ kNm}^{-3}$ .

2. The specific gravity on the other hand, was obtained from the specific gravity test. The first and third samples had identical specific gravity values, which were within the typical range for clay and similar cohesive soils (2.60-2.75). The value of 2.61 was consistent with standard values for cohesive soils like clay, indicating that these two samples are likely dense and mineralogically stable, as there was a relatively low organic matter content (Mulatu Tamiru, Worku Firomsa Kabeta, et al. 2024).

#### 4. COEFFICIENT OF PERMEABILITY

The average coefficient of permeability (K) was found to be  $1.545 \times 10^{-7}$  m/s, while the average infiltration rate was as high as 27.3cm\hour, which is considered to be in the category of very rapid according to Poesen and Deckers, 2009. The falling head permeability test was repeated three times on the three samples, enabling to determine a relationship between the soil saturation, the infiltration rate, and the time.

The infiltration rate was observed to decrease as with the cumulative experimentation. This suggested a tenancy of accumulation of water in the soil profile as the soil reaches saturation as explained by Makabayi, Musinguzi and Otukey, 2021b.

**FIG 23** depicts the graph of cumulative infiltration, which is observed to gradually decrease.

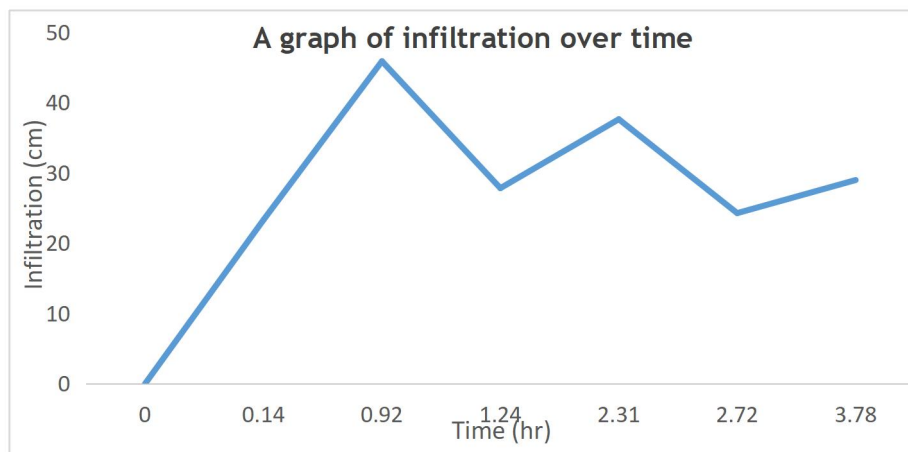


**Figure 23.** Infiltration rate graph

## 5. COHESION AND ANGLE OF FRICTION

### *a. Unconsolidated undrained conditions*

The soil samples underwent barreling which is a kind of distortion where the specimen became wider in the middle and narrower at the ends resembling the shape of a barrel.

The average cohesion value was within the range for cohesive soils such as clay (10 Kpa-100 Kpa) according to BS 1377 Part 7. The friction angle on the other hand, was low, also characteristic for clay, where the internal friction angle tends to be smaller ( $10^{\circ}$  to  $20^{\circ}$ ) compared to granular materials such as sands.

Considering the fact that the test was undrained, these values of effective stress reflect the initial effective stress (taking pore pressure into account).

### **b. Consolidated and drained conditions**

Table 16 depicts the findings of the direct shear box test. The low value of cohesion (4 Kpa) indicates that the soil had a lower inherent resistance to shear forces when pore water pressures were not a factor. The high angle of friction on the other hand, showed that the soil had a greater resistance to shear forces when pore water pressures were dissipated (ABG. No date).

## 4.2 STUDY OF THE HYDROLOGY

### 4.2.1 WATERSHED DELINEATION

The Watershed of river TSUTSU was delineated using QGIS, then further sub divided into three main sub catchment.

**Figure 24** illustrates the watershed delineation map for river TSUTSU. It comprised 3 main sub catchment, where the fourth was the extent of the slope of interest.

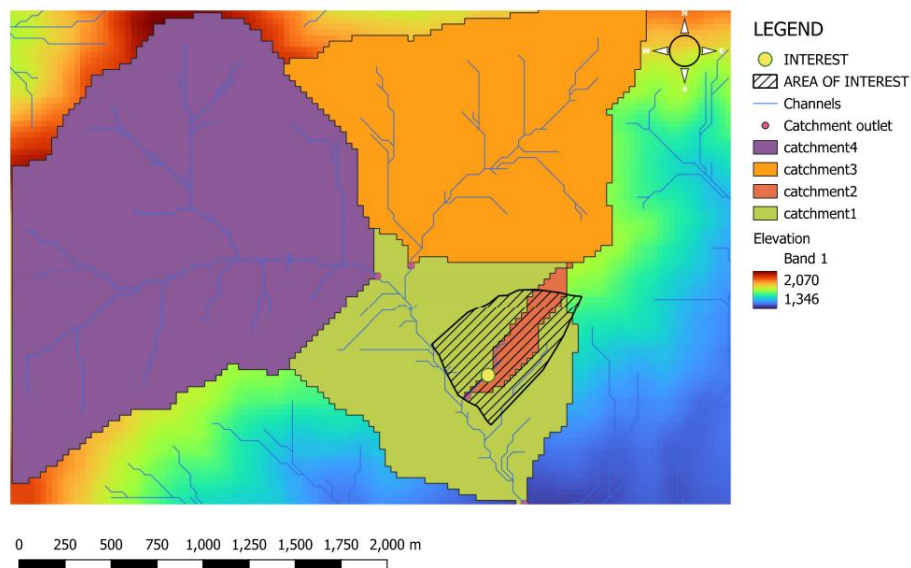


*Figure 24. Watershed delineation map*

**Table 14** summarizes the characteristics of the 3 main sub catchments.

*Table 13. Characteristics of sub catchments*

Sub catchment	Surface area (Km <sup>2</sup> )	Longest river path (Km)	Slope ( $\frac{m}{m}$ )
1	1.5	1611	0.033
2	1.9	3410.236	0.1

3	3.3	3999.615	0.093
---	-----	----------	-------

#### 4.2.2 RAINFALL

##### 1. *MONTHLY RAINFALL PATTERN*

The sum of monthly rainfall was computed to determine the rainfall trend throughout the year. October was found to be the month with the highest rainfall value whereas January was the month with the lowest value.

The amount of rainfall has a considerable influence on the moisture content and pore water pressure in soils. It has been observed that landslides are more likely to occur if high amounts of intense precipitation are preceded by a period of light yet incessant precipitation. In fact, saturation of soils needs a much longer period. This explains why there are more landslides recorded in the last quarter of the year than in the middle, where the high rainfall is first absorbed by dry soils, and towards September, the soil becomes saturated resulting in higher chances of slope failure (Kitutu et al, 2010).

**Figure 25** shows the graph for the average monthly rainfall, which October having the highest value (125364.24 mm), followed by August (125168.64 mm) and April (124452.38 mm).

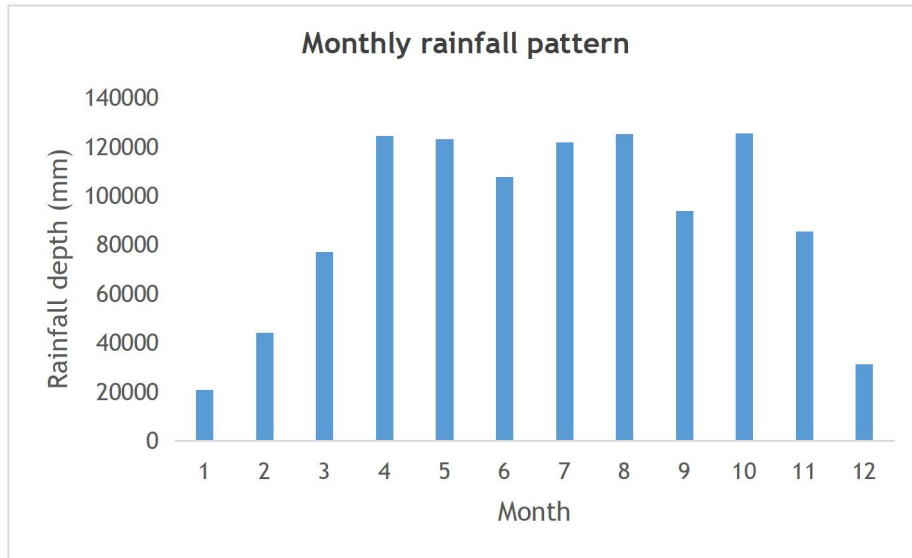


**Figure 25. Monthly rainfall pattern**

## 2. YEARLY RAINFALL INTENSITY

### a. The yearly rainfall intensity

The highest magnitudes were observed in 2010 and 2011 with values as high as 132.992mm/year and 142.01mm/year respectively.

Scientists have observed a relation between the increase in rainfall pattern in Eastern Africa, and the El Niño phenomenon, which refers to the oscillation of the ocean-atmosphere system in the tropical Pacific having important consequences worldwide. For example, 27 landslides were recorded in 1997, corresponding to a year of strong El Niño (Kitutu et al, 2010).

In the year 2010-2011, a significant El Niño episode was observed in the tropical Pacific Ocean, with effects extending into adjacent ocean basins. For this time period, the atmospheric indicators showed that the episode

was one of the strongest in the previous century, while oceanic indicators were at moderate to strong levels. This conditions continued through the first quarter of 2011 (World Meteorological Organization, 2011). This explains the high yearly intensity observed, where 2010 corresponds to the year of occurrence of the Nametsi landslide, the deadliest on record in the district (Nantumbwe, Bob R. Nakileza et al. 2017).

**Figure 26** illustrates the graph for yearly rainfall intensity, which was observed to be related to global meteorological phenomena such as the El Niño.

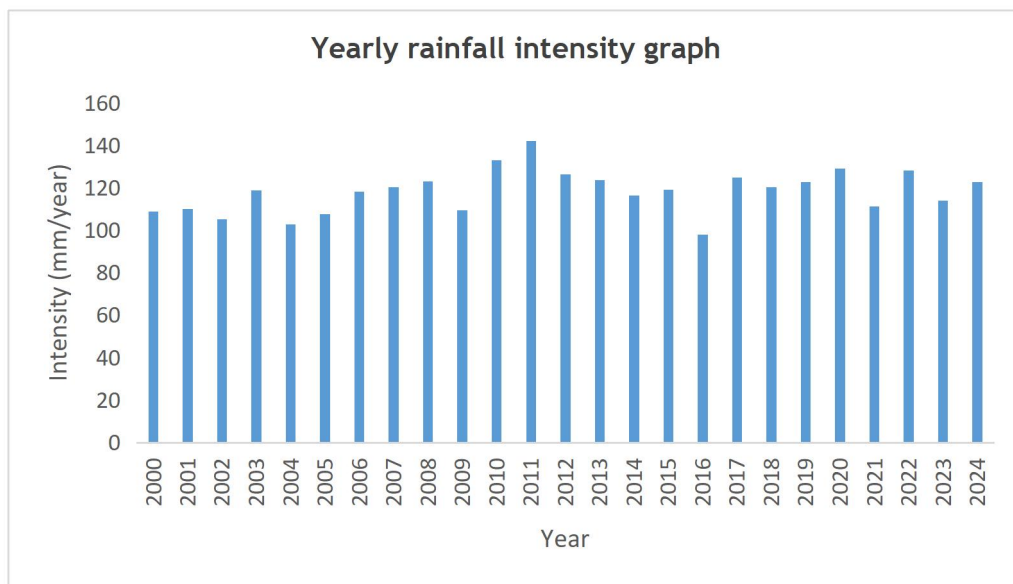


**Figure 26.** Yearly rainfall intensity

b. The maximum yearly daily rainfall intensity

The maximum daily rainfall intensity was observed in 2007, with a value of 1330.96mm.

**Figure 27** illustrates the graph for maximum yearly daily rainfall intensity.

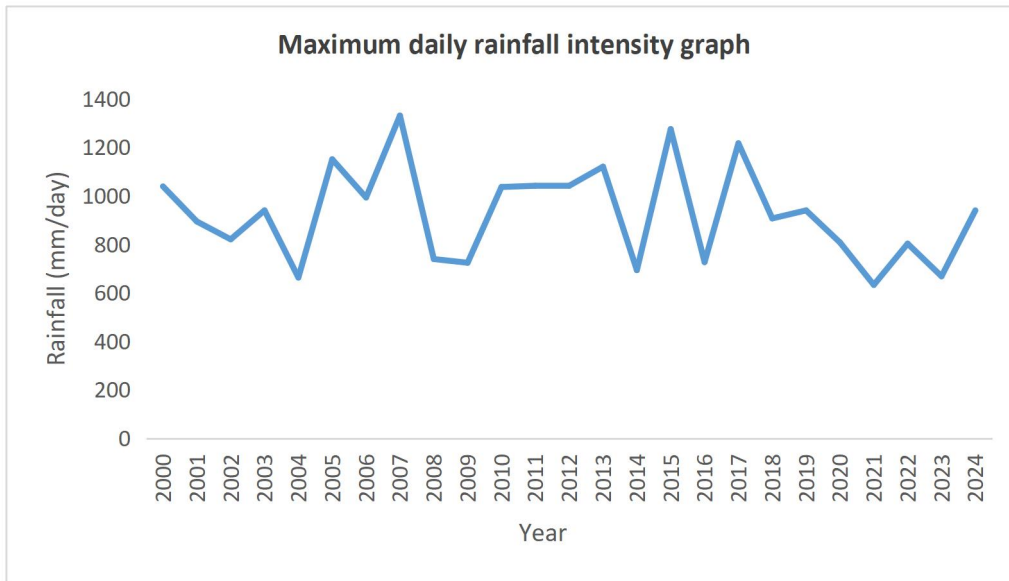


**Figure 27. Maximum daily rainfall intensity chart**

c. The average daily rainfall intensity on rainy days

This analysis only considered the rainy days count for every year. It was observed that 2011 held the highest value with 239.971mm/day, for the same reasons stated above.

**Figure 28** shows the graph for average yearly daily rainfall intensity on rainy days.

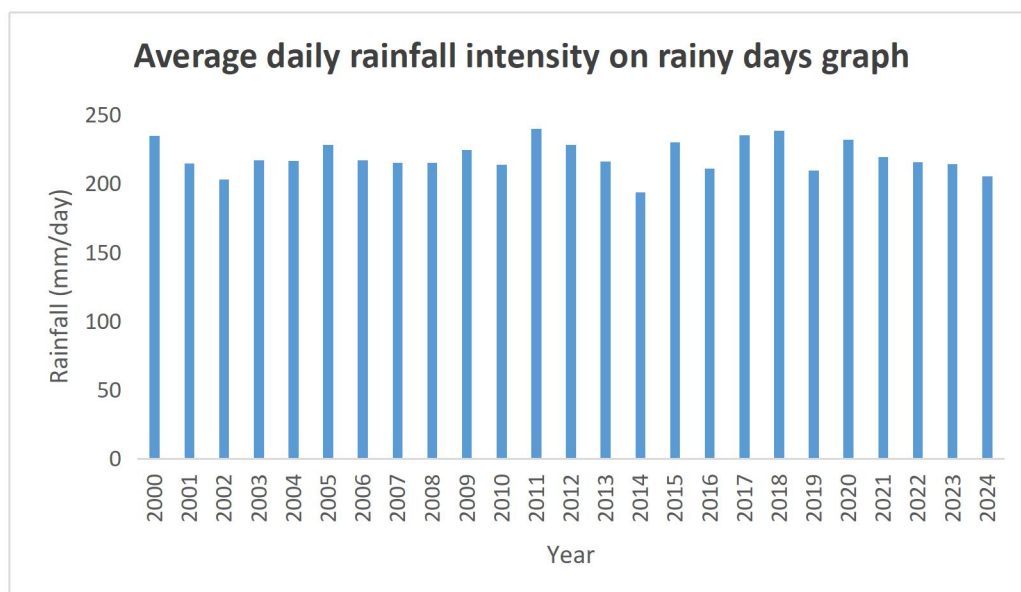


Figure 28. Average daily rainfall intensity on rainy days

### 3. RAINFALL RETURN PERIOD

The return time period is an average recurrence interval that gives an insight on the occurrence of a particular rainfall magnitude. However, the 25-years rainfall dataset obtained was relatively short for long-term rainfall analyses since usually, 100-years or 1000-years rainfall datasets are used for rainfall return time estimations (M. Amoakowaash, L. Kofiste, A. Omari-sasu et al. 2021).

Figure 29 Shows the graph of the return period against the maximum yearly rainfall values.

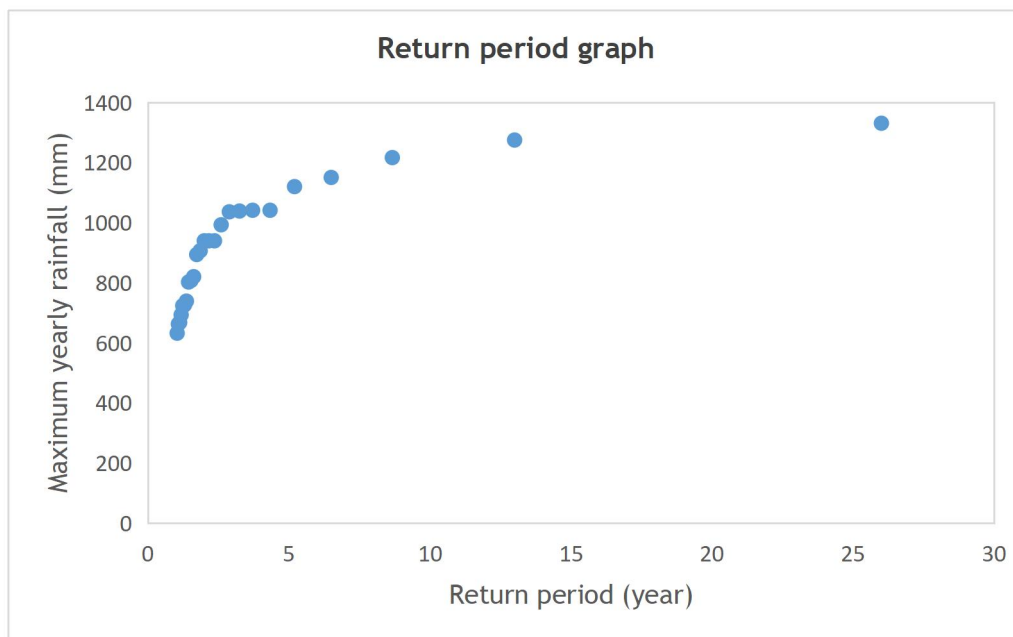


Figure 29. Return period graph

#### a. High rainfall events

The highest recorded rainfall event was 1330.96mm in 2007 and ranked as 1.

This event has a calculated return period of 26 years. The exceedance probability for this event is approximately 0.038 or 3.8%, meaning that the change of this rainfall being exceeded in any given year is 3.8%.

b. Lower rainfall events

Lower rainfall events have shorter return periods and higher exceedance probability. For example, the rainfall of 632.46mm in 2014 (rank 22) has a return period of approximately 1.18 years and an exceedance probability of about 0.85 or 85%, implying that the rainfall of this magnitude is relatively common.

#### **4.2.3 MODEL RESULTS**

##### **1. WATER LOSSES**

In a watershed system, it is not all the rainfall received over the area that is considered as the recharge (R. Carrol, T. Badger. 2013). In fact, as previously seen in FIG 11, the precipitation that fall on the land is either intercepted by the vegetation, lost as a surface run-off, infiltrates into the ground, or is taken back into the atmosphere as evapo-transpiration. Therefore, the portion that infiltrates the ground is very essential, as it is the one that recharges the groundwater. Following the stated reason, the purpose of modelling was to determine the amount of rainfall being lost in the watershed through infiltration. Infiltration made the largest portion, with a value of 67.47%. This had a relation with the characteristics of the

soil, where the infiltration rate was found to be as high as 27.03 cm/hour, as well as the absence of imperious surfaces. The run-off was equally high, provided the moderate slope of 15.5°. The evapo-transpiration portion on the other hand, was the smallest portion of the loss. This could be due to the fact that the model run for only 24 hours, where the rainy weather did not provide adequate conditions for the sun to shine for long enough to cause considerable evapo-transpiration.

**Table 15** summarizes the result of the water loss breakdown. Infiltration constituted the largest portion, with a value of 67.47%.

*Table 14. Water losses in the watershed.*

Loss	Milimeters	Percentage
Infiltration	492.9	67.47
Surface	191.25	26.18
Capony	42.8	5.86
Evapo-Transpiration	3.57	0.49

## **2. INFILTRATION**

The infiltration rate was observed to gradually increase, attaining its peak value within six hours, before gradually decreasing and stabilizing after saturation of the soil. This behaviour is similar to the one observed during the falling head permeability test, where the infiltration was observed to rapidly attain a peak value before decreasing with time. This strongly

suggested a tendency of water storage in the soil profile, as highlighted by (Makabayi, Musinguzi and Otukey, 2021a).

**Figure 30** shows the infiltration rate graph plotted by HEC-HMS.

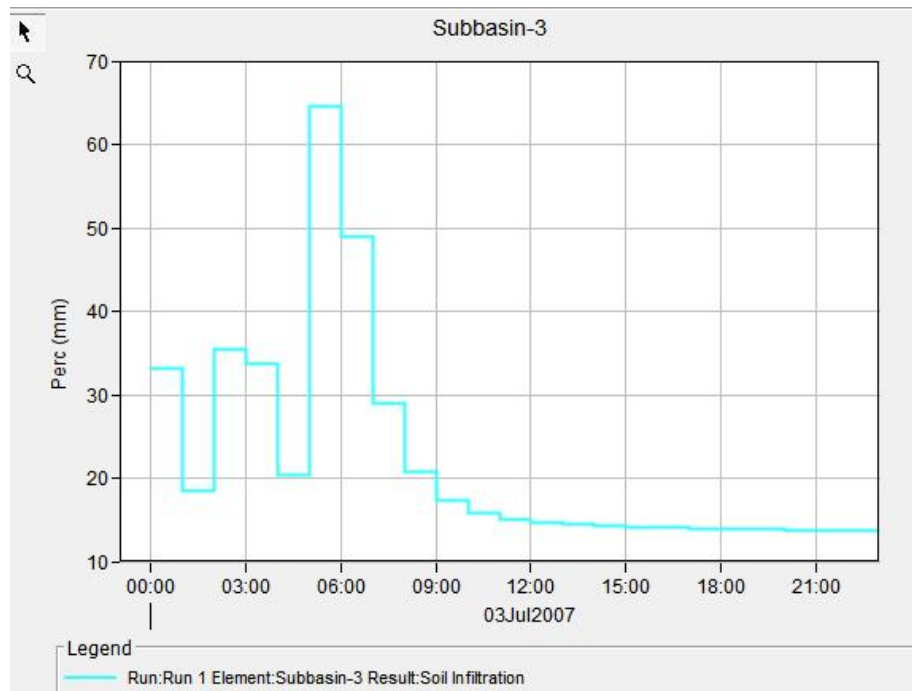


**Figure 30.** Infiltration rate graph for sub basin 3

## 4.3 DESIGN OF THE HORIZONTAL SUB DRAINAGE SYSTEM

### 4.3.1 INFLUENCE OF SUB DRAINAGE SYSTEM ON THE SLOPE STABILITY

#### *a. Influence of coefficient of permeability on the groundwater flow*

To determine the influence of coefficient of permeability on the groundwater flow, a steady state analysis was run with increased values of  $K_x$ . When the  $K_x$  was increased to 0.133 m/d and 1.33 m/d respectively, the groundwater table was observed to stabilize at lower depths than when  $K_x$  was 0.0133 m/d, where the system was flooded. This is because the low

permeability did not allow water to flow quickly through the soil profile. Rather, water accumulated, causing flooding, even at lower recharge value of 0.002 m/d.

**Figure 31** depicts the profile of the slope with the water table level after a steady state run with recharge equal to 0.002 m/day. (a) shows the piezometric line (black horizontal line) when  $K_x$  was equal to 0.133 m/day, and (b) shows the piezometric line (black horizontal line) when  $K_x$  was equal to 1.33 m/day. However, the profile with  $K_x$  equal is not shown since the system was entirely flooded.

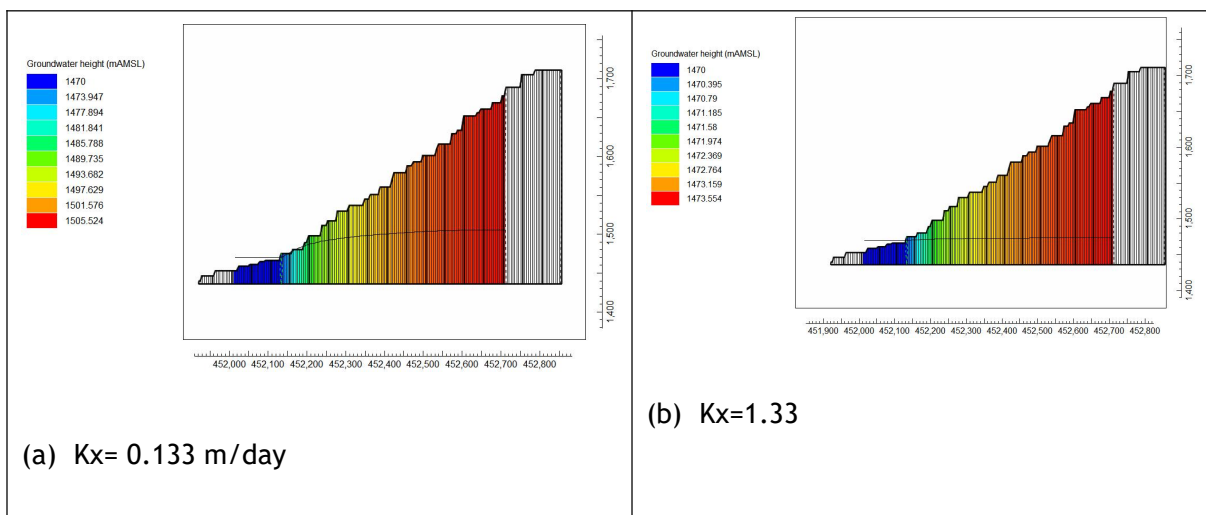


**Figure 31. Influence of  $K_x$  on the groundwater flow.**

**b. Influence of drain configuration on the groundwater flow**

**i. Steady state condiditons**

A steady state condition was run prior to the transient situation with the 25years 24-hours rainfall event, where the recharge was taken to be 0.002 m/d. Considering  $K_x = 0.0133$  m/day, and isotropy in the layer ( $K$  was the same in all 3 dimensions). As mentioned in section 3.4.1 (3), the outlet of

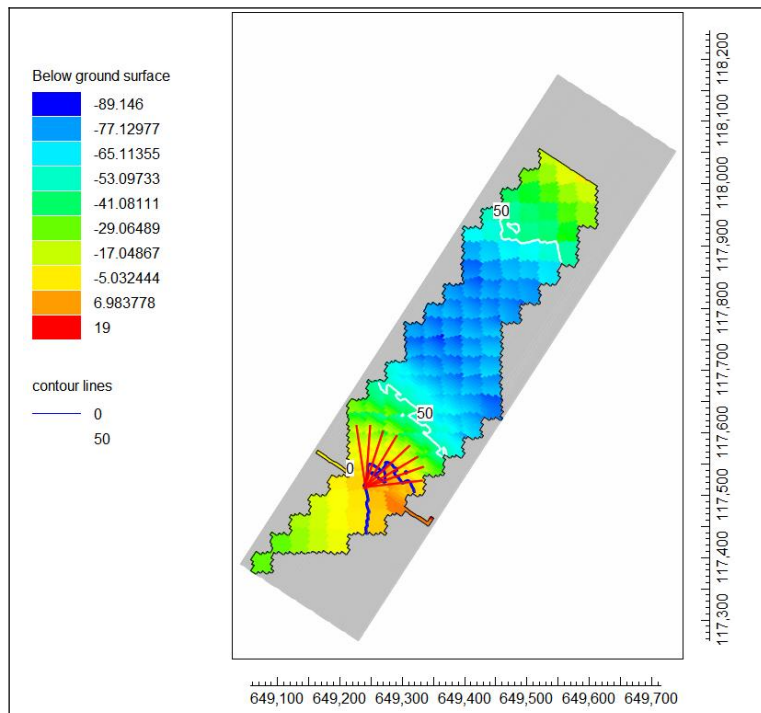
the watershed along with the drain elevation were raised to a higher elevation (from 1440m to 1469m) for design purposes, considering the irregular shape of the watershed that prevented an adequate positioning of drains downstream. Therefore, results below the elevation of the drain were ignored, and the drains assumed to be at the lowest elevation.

To interpret the results, a dataset was created, where the value of each cell was equal to the difference between the top elevation of the cell, and the groundwater head. This helped determine whether the sub drainage system was efficiently preventing flooding by maintaining the groundwater level below the ground surface.

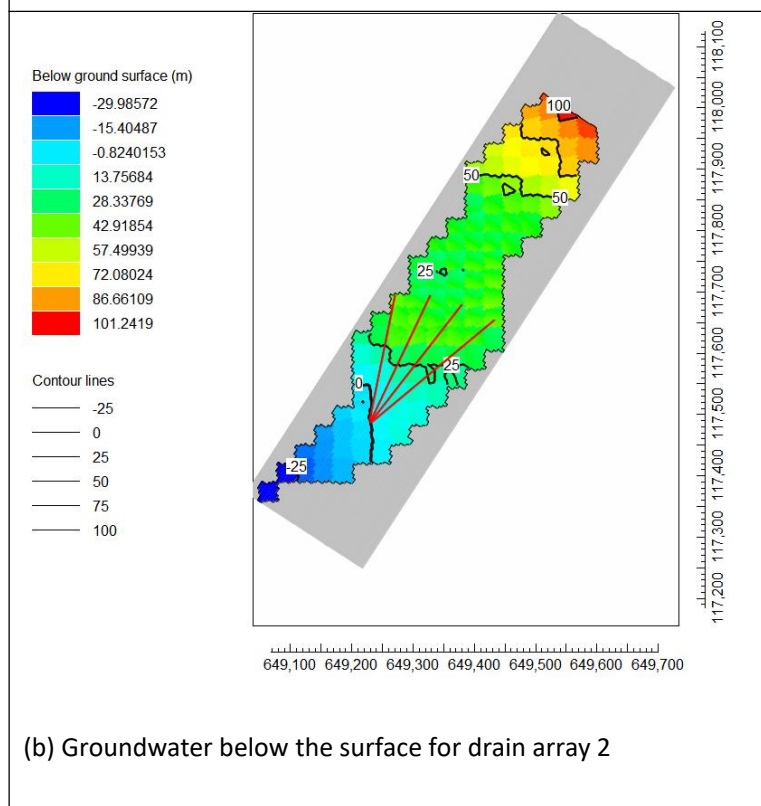
Drain array 1 was observed not to decrease the flooding when there was no drain, however not sufficiently enough for water to remain below the ground surface. Drain array 2 on the other hand, was able to decrease the flooding, and to maintain the groundwater level below the surface throughout the whole extent of the model domain.

**Figure 32** shows the plan view of the model domain. the grid cells are 5m by 5m, and coloured in accordance with the dataset specification, for instance the difference between the cell top elevation and the groundwater head. Positive values indicate that the groundwater was below the ground surface (ground surface elevation > gw head), while negative values indicate that the groundwater was above the ground surface (ground surface elevation < gw head, thus flooding). (a) is the result for drain array 1, and

(b) the result for drain array 2.



(a) Groundwater below the ground surface with drain array 1



(b) Groundwater below the surface for drain array 2

Figure 32. Plan view for steady state conditions.

Figure 33 shows the slope profile after the steady state simulation. (a) shows the piezometric line (horizontal black line) with drain array 1, which was found not effective at maintaining the groundwater below the ground surface, and (b) shows the piezometric line (horizontal black line) with drain array 2, which efficiently maintained the groundwater level below the ground surface.

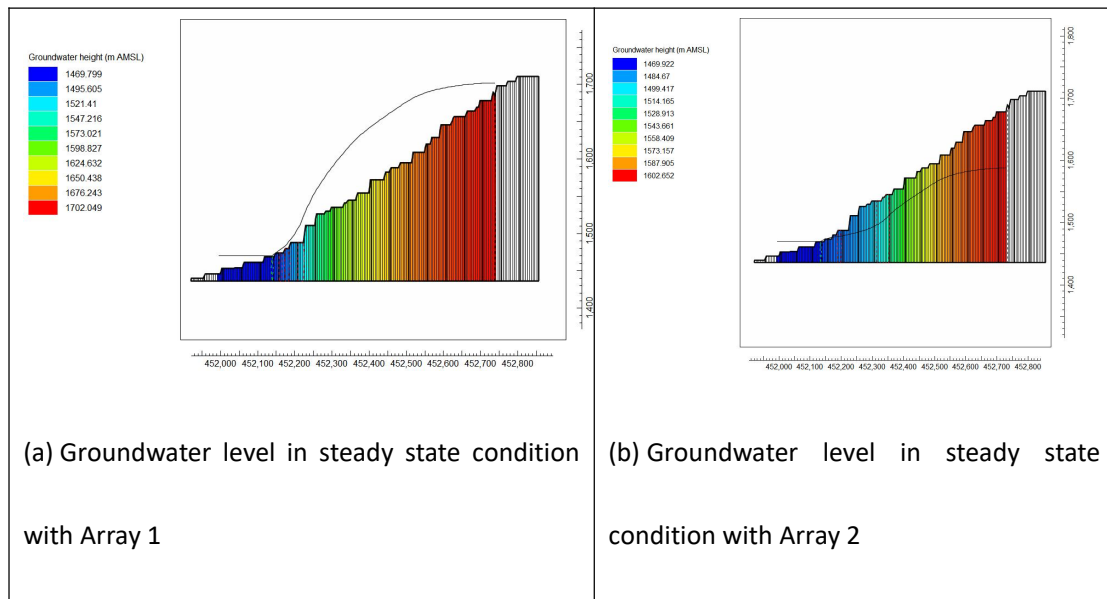


Figure 33. Piezometric line for steady state conditions.

$Kx=0.0133$ ,  $VKA=1$ ,  $sy=0.001$ ,  $recharge= 0.002m/d$ . (a) with drain array 1, and (b) with drain array (2).

## ii. Transient conditions

The transient condition was simulated with the 25years 24-hours rainfall event. The 24-hours event was divided into 24 stress periods of 0.0417 day each. The model time had a total of 25 stress periods, where the first stress period corresponded to the steady state simulation of duration 1day. The hydrological conditions are still the same, for instance,  $Kx= 0.0133$  m:day,

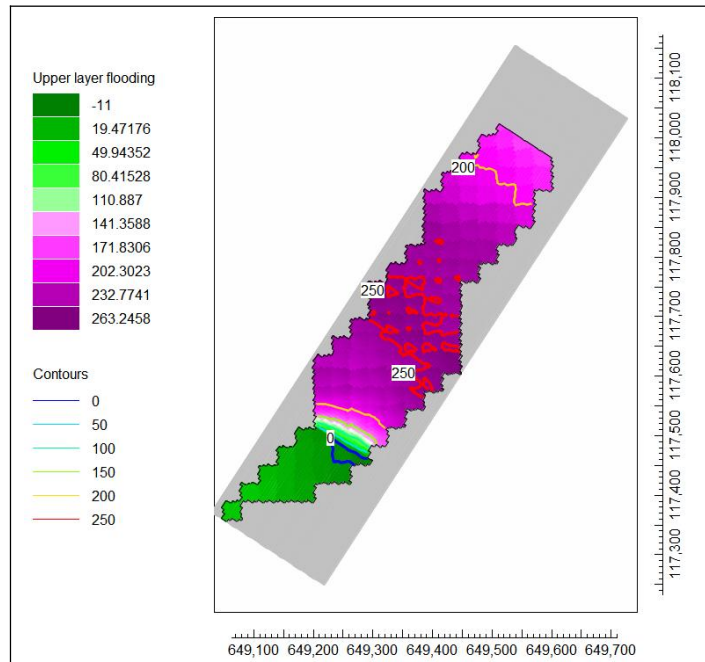
and  $VKA = 1$ . The following results are for stress period 23, which had a maximum recharge of 0.059 m/day.

To visualize the results, a dataset was created to observe the flooding of the domain. This is because flooding was expected by increasing the water influx in the system. Therefore, the goal was to check if the drain was efficient at decreasing the risk of water rising beyond the ground surface.

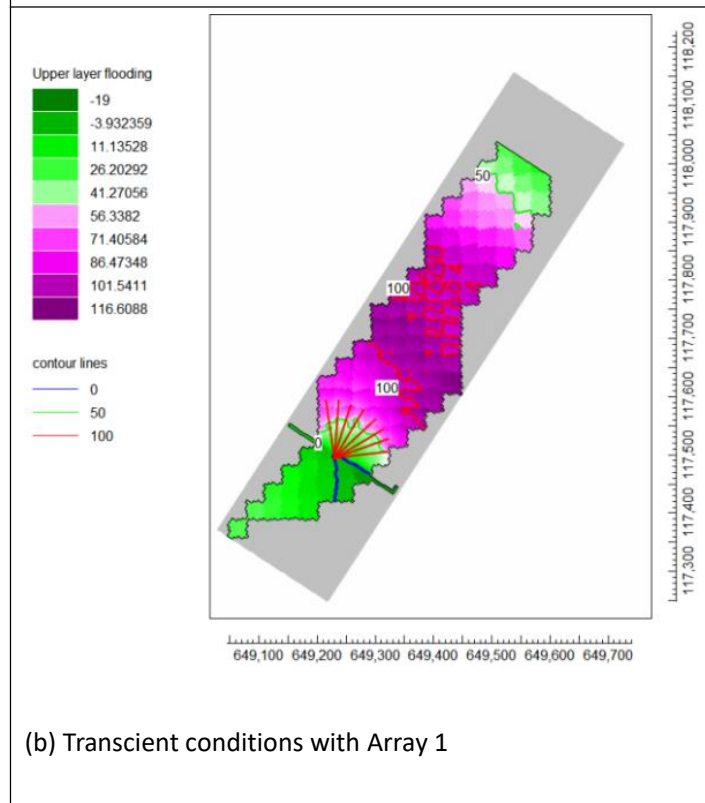
With drain array 1, the entire system remained flooded, implying that it was not efficient at decreasing the risk of flooding. Drain array 2 on the other hand, successfully mitigated the flooding risk upstream, however, it was not able to remove water above surface at the watershed outlet.

**Figure 34** depicts the plan view of the model domain after the transient simulation. The grid cell size is 5m by 5m, and the cells are coloured with respect to the dataset specifications, for instance, the difference between the groundwater head, and the cell top elevation. This implies that positive values indicated flooding ( $gw \text{ head} > \text{ground surface elevation}$ ), while negative values indicated that the groundwater was below the ground surface ( $gw \text{ head} < \text{ground surface elevation}$ ). (a) shows the domain without drains incorporated. The system was expected to be severely flooded from the slope tip to the outlet. (b) shows the domain with array 1 incorporated. It was observed to decrease the severity of the flooding, however, not enough to bring groundwater level below the ground surface. (c) show the domain with drain array 2 incorporated. It was observed to efficiently

mitigate flooding upstream, however, was not able to remove the water at the watershed outlet.



(a) Transient conditions without drains



(b) Transient conditions with Array 1

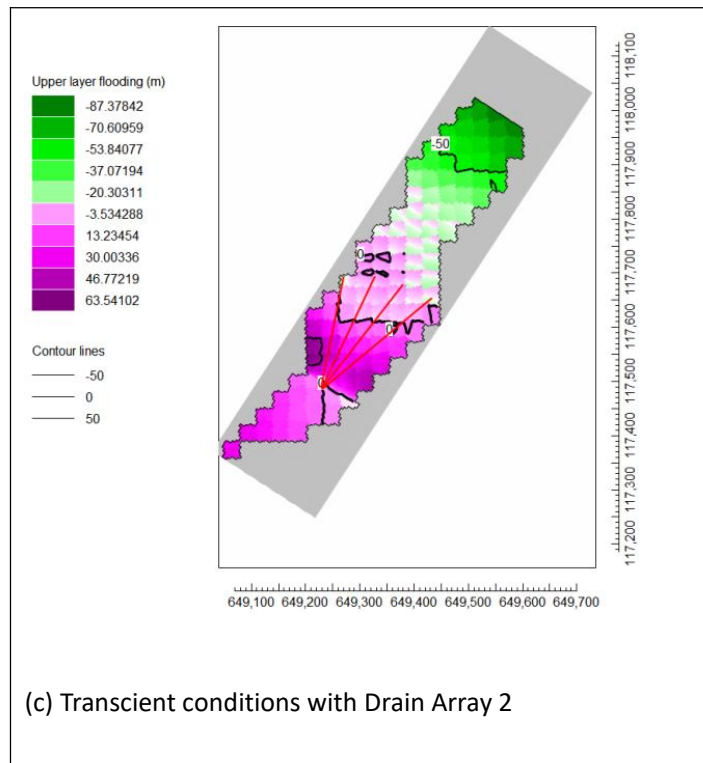


**Figure 34.** Upper layer flooding (m AMSL) in stress period 23 of the 25 year 24-hour precipitation event.

**c. Improvements to drain array 1**

From the above discussion, it was seen that drain array 2 was more efficient than drain array 1. However in practical sense, it would be hard to install horizontal drains 200 meters long. Therefore, an improvement was brought to the first configuration to check if it would improve the efficiency of the system. An additional array of four drains of about 90 meters, drilled at an angle of 10° from one another, and at an elevation of 1537m AMSL was therefore incorporated.

**Figure 35** shows the plan view of the drain configuration on the domain. The model cells are 5m by 5m, and colored with the elevation DEM. Red lines represent the drain placement. Drain array 1 is located at 1469m AMSL,

and the additional array is located at 1537m AMSL.

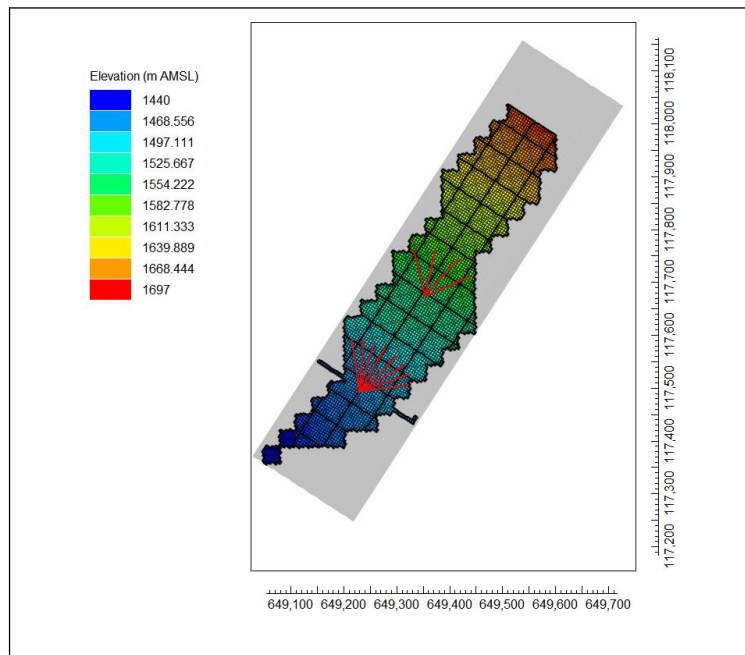


**Figure 35. Improved drain configuration**

i. Steady state conditions

Considering the same simulation conditions as used before, for instance  $K_x = 0.0133$  m/day,  $VKA = 1$ , and  $recharge = 0.002$  m/day, the new configuration was observed to have significantly decreased the risk of flooding. However, water was still above the ground surface between location of the two drain arrays.

**Figure 36:** (a) plan view of the model domain. the grid cells are 5m by 5m, and coloured in accordance with the dataset specification, for instance the difference between the cell top elevation and the groundwater head. Positive values indicate that the groundwater was below the ground surface (ground surface elevation > gw head), while negative values indicate that the groundwater was above the ground surface (ground surface elevation <

gw head, thus flooding). Flooded was only observed to occur between the location of the two drain arrays. (b) shows the piezometric line (horizontal black line), which was observed to be lower than before with only drain array 1.

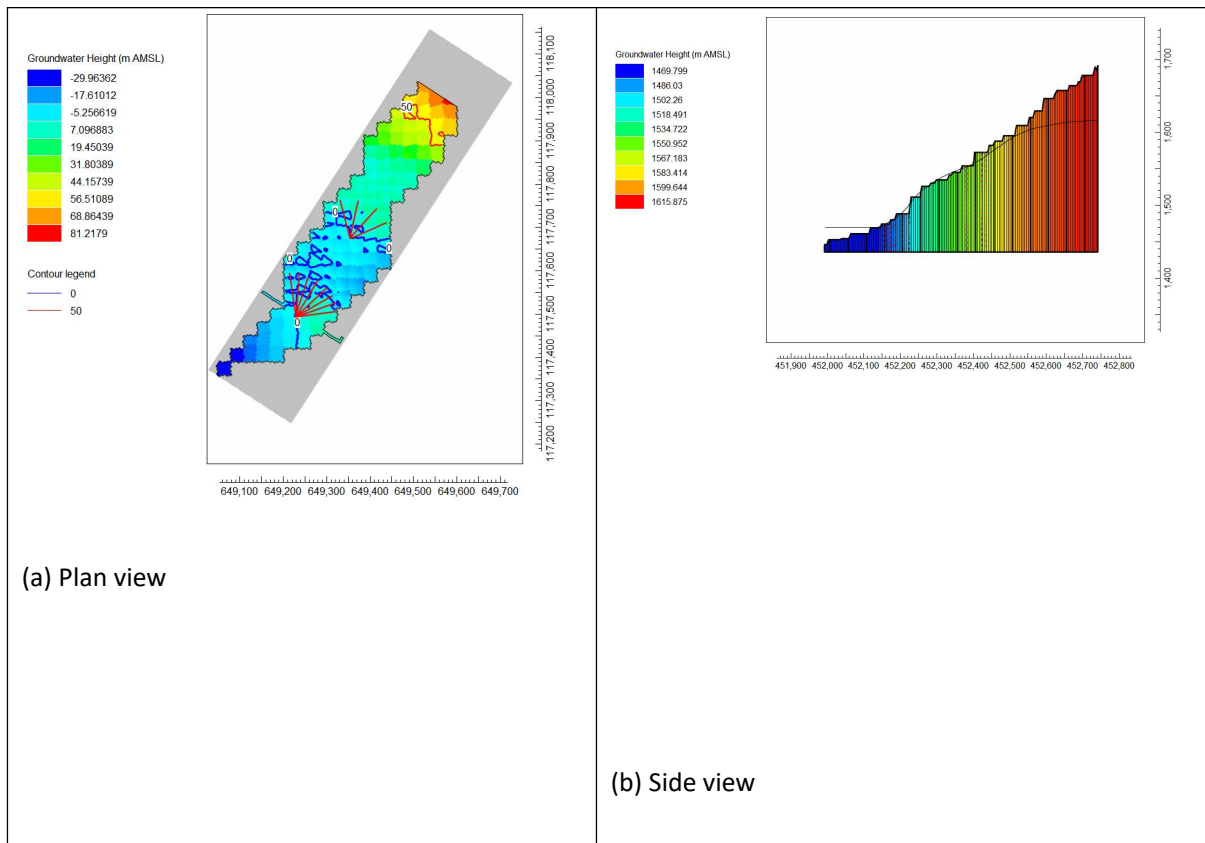


**Figure 36. Steady state simulation for improved drain configuration**

ii. Transient conditions

The transient simulation showed an improvement in the ability of decreasing the flood risk. No flooding was observed at the slope tip, while flooding occurred at the slope toe, and between the location of the two arrays.

**Figure 37** shows the plan view of the model domain after the transient simulation. The grid cell size is 5m by 5m, and the cells are coloured with respect to the dataset specifications, for instance, the difference between

the groundwater head, and the cell top elevation. This implies that positive values indicated flooding (gw head > ground surface elevation), while negative values indicated that the groundwater was below the ground surface (gw head < ground surface elevation).

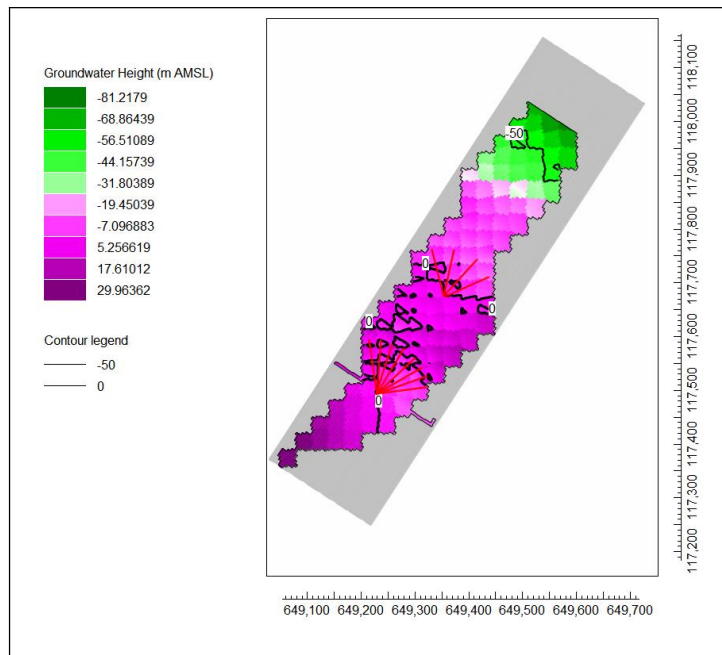


**Figure 37. Transient simulation for improved drained configuration**

From the above discussion, it was observed that long continuous drains positioned at a single lower location were more efficient than shorter drains positioned at different locations. Shorter drains had a smaller area of influence, and hence could not decrease the risk of flooding at elevations beyond their influence.

Of all the scenarios, drain array 2 was the one that provided satisfactory groundwater levels, and therefore, those were the piezometric lines considered in the geotechnical analysis of the slope.

### 4.3.2 GEOTECHNICAL ANALYSIS OF THE SLOPE

#### 1. Initial conditions

Initially, the soil was assumed to be fully saturated, with the piezometric line being at the ground surface. Under Unconsolidated and undrained conditions, the slope was unstable with a factor of safety of 0.351, while in consolidated and drained conditions however, the factor of safety was 0.897. Cahyaningsih, Catur Asteriani. 2019 provide insights of landslide susceptibility based on the value of the factor of safety. They are summarized in table 16. When the slope is assumed fully saturated, its factor of safety is below 1.07, indicating a very unstable slope, which high risk of landslide occurrence.

*Table 15. Factor of safety ranges*

<i>Factor of safety value</i>	<i>Landslide intensity</i>
FOS less than 1.07	Landslide occurred regular/ frequent (unstable slope)
1.07 < FOS < 1.25	Landslide case (critical slope)
FOS over 1.25	Rare landslide (relatively stable slope)

#### 2. Analysis

From the reasons stated before, the geotechnical analysis only accounted for the piezometric lines provided by drain array 2.

##### i. In steady state conditions

The drainage system increased the factor of safety for both conditions,

unconsolidated undrained being 0.570 (increase of 38.42%), and consolidated and drained 1.401 (35% increase). This is because groundwater significantly dropped below the ground surface from the previously position which was assumed to be at the ground surface. The pore water pressure acting on the slope thus reduced, increasing the factor of safety.

ii. In transient condition

The factor of safety decreased again provided the expected flooding. It was 0.524 (decrease of 8.07%) for unconsolidated and drained conditions, while 1.207 (decrease of 13.85%) for consolidated and drained. An increase in water influx was previously observed to increase the risk of flood occurrence. This was linked to the low permeability, where water took more time to travel through the soil profile. Groundwater levels therefore raised, flooding the slope toe where the drains were not able to mitigate the risk. This lead to an increase in pore water pressure, therefore a decrease in the factor of safety.

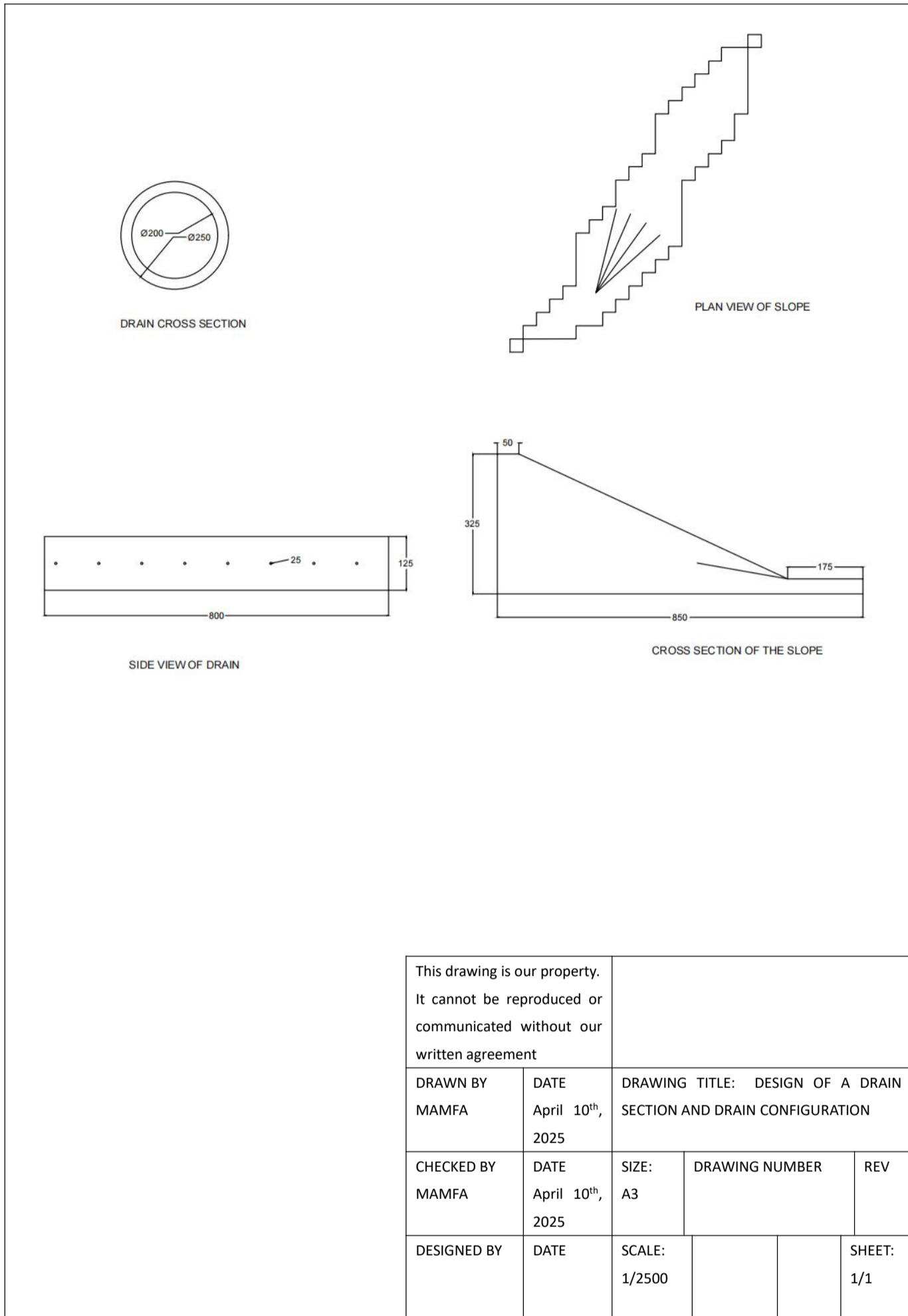
#### **4.3.3 DESIGN OF THE SUB DRAINAGE SYSTEM**

The sub drainage system consists of four drainage pipes arranged in a fan configuration. The drains, which are 200 meters long with an internal diameter of 100mm, are drilled with an angle of 12° from each other. They are perforated with circular slots of diameter 0.25mm, arranged in four longitudinal rows. Taking a section x-x along the slope, the drains are at an

elevation of 1465m AMSL, and they are drilled at an angle of  $10^\circ$  to the horizontal plane.

The drain spacing was calculated to be 10.61 meters. However, this was just an analytical estimation which is prone to changes based on expertise and site conditions as explained by Cook, Santi and Higgins (2008).

4.3.4 DESIGN DRAWING



This drawing is our property. It cannot be reproduced or communicated without our written agreement				
DRAWN BY MAMFA	DATE April 10 <sup>th</sup> , 2025	DRAWING TITLE: DESIGN OF A DRAIN SECTION AND DRAIN CONFIGURATION		
CHECKED BY MAMFA	DATE April 10 <sup>th</sup> , 2025	SIZE: A3	DRAWING NUMBER	REV
DESIGNED BY	DATE	SCALE: 1/2500		SHEET: 1/1

## CHAPTER 5: CONCLUSIONS AND RECOMMENDATIONS

### 5.1 CONCLUSIONS

This study involved the design and determination of the suitability of a horizontal sub drainage system in the context of landslide hazard mitigation, using a combination of analytical and numerical methods for groundwater and geotechnical modelling. Key findings and conclusions can be outlined as follows:

1. The site characterization showed that the area was naturally prone to the occurrence of landslide events when diving into its geological properties.
  - a. The site geometry of the area depicted high elevations (1400 - 1722m AMSL), and moderately steep slopes of maximum 28.26° .
  - b. The soil property findings were the following:
    - i. The soil was majorly composed of fine particles (clay) with a moderately high plasticity;
    - ii. The infiltration rate was very high, with a value of 0.273m/hours, yet it depicted a low permeability of  $3.7368 \times 10^{-4}$ m/hour. This situation showed a tendency of water storage in the soil profile as discussed by scholars (Makabayi, B., Musinguzi, M. and Otukei, J.R. 2021a);
    - iii. On the other hand, the strength parameters, for instance the cohesion and angle of friction were strongly influenced by the drainage conditions. In fact, they were 37.03 Kpa and 14.07° in unconsolidated and

undrained conditions, while in consolidated and drained conditions they were 4kpa and 34.2 Kpa respectively.

2. The hydrological survey showed that:

- i. Rainfall had a great impact on the stability of the slope as the landslides were rainfall-induced. Various statistical analyses were computed, and it was observed that some extreme weather conditions inducing landslides were driven by world-scale hydrological processes such as the El Niño;
- ii. The distribution of water losses in the watershed were greatly influenced by the land-use and inherent soil properties. For instance, the absence of impervious surfaces, and the high infiltration rate of the soil, along with the moderately steep slopes cause a large portion of the rainfall falling on the land (67.47%) to infiltrate the ground.

3. Design of the horizontal sub drainage system

- i. The groundwater modelling showed that the seepage was greatly influenced by the coefficient of permeability. Water accumulated in the soil profile considering its low coefficient of permeability. This increased the chances of the ground surface flood with increased rainfall intensity;
- ii. Drainage was observed to have a significant impact on the seepage of the slope. Drain array 1 consisted of 8 drains of length 100m. It was found not effective in lowering the groundwater table in both steady

state and transient conditions. Drain array 2 on the other hand, consisted of 4 drains of length 200m. It was found effective in lowering groundwater table in steady state conditions, and fairly good at lowering the ground water up slope in transient conditions;

- iii. Long and continuous drains were more efficient at regulating the groundwater levels than shorter drains installed at different locations. This is because shorter drains could not influence the seepage beyond their area of influence;
- iv. The slope was found to be more stable when it was drained. Preventing the drainage (unconsolidated and undrained conditions) lead to an increase of pore water pressure within the slope, and hence its equilibrium.

## **5.2 RECOMMENDATIONS**

1. Advanced studies should be conducted to assess the suitability of sub drains in field. This will entail installing the drains in the slope, as well as piezometers in order to monitor the groundwater over a prolonged period of time.
2. Further research should be conducted on the design of horizontal sub drainage systems, incorporating more complex geologic configurations such as multiple layers and discontinuities.
3. Also, research should be directed to the domain of hydrology in remote

areas prone to natural fatalities of this type, where scholars has shown that it is the leading cause of death and damage to property (UNDRR DesInventar Sendai, 2020). This would allow to an active collection of key data that are necessary for the design of solutions .

## REFERENCES

1. ABG. No date. Soil Properties. Online, available at: [https://abg-geosynthetics.com/wp-content/uploads/ABG\\_Soil\\_Properties\\_Shear\\_Strength\\_TECH\\_NOTE.pdf](https://abg-geosynthetics.com/wp-content/uploads/ABG_Soil_Properties_Shear_Strength_TECH_NOTE.pdf). Ahmed. August 2021. Coefficient of Permeability or Hydraulic Conductivity of Soils. Research Gate. Available at: DOI:10.1201/9781003200260-10
2. Badru, L. et al. (2022) 'Landslides Mapping and Design of IoT-based Susceptibility Prediction System: A Case Study of Bududa District in Uganda', Research Square, pp. 1-17.
3. Buchhorn.M et al. (2019). Copernicus Global Land operations "vegetation and energy" CGLOPS-1". No location: Copernicus Global Land Service (CGLS). Available at:[https://land.copernicus.eu/global/sites/cgls.vito.be/files/products/CGLOPS1\\_ATBD\\_LC100m-V2.0\\_I2.00.pdf](https://land.copernicus.eu/global/sites/cgls.vito.be/files/products/CGLOPS1_ATBD_LC100m-V2.0_I2.00.pdf)
4. Budhu, M. (no date) Soil Mechanics and Foundations. 3rd edn. Edited by I. John Wiley & Sons.
5. Census, U. (2024) 'National Population And Housing Census Preliminary Results'.
6. C Namuenge, J.E. Ssenku, et al. (2024) 'Enablers and Consequences of Landslide Outbreaks in Bududa District, Eastern Uganda.pdf', Volume 14(Issue 9), pp. 200-216. Available at: <https://doi.org/10.9734/ijec/2024/v14i94406>.
7. Cook, D.I., Santi, P.M. and Higgins, J.D. (2008) 'Horizontal Landslide Drain Design: State of the Art and Suggested Improvements', XIV(4), pp. 241-250.
8. Cahyaningsih, Catur Asteriani.2019. Safety factor characterization of landslide in Riau-West of Sumatra highway. Safety factor characterization of landslide in Riau-West of Sumatra highway Vol 17. pp 323-330. doi:10.21660/2019.63.69945
9. David L. Rpyster. No date. Horizontal Drains and Horizontal Drilling: An Overview. Transportation Research Record 783. PDF

10. Directorate of Relief, D.P. and R. (2010) 'The Republic of Uganda: The National Policy for Disaster Preparedness and Management', (October).
11. F Hutchinson and C. Gallant.2000. CHAPTER 2: Digital Elevation Models and Representation of Terrain Shape. *Terrain Analysis: Principles and Applications*. John Wiley & Sons, Inc.
12. Feldman.D. 2000. *Hydrologic Modelling System HEC-HMS Technical Reference Manual*. Davis, CA: US Army Corps of Engineers Institute for Water Resources Hydrologic Engineering Center (HEC). Available at: [https://www.hec.usace.army.mil/software/hechms/documentation/HECHMS\\_Technical%20Reference%20Manual\\_\(CPD-74B\).pdf](https://www.hec.usace.army.mil/software/hechms/documentation/HECHMS_Technical%20Reference%20Manual_(CPD-74B).pdf) .
13. GeoStudio official website. Aug 4<sup>th</sup> 2021. *GeoStudio: Geotechnical numerical analysis tool*. Online, available at: <https://www.seequent.com/products-solutions/geostudio/>
14. GEOTECHNICAL ENGINEERING BUREAU. 2015. *GEOTECHNICAL TEST METHOD: TEST METHOD FOR LIQUID LIMIT, PLASTIC LIMIT, AND PLASTICITY INDEX. STATE OF NEW YORK DEPARTMENT OF TRANSPORTATION*. Online, available at: <https://www.dot.ny.gov/divisions/engineering/technical-services/technical-services-repository/GTM-7b.pdf>
15. Gorokhovich, Y. et al. (2013) 'Landslide Science and Practice', *Landslide Science and Practice [Preprint]*, (February). Available at: <https://doi.org/10.1007/978-3-642-31337-0>.
16. Niroumand, A. Kassim, A. Ghafooripour et la; Septemner 2012. *The role of Geosynthetics in Slope stability. Electronic Journal of Geotechnical Engineering Journal Vol(7)*-. Online, available at: [https://www.researchgate.net/publication/256326625\\_The\\_Role\\_of\\_Geosynthetics\\_in\\_Slope\\_Stability](https://www.researchgate.net/publication/256326625_The_Role_of_Geosynthetics_in_Slope_Stability)
17. H. Rahardjo, V.A. Santoso, et al. (2012) 'Performance of horizontal drains in residual soil slopes', *Soils and Foundations Japanese Geotechnical Society*, 51(3), pp. 437-447.
18. 'Landslides in Uganda' (no date).

19. M. Amoakowaash, L. Kofiste, A. Omari-sasu et al. 2021. *Heliyon Estimation of the return periods of maxima rainfall and floods at the Pra River Catchment , Ghana , West Africa using the Gumbel extreme value theory. Science Direct Vol 7(5). Available at: <http://dx.doi.org/10.1016/j.heliyon.2021.e06980>*
20. M. Vijayaprakash. 2020. *Application of HEC-HMS modelling on River Storån Application of HEC-HMS modelling on River Storån. Division of Water Resources Engineering Department of Building & Environmental Technology Lund University, Lund University Sweden.*
21. Makabayi, B., Musinguzi, M. and Otukei, J.R. (2021a) 'Estimation of Ground Deformation in Landslide Prone Areas Using GPS: A Case Study of Bududa, Uganda', 2021, pp. 213-232. Available at: <https://doi.org/10.4236/ijg.2021.123013>.
22. Makabayi, B., Musinguzi, M. and Otukei, J.R. (2021b) 'Estimation of Ground Vertical Displacement in Landslide Prone Areas Using PS-InSAR. A Case Study of Bududa, Uganda', 2021, pp. 347-380. Available at: <https://doi.org/10.4236/ijg.2021.124019>.
23. Metroeconomica, N.D. and Baastel, J.G. (2015) 'Economic Assessment of the Impacts of Climate Change in Uganda Arabica Coffee Production in the Mount Elgon Nantumbwe, Bob R.
24. Mulatu Tamiru, Worku Firomsa Kabeta, et al. 2024. *Geotechnical analysis and stability assessment of a landslide event in Gera Woreda, Ethiopia. Cogent Engineering, 11(1). doi:<https://doi.org/10.1080/23311916.2024.2405745>.*
25. Nakileza et al. 2017. *Enhancing resilience to landslide disaster risks through rehabilitation of slide scars by local communities in. Jambá - Journal of Disaster Risk Studies Region (Bududa District)'*.
26. Namono, M. et al. (2019) 'The Barriers to Landslide Responses Over the Mt. Elgon in Bududa District', (September), pp. 1-13. Available at: <https://doi.org/10.20944/preprints201909.0022.v1>.
27. NCHRP (2012) *Cost-Effective and Sustainable Road Slope Stabilization and Erosion Control. Washington, D.C. Available at: [127](http://www.national-</a></i></li>
</ol>
</div>
<div data-bbox=)*

[academias.org/trb/bookstore](https://www.academias.org/trb/bookstore).

28. Oleng, M., Ozdemir, Z. and Pilakoutas, K. (2024) 'Co-seismic and Rainfall-triggered Landslide Hazard Susceptibility Assessment for Uganda Derived Using Fuzzy Logic and Geospatial Modelling Techniques', *Natural Hazards*. Springer Netherlands. Available at: <https://doi.org/10.1007/s11069-024-06744-5>.
29. Peter G. Nicholson (2015) Chapter 7 - Objectives and Approaches to Hydraulic Modification. *Soil Improvement and Ground Modification Methods*, pp. 151-187. Available at: <https://doi.org/10.1016/B978-0-12-408076-8.00007-8>.
30. Poesen, M.G.K.A.M.J. and Deckers, J.A. (2009) 'Influence of Soil Properties on Landslide Occurrences in Bududa District, Eastern Uganda', 4(July), pp. 611-620.
31. R. Carrol, T. Badger. 2013. Design Guidelines for Horizontal Drains used for Slope Stabilization. PDF
32. Rolt, J. et al. (2020) 'Rural Road Note 01: A Guide on the Application of Pavement Design Methods for Low Volume Rural Roads', (September).
33. Sikdar, P K Chakraborty, et al. 2004. Land Use / Land Cover Changes and Groundwater Potential Zoning in and around Raniganj coal mining area , Bardhaman District , West Bengal - A GIS and Remote Sensing Approach. *Journal of Spatial Hydrology*. Research gate
34. UNISDR. 2017. *Landslide Hazard and Risk Assessment: Words into Action Guidelines: National Disaster Risk Assessment Hazard Specific Risk Assessment*. Online, available at: [https://www.unisdr.org/files/52828\\_03landslidehazardandriskassessment.pdf](https://www.unisdr.org/files/52828_03landslidehazardandriskassessment.pdf)
35. Vijayaprakash, M. 2020. Application of HEC-HMS modelling on River Storån Application of HEC-HMS modelling on River Storån. Master's Thesis TVVR 20/5021. Lund University. Online, available at: <https://lup.lub.lu.se/luur/download?func=downloadFile&recordId=9035455&fileId=9035456>
36. Ward R.C. (1975). *Principles of hydrology*. London (UK): McGraw-Hill Book Company Limited.

37. World Meteorological Organization. January 25, 2011. EL NIÑO/LA NIÑA UPDATE. Online, available at: <https://wmo.int/files-el-ninola-nina-update-january-2011>
38. Zegeye, A.D. et al. (2021) 'A Low-Cost Subsurface Drainage Technique to Enhance Gully Bank Stability in the Sub-Humid Highlands of Ethiopia', pp. 311-318. Available at: <https://doi.org/10.2478/johh-2021-0019>.

# APPENDICES

## APPENDIX A: Secondary data of BUDUDA Rainfall (2000\_2025)

Year	Month	1	2	3	4	5	6	7	8	9	10	11	12	13	14	15	16	17	18	19	20	21	22	23	24	25	26	27	28	29	30	31	
2000	January	0	0	0	0	0	0	0	0	0	0	0	0	0	0	0	0	0	0	0	0	6.1	1.7	0	0	0	0	0	0	0	0	0	
	February	0	0	0	0	0	0	0	0	0	0	0	0	0	0	0	0	0	0	0	0	0	0	0	0	0	0	0	0	0	0	0	
	March	0	0	0	0	13.4	2.9	17.5	5.8	1.5	1.5	3.7	7.3	0	0	0	14.8	8.9	0	0	0	0	0	0	0	0	0	0	0	0	0	0	9.5
	April	9.2	0	0	10.3	2.3	0	8	10.2	6.8	13.7	0	0	0	0	22.8	9	3.6	0	0	3.6	0	16.1	6.9	2.3	9.2	4.5	20.9	6	13.4	19.4		
	May	15.9	7.4	8.5	7.4	9.5	0	12.8	8.5	13.9	5.3	14.2	1.1	2.2	1.6	2.2	9.6	0	0	0	0	0	0	0	0	17.3	0	0	9.8	9.8	17.7	13.8	
	June	0	0	0	4.1	12.4	0	0	9.2	12.9	0	3.3	6.5	0	0	0	0	0	0	0	22.2	3.3	0	0	13.1	16.4	5.8	9.6	11.5	9.6	7.7		
	July	0	0	10.5	5.3	0	0	0	0	27.3	31.8	16.5	14.1	0	0	2.4	8.1	6.1	0	0	14.2	13.9	17	1.5	0	12.3	0	0	0	0	0	0	
	August	9.1	9.1	0	0	0	1.9	3.7	9.3	15	22.4	3.4	25.5	20.4	17	1.7	15.5	8.6	13.7	1.7	8.6	4.8	9.6	0	0	0	7	7	7	0	0	0	

	September	6.9	1.7	0	6.9	0	0	0	8.3	0	6.6	0	0	0	0	9.9	5.2	1	3.1	0	6.2	13	7	0	1	0	1.5	0	3	0	7.4	
	October	4.7	10.6	3.5	11.7	0	8.4	13.2	20.3	8.4	6	13.5	0	5.1	5.1	8.4	1.2	6.2	18.6	11.1	40.9	0	0	0	0	7.3	0	0	0	0	0	20.5
	November	10.5	9.2	7.9	5.3	1.3	6	12	6	5	0	3.6	0	0	4.8	3.6	23.1	12	9.4	7.7	10.3	20.7	4.5	5.4	2.7	0	0	0	0	0	0	
	December	0	7.8	15.5	2.9	0	3.6	0	0	0	2.7	0	4.6	0	0	0	0	0	0	0	0	0	4.4	0	0	0	0	0	5	0	0	0
2001	January	0	0	0	0	0	0	0	0	0	0	6.2	4.5	2.2	0	3.4	0	0	0	0	4.2	4.9	2.6	7.8	0	0	0	0	0	0	0	
	February	0	0	0	0	0	0	0	0	10.9	0	8.9	0	0	0	0	0	0	0	0	0	0	10.7	2.1	0	0	0	0	0	0	0	
	March	0	0	0	0	24.2	18.7	2.9	0	8.6	0	0	0	12.7	0	7.3	0	3.3	9.9	15.8	5.3	3.7	0	3.7	0	9.2	13.4	0	3.7	3.7	9.8	2.4
	April	0	11.7	0	2.3	7	5.9	1.5	4.4	5.9	0	0	0	7.1	0	9.5	0	0	0	5.5	5.5	9.4	0	1.2	13	7.1	6.8	10.2	17	1.7	0	
	May	1.1	14.9	9.6	7.4	13.8	9.5	0	12.6	12.6	10.5	2.4	7.1	0	7.1	0	0	0	9.6	0	0	12.9	4.3	0	4.3	2.3	0	11.3	6.8	11.3	0	
	June	0	2.4	7.3	0	26.9	12.3	1.5	12.3	10.8	4.6	1.7	5	0	0	15.1	0	0	11.1	7.4	0	0	0	8	4	12	35.2	7	15.8	17.6	0	
	July	0	0	15.8	0	0	20.8	0	0	0	0	0	14.4	0	4.8	12	0	12.5	17.8	10.7	5.3	6.3	4.7	7.9	4.7	15.8	0	0	0	0	0	
	August	0	4.5	9.1	0	4.5	0	0	0	0	14.7	0	6.7	6.7	8.9	2.2	6	8	6	8	0	0	5.3	0	10.5	8.8	13.5	8.4	10.1	20.2	5.1	0

	September	2.6	0	9.1	19.5	3.9	1.6	14.4	0	0	0	0	6.7	0	0	0	2.8	0	4.6	5.5	11.1	11.5	10.6	8	0	11.5	4.8	0	1.2	13.1	0		
	October	0	1.7	0	0	10.4	1.3	6.4	11.5	6.4	11.5	0	11	0	0	6.6	0	0	0	0	17.6	0	9.5	4.8	7.1	8.3	16.4	4.1	16.4	17.8	12.3	9.6	
	November	9.7	0	13.8	4.2	0	3.1	1	2	19.3	1	0.9	11.1	7.7	12.8	11.6	10.7	0	9.8	9.8	12.4	5.1	6.3	0	0	0	0	0	0	0	0		
	December	0	0	1.3	0	10.3	0	4.8	0	0	0	0	0	3.9	0	0	0	0	0	0	0	0	0	0	0	0	3.3	0	1.1	1.1	0	0	
2002	January	4.7	10.3	0.9	8.4	19.7	3.6	0	0	0	0	1.4	5.6	0	1.4	0	1.2	0	0	1.2	3.5	0	5.6	6.3	0	0	4.8	0	0	0	0		
	February	0	0	0	0	0	0	0	0	0	0	0	8.9	0	0	0	2.9	0	5.8	11.5	0	0	0	0	0	0	0	4	14.1				
	March	3.7	7.5	24.2	0	24.2	14.9	12.8	0	4.3	0	0	0	0	16.6	0	0	8.2	7.5	3	4.5	0	0	0	0	0	0	0	0	0	0	0	
	April	0	11.9	0	0	15.9	4.9	0	0	0	9.9	5.8	26.2	8.7	10.2	2.9	0	1.4	8.2	10.9	8.2	7.3	5.5	0	0	0	0	3	6	0	6		
	May	0	11.3	20.5	17.5	15.4	18.9	20	1.1	3.2	2.1	0	0	7.2	1.4	2.9	0	3.4	5.1	8.4	11.8	26.4	9.3	14	7.8	12.4	0	0	0	0	0		
	June	8.3	8.3	0	0	0	0	3.5	5.3	5.3	10.6	6.6	3.3	4.9	8.2	0	12.3	0	14.8	9.8	0	4.4	13.1	4.4	0	0	11.5	0	6.9	4.6	2.3		
	July	0	17.8	0	0	0	0	0	32.3	0	0	3	14.8	0	3	0	0	16.9	6.3	0	2.1	0	2.4	11.9	0	0	0	0	0	0	0	21.4	
	August	0	0	0	20.1	0	12.5	5	0	0	5	13.2	0	0	0	5.3	0	0	0	9.2	0	8.8	3.5	12.3	0	0	0	2.8	0	0	13.8	0	

	September	8.2	2.1	2.1	0	0	0	0	0	0	9.8	9.1	7.8	6.5	1.3	3.9	2.9	5.8	0	0	0	0	0	2.2	4.5	7.9	3.4	0	2.3	6.8	10.1	
	October	22.7	4.5	1.1	4.5	3.4	8	2.7	8	5.3	6.6	8.4	0	4.2	2.1	4.2	1.3	0	9.3	18.6	14.6	9.8	4.3	0	22.8	17.3	10.5	0	6	0	0	22.6
	November	0	1.5	0	16.3	4.4	12.1	2.2	0	0	5.5	0	0	2.4	8.8	1.2	4.4	8.7	1.1	2.2	0	0	3.7	5.6	13	5.6	6.4	0	0	0	0	
	December	0	0	0	0	0	0	0	0	0	0	0	0	6.2	2.1	0	0	8.4	3.1	6.9	0	1.6	5.6	0	0.8	3.6	7.1	6	10.1	0	1.2	
2003	January	0	2.9	8.7	0	0	0	0	0	0	0	0	0	0	0	0	0	0	2.7	5.4	7.4	3.5	3	0	0	0	0	0	0	0	0	
	February	0	0	0	0	0	0	0	5.4	5.4	0	0	0	0	13.1	0	12.8	0	0	0	0	0	0	0	0	0	9.5	0	1.9			
	March	13.4	0	0	0	0	0	0	0	10	0	0	0	16.6	0	0	0	0	0	0	0	0	9.5	5.5	6.3	0	0	0	17.6	9.4	2.3	10.5
	April	0	0	0	0	0	6.6	4.4	0	0	0	0	5.9	23.8	0	17.8	0	17.6	5.4	6.8	0	7.9	14.7	6.8	3.4	4.5	0	8.8	0	0	22.9	
	May	0	3.2	11.7	14.9	16	6.6	0	14.3	2.2	9.9	3.9	16.6	0	9.8	5.9	7.3	2.4	0	4.9	0	0	11.6	5.8	9.6	0	8.2	20.5	0	2	12.3	0
	June	6	0	9	0	9	5.2	0	5.2	5.2	10.4	4.3	2.9	1.4	20.9	8.6	14.5	7.3	12.1	0	4.8	13.1	0	6.6	6.6	6.6	13.4	11.5	11.5	1.9	5.8	
	July	7.3	16.9	2.4	12.1	19.4	2.3	29	8.1	13.9	0	8.1	16.1	0	0	0	0	8.1	2	12.1	6.1	8.9	1.8	12.5	1.8	0	0	0	0	6.5	13	0
	August	0	0	0	14.3	0	4.7	9.3	0	0	11.7	2.3	11.5	4.6	2.3	2.3	22.7	3.2	9.7	4.9	29.2	2.9	8.8	8.8	2.9	26.4	11.5	22.9	0	8.8	0	1.8

	September	3.2	3.2	0	8.1	3.2	5.1	9	3.8	3.8	7.7	1.6	0	8.1	3.2	3.2	5.6	8.4	9.3	0	0	8.1	0.9	7.2	19.7	1.8	0	5.5	0	4.1	4.1	
	October	2.8	4.4	14.5	18.9	1.1	2.5	1.2	16	16	8.6	0	26.2	6.4	7.9	0	1.3	37	4	1.3	1.3	3	0	12.1	0	0	0	14.4	0	11.2	0	4.8
	November	5	18.7	18.7	1.2	2.5	0	0	0	21	8	0	0	0	1.8	5.5	6.7	0	0	1.7	0	0	4	0	5.3	1.3	0	0	5.7	24.1	8	
	December	4.1	0	0	4.1	12.3	0.6	3.1	5	5.9	0	0	0	0	0	0	0	0	0	0	0	0	0	0	0	0	0	0	0	0	0	0
2004	January	0	5.7	0	0	0	0	0	0	0	0	0	0	11.8	0	1.2	7.9	0	7.9	1.3	0	0	0	0	15.2	2.5	0	0	0	5.1	5.8	1.5
	February	9.8	0	0	0	0	0	0	0	0	0	0	0	0	0	8.9	0	0	15.2	15.2	0	0	9.6	21.6	12	0	0	6.9	10.4	10.4		
	March	0	19.5	0	0	0	0	0	8.4	0	0	0	0	13.2	5.7	0	0	0	0	0	0	0	0	0	0	0	2.5	16	0	0	9.8	3.7
	April	0	0	5.3	17.7	15.1	8.6	0	5.4	23.2	16.2	0	0	8.1	8.1	4.1	0	8.3	10.7	26.1	10.7	4.9	0	0	13.5	8.6	2.1	0	0	0	19.2	
	May	0	9.4	7	5.9	4.7	3.2	9.5	9.5	12.7	8.5	11.7	7.8	0	12.7	3.9	0	8.3	0	0	0	0	0	0	0	0	0	0	0	21.9	0	0
	June	0	0	18.4	0	0	0	0	0	0	0	0	9.8	0	0	0	10.6	8.5	14.9	10.6	25.5	9.8	6.6	0	16.4	0	0	0	0	0	0	
	July	0	0	0	0	11.8	0	0	0	0	0	0	0	10.2	0	0	2.2	6.7	0	0	13.4	3.5	10.5	12.2	0	0	16.6	22.9	0	16.6	0	9.4
	August	14.5	10.9	12.1	0	14.5	0	2.8	0	0	16.6	19	1.9	9.5	5.7	1.9	0	15.4	15.4	0	0	0	12.8	0	1.8	7.3	0	10.2	0	3.4	0	0

	September	6.2	4.1	2.1	0	0	0	12.9	0	0	0	0	8.7	2.2	0	0	4	1	0	12.1	0	5.8	7.7	1	6.7	3.8	1.1	8.5	4.2	5.3	10.6	
	October	19.5	5.7	4.6	4.6	0	6.1	0	3	7.6	3	2.5	12.5	0	0	0	7.7	0	1.9	3.8	1.9	0	0	13.2	0	1.5	6	6	10.5	13.5	3	
	November	1.5	7.4	0	10.4	3	0	0	0	8.1	4.1	10.1	0	4	4	0	0	0	2.2	6.5	7.6	0	10.6	7.9	8.8	11.5	0	0	0	0	0	
	December	3.7	0	8.7	0	0	1.9	1	0	2.9	0	0	0	0	0	10.7	9.4	2.3	5.5	0	0	4.5	1.5	3	0	0	0	0	0	4.1	0	2
2005	January	0	0	0	0	0	0	0	0	0	0	0	0	0	0	0	0	0	0	0	0	0	0	0	0	5.2	3.7	1.8	6.2	9.2	0	5.5
	February	11.1	0	0	0	0	0	0	0	0	0	0	0	0	13.1	0	0	0	0	0	0	0	0	0	0	0	14.7	13.6	14.7			
	March	14.9	5	0	7.4	0	0	13.9	0	0	0	0	4.8	0	9.6	0	18.9	13	11.8	9.4	9.4	11.5	2.6	0	2.6	24.2	0	7.8	2.6	0	0	0
	April	0	0	0	12.3	7.4	10.7	5.4	0	4	1.3	15.7	0	14.1	7.9	0	0	0	0	0	7.8	1.3	5.1	11.6	5.1	0	12.4	17	1.5	12.4	9.3	
	May	9.4	10.4	11.5	14.6	10.4	24.7	9.3	12.4	2.1	5.1	3.1	10.3	5.2	7.2	1	10.3	0	6.9	3.4	6.9	31.7	11.7	0	0	1.7	18.6	2.1	10.3	0	10.3	0
	June	8.3	8.3	0	0	0	0	0	3.5	7	0	0	0	0	8.6	0	0	9.9	0	0	4.9	29.6	11.9	0	0	0	0	6.9	9.2	6.9	2.3	
	July	5.3	0	0	0	10.5	17.7	5.9	2.9	0	0	0	0	0	0	15.5	0	0	0	0	8.8	14.3	4.8	3.2	9.5	6.4	9.8	45.3	15.7	23.6	0	9.8
	August	0	0	14.3	0	0	0	0	0	0	16.3	10	0	6	10	6	13.8	13.8	8.6	10.4	0	8.1	0	13	0	9.7	16.4	0	10.3	0	0	0

	September	0	6.9	0	3.5	5.2	12.7	8.9	3.8	0	5.7	0	7.9	5.3	1.3	13.1	9.5	13.8	4.3	9	0	1.5	1.5	6	0	0	0	0	0	0	0	5.7
	October	5.6	0	5.6	0	0	0	0	0	0	0	10.6	1.5	9.1	25.8	4.6	12.7	0	11.3	2.8	5.6	14.4	0	12.2	14.4	3.3	6.7	6.7	0	0	5	8.4
	November	4.4	8.9	3	0	5.9	0	9.9	1.4	0	0	0	0	0	0	0	6	0	0	0	0	0	0	0	0	0	0	0	0	0	9.3	
	December	1	1	1	15.4	2.1	2.8	1.4	0	0	0	5.2	0	0	0	0	0	0	0	0	0	0	0	0	0	0	0	0	0	0	0	0
2006	January	0	0	0	0	0	0	0	0	0	0	0.8	4.9	0	0	0.8	6.9	0	0	0	0	0	0	0	0	0	0	0	0	0	0	0
	February	0	0	0	0	0	0	0	0	0	0	0	0	10.3	11.6	12.9	0	0	17.3	2.9	0	0	0	4.3	0	8.6	10.7	1.2	13			
	March	0	0	0	0	0	1.6	6.5	12.9	1.6	0	0	15.9	1.8	0	3.5	0	8.4	17.6	0	1.4	1.3	18.4	2.5	15.3	3.8	11.5	0	0	0	1.9	0
	April	20.3	0	17.9	16.2	0	0	1.2	7.4	11.7	7.4	6.5	0	6.5	0	0	9.9	11.1	4.9	14.8	3.7	14.5	18.6	14.5	7.2	15.5	20.4	0	3.7	0	3.7	
	May	1.1	5.6	14.1	5.6	5.6	0	7.4	9.5	10.6	14.8	17.8	2.8	1.9	12.2	15	23.4	21.2	1.5	8.8	0	0	0	4.2	2.1	16.6	0	12.6	19.9	28.9	19.9	7.2
	June	9.8	0	0	4.9	0	0	12.7	2.1	2.1	0	1.6	9.3	0	9.3	7.8	0	0	0	0	0	0	0	28.6	6.4	0	11.7	7.8	0	17.6	3.9	
	July	0	0	0	0	0	0	0	20.1	0	1.7	9.7	0	5.8	0	0	0	0	8.9	0	13.4	0	0	18.2	0.9	7.8	3.6	16.8	0	6	0	8.4
	August	1.1	9.2	19.5	16.1	20.7	39.1	28.6	0	20	0	11.8	0	0	0	0	0	10	5.7	0	0	4	0	0	0	4	5.9	9.8	0	6.9	7.8	0

	September	0	2.3	9	0	0	0	4.2	3.3	7.5	0	0.8	4	9.7	0	1.6	5.2	3.8	2.3	7.5	3.3	3.8	2.7	2.7	2.7	4.3	4.3	0	3.2	8.5	12.8	
	October	5.7	8	3.4	7.4	10.9	0	0	6	9	5.3	0	0	0	0	0	0	0	0	0	0	0	9.4	10	6.5	5.9	9.8	16.8	22.4	4.9	7.7	0
	November	11.6	0	1	1	0	7.1	0	0	0	0	6.1	1.8	0	2.4	1.2	6.1	20.6	12.3	0	8.8	16.2	18.8	6.8	2.6	10.2	0.7	2.2	10.3	2.9	0	
	December	0	0	0	0	0	6.7	6.4	0	0	0	0	0	10.3	0.4	0	0	0	0	0	4	0	4.2	1.9	2.3	0.4	0	4.1	0.2	7.5	3.3	1
2007	January	0	0	0	0	0	0	0	0	0	0	0	2.2	0.4	0	3.1	1.4	0	6.1	0	0	0	0	0	0	0	0	0	0	7.8	8.4	0
	February	0.7	11	20.6	19.9	12.5	5.8	4.4	5.1	3.6	3.6	1	3.1	9.4	0	0	0	0	0	0	0	0	0	0	0	8.3	0	10.8	7.4			
	March	9.3	21	0	0	0	0	0	0	0	0	11	0	0	0	0	0	0	2.9	5.7	0	0	0	0	0	0	0	0	0	0	0	0
	April	0	0	0	0	0	8.7	0	0	8.1	18.5	10.7	2.8	19.2	17.1	12.1	0	4.4	1.9	6.3	25.4	1.4	1.4	2.2	0	12.9	5.6	0	0	0	9.9	
	May	4.9	1.8	1.8	6.1	8	2.8	0	0	7.7	4.9	3.1	3.1	2.6	10.4	6.7	11.3	6.4	14.5	1.6	0	0	0	2	16.4	5.1	18.6	0	2.8	14.9	16.7	17.7
	June	19.6	13.9	3.5	5.2	2.3	9.4	2.2	11.5	38.2	2.2	11.5	10.2	16.9	14.9	4.1	0	6.8	21.8	0	0	0	0	0	0	0	0	0	9.6	0	0	
	July	0	9.5	52.4	1.2	0	0	0	10.2	0	0	0	4.6	4.6	7.6	3.1	1	6.9	2.9	6.9	13.7	0	6.9	0	8.1	0	15.6	12.7	14.6	37	33.1	5.8
	August	6.9	6.9	1.4	15.2	4.2	2.2	3.3	13	11.9	0	0.9	24.1	23.2	6	7.7	10.6	0.9	9.7	17.7	2.7	5.1	1.7	10.1	3.4	6.8	0	5.2	6	9.5	6	24.1

	September	8.8	6.8	4.7	4.7	4.1	12.6	9.7	8	16.6	13.7	14.3	7.2	4.2	7.2	13.1	2.4	4.9	0	2	9.8	4.3	1.9	7.2	5.8	5.3	0.6	0	11.3	2.5	1.9		
	October	1.2	12.1	11	0	8.7	0	6.5	5.1	7.6	3.3	6.4	0	0	19.1	0	4.5	0	0	7.9	0	6.4	13.4	1.7	3.5	8.7	0	5.9	0	0	5.9	0	
	November	0	0	15.5	5.4	9.5	0	4.1	0	0	7.6	6.8	7.8	0	2.1	0	6.8	0	0	0	0	0	6	0	4.6	0	0	0	0	6.3	1.6		
	December	0	0	0	0	0	0	0	5.8	10.9	0.3	0	12.9	0	0	0	0	0	0	0	0	0	0	3.6	0	0	0	0	0	0	0	0	
2008	January	0	0	0	0	0	0	0	0	0	0	0	0	0	0	6.9	0	0	0	0	0	0	0	0	1.6	3.1	1.7	3	0	0.7	2.3	9	
	February	9.8	0	0	0	0	5.5	18.6	0	0	2.1	9.4	4.2	0	0	0	0	0	0	0	0	0	0	0	0	0	6.9	0	0	0			
	March	1.4	0	0	0	22	10	0	0	0	0	0	0	7	11.3	3.5	3.4	0	0	19.8	6.8	0	15	0	1.6	4.7	14.1	0	0	5.1	3.2	5.1	
	April	10.2	0	0	0	0	0	0	0	0	14.3	24.9	0	14.7	2.2	9.5	0	0	9.6	26.4	16.2	6.5	3.2	1.9	9.1	1.9	0	0	0	0	11		
	May	11.2	0	1.3	5.9	0	0	0.7	0	13.2	0	0.5	15.3	7.4	2	8.9	0	0	3.5	0	22.7	8.5	10.1	12.4	28.7	12.4	2.1	8.4	9.4	9.4	7.3	3.1	
	June	1.1	5.4	14	21.5	19.4	9.4	8.5	0	8.5	0.9	0	0	0	13.2	3.8	13.5	10.5	0	0	0	0	0	0	0	0	0	0	0	0	0	11.9	
	July	0	0	29.1	9.3	2.6	7.1	16.6	1.2	13	10.7	2.2	8.6	21.6	11.9	0	8.4	0	9.3	15.9	3.7	11.7	15.8	18.8	2.3	4.5	1.3	0	0	17.7	5.1	6.3	
	August	6.3	21.5	7.6	6.3	2.5	1.9	7.7	15.5	12.6	6.8	9.1	2.7	20	12.7	0.9	0	7.9	15.8	11.4	8.8	7.6	14.4	0	9.1	10.6	10	2.5	6.7	25.1	4.2	11.7	

	September	1.6	9.4	3.9	0	3.9	2.2	0	1.1	4.3	3.2	5.3	4.7	4.7	0.7	10.7	0	3.4	6.3	1.9	7.8	4	9	4.5	12.5	7.6	6.4	1.9	0.6	0	7	
	October	7.7	0	16.5	20.4	0	0	4	9.3	13.3	4	6.6	14.1	2.8	0	0	3.5	4.3	10.4	0	0	1.1	0	7.9	25.3	6.7	21.7	1.4	0	20.3	9.8	8.4
	November	10.5	8.7	18.7	16.3	6	8.4	14.9	4.5	0	2.2	5.7	0	0	6	0	4.9	0.5	3.2	8.1	0	0	0	0	0	0	0	0	9.6	2.6	0	
	December	0	5.2	0	0	0	0	0	0	0	0	4.9	0	0	0	0	0	0	0	3.2	4.8	0	0	0	0	6.2	1.4	3.4	0	0	0	0
2009	January	0	0	0	0	0	0	0	4.2	0	0	0	0	0	0	0	0	0	0	0	3.7	1.4	0	0	4.5	1.4	0	8.5	0.7	0	0	2.9
	February	8.5	13.2	0	4.7	0	7.3	0	0	0	0	0	0	0	0	0	0	0	14.2	0	0	0	0.8	17.6	0	0	0	0	0			
	March	0	0	0	0	12.6	0	0	0	0	0	0	6.6	4.1	13.2	0	0	14.6	3.4	0	0	0	10.2	0	0	0	0	0	6.1	21.1	28.3	
	April	22.1	16.4	11.5	0	2.5	2.3	7.6	0	0	6.8	0	15.9	6.1	6.1	15.2	3.8	2.3	4.6	0	10.7	1.3	10.8	5.1	0	7	0	5.5	16.6	0	25.2	
	May	9	0	0	0	0	0	0	1.7	2.3	22	22.1	0	15.2	16.6	7.4	21.5	7.2	0	21.5	14.3	12.7	14.6	0	0	4.5	15.9	14	20.6	6.5	3.7	7.5
	June	0	5.5	0	0	8.3	4.4	4.4	2.9	0	0	0	0	0	11.5	11.5	0	15.9	6.3	0	0	0	0	0	0	0	3.8	0	28.5	8.5	5.7	
	July	3.4	10.3	0	0	0	0	0	0	13.1	0	0	0	0	1.6	17.4	16.3	0	0	0	0	0	0	9	8.1	7.2	0	0	0	0	0	0
	August	0	0	0	14.7	7.3	0	0	11.6	0	0	0	0	16.6	5.5	20.3	9.1	8.2	6.4	7.3	6.4	8.1	10.1	0	0	0	0	1.3	6.6	0	9.3	0

	September	0	21	5.4	0	2.7	4.8	0	2.4	0.8	8	0	0	9.6	14.4	0	1.7	0.4	14.4	10.5	5.7	0	2.1	7.4	7.9	0	4.6	8.2	1	15.9	5.6		
	October	4	6.3	8	8	8	13.4	2.7	7.4	2	4	13.7	6.9	0	0	9.4	6.6	21.6	19	0	0	0	0	0	11.7	0	0.8	8.4	7.6	19	1.5	0	
	November	0	0	0	0	11.4	4.8	5.5	0	0	1.4	0	2.6	7.8	0	0	14.4	0	0	1.1	0	0	0	0	0	0	2.8	0	9.1	6.3	0		
	December	0	2.3	4.5	0	0	0	0	0	3.6	13.1	18.4	9	0	0	1.7	4.5	4.5	0	0	0	0	0	7	5.1	8.5	8.6	10.3	11.7	7.4	0	7.4	
2010	January	15	2	6.5	5	1	2.2	0	0	1.1	2.7	7.2	0	0	0	0	1.6	2.4	0	0.8	4.4	0	0	0	0	0	0	0	0	0	0	0	0
	February	0	0	0	6.7	13.3	9.7	15.9	0	0	0	0	0	0	0.9	16.1	26.8	0	1.9	0	16.9	8.9	13.3	9.4	6.4	40.8	0	15	9				
	March	1	11.6	29.1	6.8	1.9	5.1	2.6	11.1	0	1.7	0	0	0	0	0	0	0	0	14.3	0	5.6	13	20.4	1.9	8	12.9	5.3	0	2.9	16.4	2.9	
	April	6.2	7.8	0	1.6	0	0	0	0	0	0	0	14.7	22.4	13.3	19.6	0	14.9	3.5	4.3	2.8	4.8	10.2	12.6	1.2	0	9.4	0	1.3	2.7	2.7		
	May	3.2	0	0	1.6	8	9	18.5	9.5	6.3	0.5	12.5	4.8	6.2	8.7	8.7	14	5.8	0	7.4	4.1	0	9.9	6.3	10.8	5.4	14	0	1.2	7	7	0	
	June	0	0	18.9	15.1	0	4.4	11.5	0	2.6	6.2	4.2	9.8	2.8	25.1	3.8	22.7	21.1	17.9	11.6	0	1.6	17.2	17.2	0	0	0	0	0	0	0	0	
	July	2.5	12.5	32.5	2.5	0	0	0	11.2	0	0	5.7	10.3	0	8	11.5	3.2	0	0	0	6.4	2.5	10.7	3.3	0	16.4	5.1	5.1	18.3	0	19.3	30.5	
	August	19.3	3	7.4	0	0	0	0	2.5	0	9.9	19.3	0	4.1	0	7.1	5.7	10	0	0	0	3.2	0	3.2	5.6	20.8	7.1	0	5.3	23	1.8	7.1	

	September	4.9	0	7.4	4.9	0	10.8	1.3	0	4.7	7.4	12.7	7.3	8.5	3.6	9.7	5.8	5.3	5.8	2.4	0	10.6	2.4	6.3	5.3	0	0	8.5	4.3	0	0	
	October	0	0	0	0	16	7.2	9.1	2	11.1	3.3	0.8	10.6	11.8	7.6	21.2	0	5.1	13.4	22.3	17.2	4	8.6	13.7	5.7	5.1	9	13.1	3.3	0.8	2.5	0
	November	12.1	10.2	3.2	6.4	8.3	3	0	10.7	0	1.8	3	2	6.5	7.5	0	0	0	0	0	0	0	2.2	7.2	0	0	0	0	0	0	0	
	December	10	0	0	0	0	5.4	2.6	5.4	6	4.9	7.5	3.5	0	0	0	0	0	0	0	0	0.3	0	0	7.4	7.7	8	4.6	4.9	1.8	2.2	0
2011	January	0	0	0	0	0	0	0	0	0	0	0.7	3.1	4.5	0	0	0	0	0	0	8.3	0	0	0	0	0	0	0	0	0	0	0
	February	6.3	3.2	4.8	0	0	0	0	0	0	0	0	0	10	0	0	0	0	12	0	0	0	0	0	0	0	0	0	0	0	0	0
	March	0	0	0	0	0	0	14.9	0	0	0	0	0	0	0	8.1	7.7	0	1.9	0	0	8.6	7.9	7.2	2.9	0	0	10.7	6.6	2.4	10.7	6
	April	9.5	0	0	0	0	0	13.8	6.2	0	0	0	0	0	0	0	0	7.3	0	0	0	2.9	5.8	0.6	11.1	12.2	11.4	13.8	0	9.8	6.5	
	May	20.5	0	3.2	0	18.3	15.1	22.2	9.1	7.1	13.1	0	0	12.8	0	0	15.9	0	9.9	4.6	13.7	0	0	0	11.1	19.4	6.9	10.3	2.3	0	1.1	10.3
	June	16.6	12.2	11.1	13.3	0	2.2	3.7	9.6	11.1	26.6	9.3	14.6	23.3	16.6	4	11.3	6.3	0	2.5	15	0	0	10.6	16.6	12.1	16.7	32.5	11.4	8.8	7	
	July	28.5	41	9.1	5.7	0	9.7	5.5	0	5.5	9.7	0	0	14.3	6.5	5.2	7.5	0	0	4.3	12.8	10.7	11.5	1.5	9.2	14.5	0	25	10	30	8.5	15
	August	2.8	7.1	1.4	0	21.9	11.8	16.7	11.3	1.5	0	10.5	2.6	22.8	15.8	2.6	9.9	11.7	10.8	0	7.2	6.5	8.9	0.8	7.3	8.1	0.8	13.4	17.6	3.3	7.5	17.6

	September	14.1	4.4	3.1	6.9	13.2	9.8	13.8	14.9	12.1	6	9	6.6	1.2	15	12	4.2	11.9	0	7	0	0	0	4.7	14	9.8	0	8	11	14	10	
	October	13.3	1.2	2.3	4.6	11	5.6	16.6	4	0	4	6.8	6.8	21.2	15.1	3	0	2	22.5	10.2	2.7	0	4.1	11.5	3.4	0	4.3	10.1	3.6	10.8	10.1	12.2
	November	3.7	9.9	9.3	4.3	20.5	6.7	8.6	13.8	10.9	0	0	4.8	0	0	0	1.1	0	4.5	1.1	0	0.5	0	2.3	15.9	8	5.5	10.5	10.5	9.4	13.8	
	December	0	7.3	8.3	2.9	1	0	0	3.2	0	0	0	0	2.5	1.6	0	3.7	2.2	0	0	0	0	0	0	0	0	0	0	0	0	0	0
2012	January	0	0	0	0	0	0	0	0	0	0	5.3	0	0	0	0	0	0	0	0.5	6.1	0	0	0	0	0	0	0	0	0	0	0
	February	0	0	0	0	0	0	0	0	0	0	0	0	0	0	0	0	0	13.5	0	0	0	0	0	0	0	7.6	0.8	2.5	1.7		
	March	1.9	0	11.5	0	3.8	0	0	0	0	0	0	0	0	0	0	0	0	0	0	0	0	0	0	0	0	0	0	0	0	1.9	27.2
	April	8.3	12.4	14.9	0	14.1	5.1	11.4	1.7	15.9	4.6	3.5	12.5	2.1	13.9	41	19	0	13.5	8.6	4.9	15.5	5.6	0	3.1	1.2	20.6	11.5	0	2.5	4.9	
	May	13.8	1.6	8.5	8.5	16.4	7.4	11.6	7.9	7.9	7.9	0	4	14.5	1	12	10.1	9.2	0.8	4.2	5	1.7	8.3	24.9	0	11.6	0	9.7	0	0	0	0
	June	0	10.9	9.7	17	0	2.2	5.8	15.9	25.9	14.4	5.5	9.1	0	0	3.6	0	0	19.4	0	12.9	15.3	9.8	25.1	0	0	5	5	13	9	5	
	July	13.3	10.7	9.3	0	6.7	0	9.8	0	17.2	15.3	6.3	0	0	0	12.6	5.2	16.6	14	0.9	14.9	0	18.2	15	4.8	0.8	0	13.4	7.2	15.5	15.5	18.5
	August	19.5	12.2	0	17	2.4	0	1.1	9.9	18.6	0	3.9	21.2	3.9	6.8	0	0	1	3.9	14.4	11.6	0	6.9	8.5	4.6	18.5	0	15.8	8.8	7.5	8.8	4.4

	September	8.9	19.1	3.2	0	7.6	0	6.6	10.8	10.2	12.6	5.2	9.2	12.7	23.1	8.7	2.1	4.8	1.1	6.9	0	2	6	3	9.4	1	11.6	3.2	6.8	4.7	4.7	
	October	3.2	6.4	0	0	0	0	2.3	0	0	16.9	0	24.9	0	9.6	4	0	0	0	0	0	11.2	0	0	0	0	9.5	18.3	0.7	0	15.4	1.5
	November	7	5.1	12	14.5	3.8	2	11.3	6.4	12.7	0	0	0	6.2	2.5	2.5	9.4	4.7	0	4.7	0	0	7.7	1.7	1.7	3.9	0	7.8	14.3	0	0	
	December	0	0	0	0	13.3	4.5	4.1	0	0	0	0	0	0	0	0	4.3	0	0	0	0	0	0	2.9	2.3	0	0.3	0.7	7.7	0	5.4	0
2013	January	0	2.8	4.2	0	0	0	0	6.6	0	3.1	0	0	0	0	0	0	0	0	0	0	0	0	0	0	0	0	0	0.4	0.4	7	0.4
	February	18.7	0	0	0	0	0	0	0	0	0	0	0	3.3	6.6	0	0	0	0	0	0	8.8	0	0	0	0	0	0	0	0	0	
	March	0	0	0	0	0	0	9.8	11.1	12.5	10.5	2.3	6.2	10.1	9.3	0	0	1.5	7.4	14.8	0	15.8	0.6	9.5	16.4	0.6	19.4	15.6	14.5	1.6	8.1	13.5
	April	0	13.5	11.7	10.8	0	19	10.6	7.4	16.4	11.1	12	6.4	10.4	2.4	4	0.7	0	1.4	2.1	22.9	0	9.1	2.8	0	7	10.4	14.4	0	11.2	8	
	May	9.5	6.1	3.9	0.6	13.9	14.3	10.1	8.5	7.9	1.6	5.7	7	0	1.3	0	0	0	4.8	4.8	0	0	0	0	0	18.7	13.2	9.6	4.8	0	0	0
	June	9.7	0	0	0	3.2	0	0	0	13.2	11.5	2.9	7.9	15.1	8.6	4.3	19.4	35.5	1.1	6.5	2.2	0	0	0	0	0	0	5.6	0	5.6	0	
	July	0	1.5	16.7	9.1	1.5	0	0	0	0	0	10.1	0	0	17.6	0	0	1.7	21.8	16.5	13.1	0	6.7	5.7	8.6	0	0	1	25.4	44.1	0	8.1
	August	16.1	0	0	0	14.6	6.5	14.8	9.3	10.2	13.9	12.9	0	0	9.9	9.9	12.6	12.6	0.9	5.4	7.2	12.8	5.6	5.6	8.8	0	0	0	0	0	4.8	9.6

	September	11	4.5	7.8	7.8	4.5	1.3	3.3	9.4	4.7	6	3.9	16.2	0.6	6.5	1.9	3.6	9.9	4.5	4.1	4.5	0.9	0.9	6.8	14	13.5	11.2	12.2	5.8	0	0	
	October	0	10.5	8.8	4.1	7.6	3	16.3	4.8	22.4	4.8	22.7	7.6	11.3	2.3	9.1	6.3	9.4	0	0	7.1	1.8	10.2	0	5.4	12	9.4	13	0	23.1	4.3	0
	November	0	0	0	0	0	3.4	1.7	0	5.6	7.8	3.5	2.6	5.6	10.4	18.6	0	0	8.7	7.6	0	0	8.9	7.5	9.9	0	4.1	0	0	0	6.2	
	December	0	0	0	0	0	5.5	0	0	2.3	0	7.5	0	1.8	1.8	0	0	0	0	0	0	0	0	0	0	0	0	0	0	0.7	6.1	6.8
2014	January	12.2	3.1	0	0	0	0	3.9	2.1	2.1	0	0	0	0	0	0	0	0	2.9	0.8	5.4	0	3.6	3.6	0	0	0	0	0	0	0	0
	February	0	0	0	0	16.8	9.5	0	0	1.4	0	0	7.9	0	0	0	0	0	0	14.2	16.3	2.9	6.4	0	13.2	0.7	0	0	0			
	March	0	0	0	0	0	8.4	0	0	0	6.4	1.4	17.2	6.4	5	13.3	0	0	0	0	0	0	0.6	27.3	13.3	0.6	0	0	3.4	2.3	5.7	0
	April	2.8	0.9	6.5	15.7	7.4	14.4	2.3	0	0	0	0	10.6	10.2	3.4	5.1	0	0	0	0	8.3	6.9	6.2	4.8	1.4	0	6	0	8	0	10	
	May	9.4	0.6	4.4	2.8	18.3	17	10.8	9.2	9.5	8.2	14.6	6.8	5.8	1.9	8	0	8.4	5	15.9	0	7.8	9.5	14.7	6.1	0	7.5	7.5	11.7	0	6.4	4.3
	June	2.5	12.3	8.6	11.1	1.2	0	0	0	3.1	14.5	4.5	5.6	3.3	0	0	0	0	3.8	10.1	20.2	16.7	6.3	0	0	0	0	0	2.6	18	0	
	July	0	14.8	0	0	0	0	17.3	0	0	3.5	0	0	0	0	12	0	0	0	0	12.5	20.8	5.4	11.2	7.7	0	9.2	19.6	10.4	1.2	0	0
	August	1.6	0	0	19.4	4.9	9.5	23.8	0	5.7	9	2.4	4.8	8.4	0	6	1.9	13.2	4.7	7.5	5.7	13.9	2.5	0	4.1	9.8	4.1	12.3	4.9	20.5	9.8	17.2

	September	8	19.1	0.9	8.6	11.7	9.3	0	2.5	2.5	0	5.9	0	0	11.1	2.2	0	4.7	0	7.5	10.3	4.1	5	10.9	6.8	6.8	1.8	0	6.7	4.3	4.9	
	October	0	4.2	0	7.8	4.9	5.2	5.8	9	13.5	1.3	0.8	4	5.5	7.9	23	6.5	2.6	0	13.8	24.9	13.9	0	4.2	4.8	5.4	3.7	1.8	0	0.9	0	14.7
	November	0	17.8	2.2	2.2	0	5.6	9.3	0	7.1	5.6	8.8	0.5	1.1	4.8	0	12.4	2.4	1.4	1.9	8.8	3.1	4	10.6	11.9	9.7	5.5	0	3.1	6.8	11.7	
	December	11.4	6.5	5.5	0	0	0	0	1.2	3.1	3.5	0	0	0	0	0	3	0	0	0	2	0	0	0	8.1	0.8	0	0	0	0	0	0
2015	January	0	0	0	0	0	0	0	0	0	0	0	0	0	0	0	0	0	0	0	0	0	0	0	0	0	0	0	0	0	0	0
	February	0	0	0	0	0	0	0	0	0	0	0	0	0	0	0	15.8	0	4.3	0	0	0	0	0	0	0	4.9	2.4	0			
	March	0	0	0	5.7	8.5	0	0	0	0	0	0	0	0	0	0	0	0	0	0	0	0	0	8.7	14	11.3	9.2	0	10.9	8	6.9	9.2
	April	1.5	15.8	50.2	9.1	13.6	10.7	1.3	13.8	0	0	0	0.8	0	0	31	6.9	4.6	4.6	1.5	3.8	20.5	5.9	18	3.8	1.6	18.6	1.6	0	2.8	19	
	May	13.3	5.8	7.2	3.3	5	23.9	0	7.7	1.6	8	9.3	2.2	0	0	0	13.8	0	8.4	13.8	6.1	10.4	0	0	0	0	1.1	5.7	1.1	8.6	11.5	2.3
	June	11.1	0	19.6	21.7	14.8	3	0	11.9	3	1	0	8.3	6.3	7.9	3.9	23.2	21.1	13.2	8.4	7.4	6.6	0	0	0	25.6	12.9	3.4	0	6.2	4.5	
	July	15.8	0	0	0	0	0	0	0	0	10.7	0	0	0	0	0	0	0	16.9	8.9	4	5.8	2.9	5.8	6.2	11.6	19.3	4.6	12.5	0	5.7	0
	August	18.2	23.7	0	0	9.7	5.5	4.1	0	7.5	2.7	0	0	9.9	0	0	7.7	13.4	4.6	0	0	10.8	13.2	5	0	0	0	0	0	0	0	22.4

	September	7.6	15.8	0	3.4	0.7	13.2	0	8.8	1.4	0.7	0	0	11.5	13.5	0	0	0	10.5	3.7	3.5	2.7	4.6	2.2	0	7	5.9	3.9	0	0	5.2	
	October	12.2	2.3	0	0	0	0	0	0	4.6	14.6	27	0	22.1	7.5	0	17.3	6.4	10.6	9.9	11.2	10.4	9.6	4.9	4.1	4.9	5.4	10.4	21.7	33.8	13.7	13
	November	5.9	1.2	9.1	27.5	2.2	0	5.5	6.6	3.2	7.1	11	5.5	0	0	5.3	14.8	0	14.8	4.5	1.4	8.3	1.7	0	0	0	17	4.6	2.8	1.9	0	
	December	8.3	5.9	0	9	7.3	0	6	0	0	0	0	7.2	1	0	0	0	1.2	4.8	1.2	0	0	0	0	0	0	1.6	7.3	0	0	0	0
2016	January	0	0	0	6.6	0	0	0.7	1.6	1.2	9.1	2.7	3.8	5.4	3	5.4	0	8.5	0	6.6	3.9	2.6	1.3	0	0	0	0	0	0	0	0	0
	February	0	0	0	0	0	0	0	0	0	0	0	0	0	0	0	0	0	0	0	0	0	0	0	0	0	0	7.1	0	0		
	March	0	16.8	0	0	0	0	3.2	20	9.8	0	0	0	0	0	0	0	10.7	5.1	0	0	0	8.6	7.1	5.9	0	0	0	0	0.6	12.7	17.7
	April	28.6	0	16.4	23.1	0	6.4	18.4	5	3.1	10.3	13.2	7.5	14.3	0	9.4	15.4	7.4	2.7	3.7	1.7	5	3.6	4.2	12.8	15.8	20.2	7.3	2.8	2.8	9.3	
	May	0	5	17.5	13.8	11.9	7.6	0	0	0.7	7.3	11.7	12.7	5.5	5	7.7	0	7.7	6	0	13.7	3	9	0	0	2.2	0	0	0	0	0	0
	June	8.9	0	0	3.6	0	0	0	0	0	0	0	0	5.6	6.3	0	4.4	0	15	0	4.8	0	23.8	0	26.5	11.1	0	0	0	0	0	
	July	13.3	0	0	0	0	0	3.5	0	3.5	13.2	11.5	0	0	0	0	0	9.2	4.3	6.3	13	6.8	1	5.4	0	6.8	12.5	6	11.3	0	6	0
	August	0	20.4	3.6	19.8	10.2	16.4	23.7	0	2.9	1.9	7	4	15.4	6	0	0	0	0	0	0	3.5	5.9	9.4	0	0	0	11.4	0	0	0	0

	September	0	0	0	0	0	0	0	0	12.6	0	0	0	5.1	8.3	7.2	0	5.9	4.7	6.4	1.7	1.8	2.5	0.8	7.3	8	9.9	10.2	12.4	1.3	4.3		
	October	4.3	16.7	12.4	9.7	9.2	0	8	0	0	0	13	0	0	0	0	0	0	0	0	9.1	3.3	5.9	7.2	5.2	0	15.2	10.6	12.1	0	0	0	
	November	3.8	7	16.5	12.7	1.3	6.9	5.2	3.4	0	1.7	0	0	0	0	0	10.3	4.4	1.5	7.3	0	0	0	4.7	13.6	8.4	0	7.3	9.1	11.6	0		
	December	0	0	0	0	0	0	0	0	0	0	4.9	0	0	0	0	0	0	0	0	0	0	0	0	0	0	0	0	0	0	0	0	
2017	January	0	0	0	0	0	0	0	0	0	0	0	0	0	0	0	0	0	0	0	0	0	0	0	0	0	0	0	0	109.	22	0	0
	February	312.42	0	0	0	0	0	0	0	0	0	0	0	0	0	0	0	99.06	322.58	223.52	373.38	327.66	132.08	0	279.4	66.04	0	215.9	0				
	March	0	0	431.8	144.78	0	182.88	0	0	294.64	0	0	0	0	0	508	596.9	53.34	35.56	17.78	35.56	187.96	40.64	0	0	271.78	106.68	299.72	157.48	0	0	0	
	April	0	0	0	0	640.08	213.36	363.22	15.24	0	0	0	0	0	0	0	515.62	439.42	198.12	30.48	198.12	91.44	30.48	368.3	0	215.9	0	474.98	673.1	0	119.38		
	May	124.46	383.54	398.78	149.86	0	365.76	243.84	190.5	0	215.9	0	0	170.18	152.4	0	101.6	226.06	182.88	182.88	162.56	332.74	0	0	0	0	243.84	0	0	121.92	213.36	121.92	
	June	66.0	302.	0	0	401.	101.	127	0	251.	0	0	0	0	0	264.	0	0	187.	281.	0	274.	353.	314.	0	0	256.	0	256.	332.	76.2		



	April	231. 14	231. 14	441. 96	358.1 4	0	193. 04	741. 68	165. 1	0	246. 38	447. 04	71.1 2	482. 6	0	695. 96	185. 42	0	111. 76	149. 86	149. 86	162. 56	205. 74	132. 08	325. 12	0	241. 3	381	200. 66	381	0		
	May	200. 66	15.2 4	243. 84	129.5 4	215. 9	515. 62	215. 9	271. 78	0	27.9 4	55.8 8	40.6 4	0	347. 98	83.8 2	165. 1	292. 1	281. 94	538. 48	309. 88	731. 52	40.6 4	0	0	439. 42	0	238. 76	612. 14	53.3 4	25.4	78.7 4	
	June	137. 16	220. 98	332. 74	248.9 2	525. 78	0	467. 36	45.7 2	0	45.7 2	93.9 8	0	0	0	353. 06	464. 82	33.0 2	266. 7	33.0 2	0	0	269. 24	0	403. 86	906. 78	411. 48	482. 6	205. 74	137. 16	342. 9		
	July	871. 22	528. 32	0	0	0	104. 14	0	104. 14	276. 86	312. 42	0	335. 28	0	0	302. 26	0	0	0	0	0	0	0	0	0	0	0	0	0	0	279. 4	238. 76	0
	August	0	0	0	0	0	0	340. 36	0	114. 3	0	0	0	0	0	0	0	0	0	185. 42	449. 58	665. 48	144. 78	558. 8	269. 24	0	500. 38	347. 98	0	109. 22	238. 76	129. 54	
	September	0	185. 42	302. 26	116.8 4	200. 66	0	0	0	236. 22	0	78.7 4	642. 62	203. 2	0	15.2 4	45.7 2	73.6 6	0	134. 62	45.7 2	0	0	129. 54	0	0	116. 84	91.4 4	0	477. 52	271. 78		
	October	167. 64	287. 02	0	50.8	0	0	53.3 4	53.3 4	190. 5	383. 54	96.5 2	355. 6	172. 72	452. 12	269. 24	259. 08	370. 84	386. 08	530. 86	0	0	0	0	0	0	0	218. 44	91.4 4	398. 78	345. 44	144. 78	144. 78
	November	236. 22	383. 54	104. 14	0	0	40.6 4	0	25.4	223. 52	335. 28	152. 4	0	101. 6	0	0	15.2 4	0	45.7 2	284. 48	0	119. 38	0	0	0	0	0	0	0	0	0	0	0
	December	0	0	0	0	0	0	132. 08	111. 76	261. 62	228. 6	38.1	0	0	205. 74	0	0	0	0	0	0	0	0	0	0	0	0	45.7 2	0	15.2 4	73.6 6	0	
20	January	0	0	0	0	0	0	0	0	0	0	0	0	0	0	205. 205.	0	0	0	0	0	0	0	0	76.2 60.9	0	0	0	0	0	0	0	0



	Novem ber	670. 56	137. 16	426. 72	274.3 2	76.2	546. 1	73.6 6	279. 4		60.9 6	381	518. 16	76.2	0	0	99.0 6	20.3 2		0	0	109. 22	205. 74	581. 66	170. 18	121. 92	33.0 2	208. 28		0	0	83.8 2	251. 46			
	Decem ber	439. 42	40.6 4		0	0	48.2 6	104. 14	86.3 6	86.3 6	40.6 4	0	0	99.0 6	0	0	0	254	0	0	0	7.62	45.7 2	91.4 4	53.3 4	388. 62	101. 6		38.1	38.1	38.1	20.3 2	0			
20 20	Januar y		0	0	0	0	0	0	0	0	0	0	0	0	0	0	111. 76	0	0	0	0	0	0	0	0	190. 5	83.8 2	406. 4	314. 96	96.5 2	76.2	0				
	Februa ry		0	0	0	0	0	0	0	0	0	0	0	0	0	0	0	0	0	0	0	210. 82	0	0	88.9	0	0	281. 94	185. 42	205. 74						
	March	657. 86		0	76.2	419.1	0	147. 32		383. 54	17.7 8	218. 44	271. 78		139. 7	0	665. 48		375. 92	226. 06		0	0	0	0	325. 12	510. 54		177. 8	111. 76	88.9	0	0			
	April		0	0	0	0	0	0	0	0	266. 7	0	408. 94	551. 18	657. 86	106. 68	632. 46	190. 5	157. 48	78.7 4		0	0	154. 94	45.7 2	63.5	406. 4	248. 92	165. 1	320. 04	40.6 4	279. 4				
	May	203. 2	236. 22	167. 64	180.3 4	167. 64	142. 24	142. 24	86.3 6	373. 38		0	38.1	0	132. 08	0	111. 76	238. 76	22.8 6	144. 78	144. 78		279. 4	228. 6	127	0	0	0	119. 38	314. 96	40.6 4	0	0			
	June		0	0	0	652. 78		83.8 0	83.8 2	226. 06		0	0	0	0	88.9 64	421. 0				58.4 2	342. 9		0	0	0	304. 8	304. 8	391. 16	129. 54	104. 14	236. 22	0			
	July		0	0	340. 6	226.0 0		190. 5	558. 8	543. 56	271. 78	652. 78	312. 42		0	25.4 42	312. 72	807. 508	553. 72		0	0	0	149. 86	43.1 8	0	0	584. 2		208. 28		0	177. 8	254	42	
	August	0		0	0	421.	248.	408.	421.		0	0		213.	256.	213.	662.	469.	515.	172.	160.	203.	289.	0	223.	93.9	48.2	177.	134.	88.9	236.	180.	203.	269.		

			82			64	92	94	64			36	54	36	94	9	62	72	02	2	56		52	8	6	8	62		22	34	2	24
	Septem ber	203. 2	172. 72	0	81.28	0	353. 06	0	96.5 2	0	114. 3	0	86.3 6	0	127 18	18	0	104. 14	0	91.4 4	220. 98	106. 68	142. 24	76.2	1	78	96	68	266. 7	0	220. 98	
	Octobe r	27.9 4	254 4	27.9 4	137.1 6	462. 28	0	55.8 8	0	350. 52	165. 1	0	215. 9	236. 22	647. 7	78.7 4	0	81.2 0	8	0	467. 36	38.1	137. 16	137. 16	137. 16	289. 56	0	416. 56	294. 64	797. 56	485. 14	0
	Novem ber	40.6 0	4 4	0	60.96	365. 76	340. 36	203. 2	177. 8	0	38.1	22	0	25.4	139. 7	279. 4	63.5	62	38.1	25.4	63.5	0	106. 68	0	269. 24	40.6 4	292. 1	292. 1	480. 06	243. 84	0	
	Decem ber	66.0 0	4 4	381	66.04	0	0	0	172. 72	0	0	132. 08	0	0	0	0	0	0	180. 34	0	0	0	78.7 4	0	0	0	0	0	0	0	0	134. 62
20 21	Januar y	330. 2	15.2 4	0	0	0	0	0	0	297. 18	30.4 8	38.1	25.4	63.5	0	0	0	0	0	0	0	0	104. 14	0	0	0	0	0	0	0	0	0
	Februa ry	0	0	0	0	0	0	0	0	0	495. 3	15.2 4	330. 2	281. 94	236. 22	203. 2	462. 28	0	462. 28	0	0	0	104. 14	185. 42	124. 46	40.6 4	0	0	0	0	0	
	March	0	0	0	457.2	0	0	0	292. 1	58.4 2	0	0	0	0	0	0	0	190. 5	0	213. 36	0	48.2 6	342. 9	0	0	0	182. 88	134. 62	0	398. 78	0	33.0 2
	April	66.0 4	220. 98	0	398.7 8	332. 74	182. 88	0	271. 78	332. 74	0	474. 98	548. 64	147. 32	0	274. 32	424. 18	213. 36	198. 12	30.4 8	485. 14	388. 62	335. 28	200. 66	373. 38	226. 06	20.3 2	76.2	441. 96	632. 46	345. 44	
	May	109. 22	325. 12	187. 96	93.98	472. 44	449. 58	487. 68	170. 18	154. 94	182. 88	142. 24	243. 84	175. 26	335. 28	0	127	0	0	284. 48	0	0	0	0	0	0	0	109. 22	0	403. 86	0	0

	June	0	71.1 2	375. 92	579.1 2	172. 72	0	0	0	0	0	0	0	0	0	185. 42	187. 96	48.2 6	236. 22	0	0	0	0	0	0	0	0	0	223. 52	0	0	
	July	0	370. 84	91.4 4	91.44	0	0	0	0	284. 48	104. 14	0	0	419. 1	68.5 8	381	292. 1	157. 48	279. 4	134. 62	213. 36	0	0	0	0	0	0	0	157. 48	0	236. 22	
	August	0	0	0	363.2 2	185. 42	0	421. 64	157. 48	106. 68	0	45.7 2	563. 88	474. 98	203. 2	0	254	0	50.8	0	292. 1	93.9 8	0	0	53.3 4	0	99.0 6	48.2 6	0	220. 98	441. 96	
	September	160. 02	0	142. 24	142.2 4	195. 58	15.2 4	198. 12	243. 84	396. 24	182. 88	111. 76	160. 02	96.5 2	271. 78	223. 52	160. 02	309. 88	12.7	160. 02	45.7 2	170. 18	215. 9	147. 32	297. 18	101. 6	241. 3	119. 38	119. 38	119. 38	172. 72	
	October	0	248. 92	320. 04	175.2 6	132. 08	213. 36	241. 3	0	177. 8	0	464. 82	485. 14	96.5 2	213. 36	20.3 2	157. 48	297. 18	17.7 8	436. 88	0	0	0	0	0	0	0	0	0	0	0	0
	November	33.0 2	444. 5	358. 14	317.5	0	104. 14	284. 48	0	0	15.2 4	0	40.6 4	109. 22	274. 32	0	0	0	248. 92	309. 88	342. 9	124. 46	0	0	0	0	0	0	0	0	0	
	December	0	0	0	0	0	0	0	0	0	0	0	0	0	0	109. 22	0	0	0	0	116. 84	0	241. 3	307. 34	187. 96	38.1	0	58.4 2	106. 68	0	38.1	
20 22	January	134. 62	0	0	0	0	0	0	0	0	0	0	0	175. 26	30.4 8	304. 8	30.4 8	0	7.62	43.1 8	104. 14	0	114. 3	0	0	0	0	0	0	165. 1	0	
	February	0	281. 94	0	0	0	0	0	0	185. 42	0	198. 12	73.6 6	0	99.0 6	22.8 6	167. 64	358. 14	287. 02	332. 74	0	116. 84	0	284. 48	350. 52	231. 14	0	0	0	0	0	
	March	0	0	0	0	0	0	0	0	0	0	0	0	0	0	193.	76.2	0	0	0	33.0	256.	50.8	325.	170.	127	48.2	205.	396.	0	0	





20	Januar	8.1	1.1	2.3	2.4	0	2.6	2	4.2	2.2	2.6	22.4	0.1	2.1	1	0	0	0.1	0	0	1.5	tr	0	0	0	6.6	0.5	tr	0	0	0.8	0
24	Februa ry	4.5	0	1	1	2	1	0	0	11.4	11	3.7	0	1.4	28.5	4.3	0	0	0	0	2.1	0	0	0	0	8.1	23	1.1	0.1			
	March	25	0	20	5.4	4.5	4	15.7	4.8	0.1	17.2	0	0	0	0	0	0	0	0	0	0	0	0	0	0.7	6.3	3	16.1	18.5	38.4	2.5	22.6
	April	4.5	22.7	35.5	1.1	28.7	12.8	3.3	0.5	0	0.7	0	0	2.9	0	2.6	8.5	3.8	14.5	2.8	34.1	6.5	6.9	6.8	7.8	4.7	0.1	32.5	33	2.5	8.8	
	May	24	7.5	4.2	15.5	0.1	0	0.7	0.5	44.7	20	5.7	0.1	0.9	0.1	2.5	0.1	0	15.7	6.7	16.3	9.7	18.9	23	0.9	0	0	0	0	0	0	0
	June	0	0	1.3	3.4	0	2.4	15.3	3.5	1.4	0	0	2.6	0	0	2.5	3.5	3.7	0	4.6	2	44.6	1.5	4.4	11.4	1.1	0	1.4	3	2	0	
	July	0	1	0	0	tr	2.1	5.1	0	3.4	tr	4.2	3.2	8.4	0	0.8	9.1	0	1	28.3	0	0	20.5	0.6	0.7	0	0	0.5	0	4.3	0	0
	August	0	0	30.1	0	2.4	0	0	7.2	30.2	6.1	7.7	12.5	1	0.7	tr	2.7	14.1	0.7	2.8	0	2.3	tr	0	tr	3.9	6.1	0	17.8	13.4	25	0
	Septe mber	3.5	0	11.1	22.3	0.8	3	2.4	0	4.2	1.2	12.4	0.6	4.1	tr	0	19.3	26.6	2.2	4.2	0	5	2.8	0.1	5.7	3.4	0	9.4	2.6	2.7	2.1	
	Octobe r	20	0	0	0	27	57	16.2	2.7	tr	10	1.2	0.6	6.5	26.4	17.4	tr	tr	16.3	0	18.4	7.4	13.4	32.5	1	15.1	11.4	0	1.3	18.4	tr	2.1
	Novem ber	2.2	9.2	tr	tr	3.3	11	9.2	0.1	0	0	6.8	0	0	3.4	8.2	0	tr	0	tr	3.9	1.4	24	2.4	30.4	0	21	13.7	16.2	3.7	0	
	Decem ber	0.5	5.9	1.8	0.0	0.0	0.0	0.0	0.0	0.0	0.0	0.0	0.5	0.0	0.0	0.6	0.0	0.0	0.5	16.0	2.0	16.3	tr	1.3	2.3	2.5	tr	0.0	0.0	0.0	0.0	0.0

20 25	Januar y	0	0	0	0	0	0	0	0	0	7.9	0	0	0	0	0	0	0	0	0	0	0	0	0	0.8	5.1	3.2	1.8	2.7	0	0	0	0
	Februa ry	13	0	0	0	0	no data	no data	no data	no data	no data	no data	no data	no data	no data	no data	no data	no data	no data	no data	no data	no data	no data	no data	no data	no data	no data	no data	no data	no data	no data	no data	no data

## APPENDIX B: Secondary data of BUDUDA borehole

Borehole Number	Li/BUD/ 004	Li/BUD/0 03	MBL/05/ 440	Li/BUD/00 6	DWD32763	MBL/05/ 030	MBL/05/04 5	MBL/05/0 32	Li/BUD/00 1	Li/BUD/005	Li/BUD/002	DWD51922	DWD41494
Water Point	Deep Well	Deep Well	Deep Well	Deep Well	Borehole	Deep Well	Deep Well	Deep Well	Deep Well	Deep Well	Deep Well	Borehole	Borehole
Latitude					0.362853	0.083333 333		0.1				1.012400314	1.183333333
Longitude					33.779708	32.11666 667		32.1				34.37051575	33.98333333
Altitude(m)					0.362853	0.083333 333		0.1				1.012400314	1.183333333
UTM Zone	36S	36S	36N	36S	36	36N	36N		36S	36S	36S	36N	36N
WM Zone													
District	BUDUD A	BUDUDA	BUDUDA	BUDUDA	BUDUDA	BUDUDA	BUDUDA	BUDUDA	BUDUDA	BUDUDA	BUDUDA	BUDUDA	BUDUDA
County	MANJIY A	MANJIYA	MANJIYA	MANJIYA	MANJIYA	MANJIYA	MANJIYA	MANJIYA	MANJIYA	MANJIYA	MANJIYA	MANJIYA	MANJIYA
Subcounty	SHAFAT	BUMAY	BUSKIKA	BUDUDA	TOWN	BAKIGAI	BUKIGAI	BAKIGAI	BUDUDA	BUDUDA TC	BUSKIKA	BUBIITA	BUKIGAI

	SA	OILA			COUNCIL								
Parish	BUWALI	BUNADU TU	BUFUTSA	BUDUDA T/C	NASHULA	BUNAMU BI	BULOBI	BUMATA NDA	BUSHINYE KWA	BULOLI M/WARD	BUSHUNYA	BUWALI	BUMATANDA
Village	BUBISK WA	NAGOBE	NANGOK O	BUDUDA CELL	BUNAEMEB E	BUNAMU BI	NAMAWUL ULU	BUMUKO YA	WAMARA	BULOLI	BUMATAYA	BUWASHI	BUMUKOYA
Source Name													
Owner Ship					Communal							Communal	Communal
Owner Contact Number												0	1010101010
Water Use					Communal							Domestic	Domestic
Organization												DRACO (UGANDA) LIMITED	DRACO (U) LTD
Site Investigation Method											Electrical Resistivity Method		
Date of Investigation												29-01-2018	41671
Recommended Depth of Borehole(m)												55	
Date of Completion	34004	34004	34004	34004	34004	34004	34004	34004	34004	34004	34004	43314	18-01-2014

Drilling Method												Direct Air Rotary	Direct Air Rotary
Casing Material					PVC							PVC	127
Casing Diameter(mm)					127							127	
Total Casing Length(m)	0	0	0	0	2.75	0	0	0	0	0	0	45	
Height of Surface Casing(m)	0	0	0	0		0	0	0	0	0	0	0	
Datum Elevation(m a.g.l)	0	0	0	0		0	0	0	0	0	0		
Borehole Seal Type												Cement	
Well Development Method					Airlift							AirLift	Airlift
Duration of Development(hrs)					1							1	1
Borehole Filters												Gravel Pack	
Depth at slot size1												34.5	
Depth at slot size2												40	
Depth at slot size3												48.25	
Depth at slot size4													
Depth at slot size5													

Slot Size1													1	
Slot Size2													1	
Slot Size3													1	
Slot Size4														
Slot Size5														
Total Drilled Depth(m b.g.l)	0	0	0	0	55	0	0	0	0	0	0	0	52	66
Date of Installation													23-02-2018	21-01-2014
Pump Type													Hand pump	Hand pump
Name of Pump													U2	U-2
Pump Capacity(m3/hr)													1	1
Pump Installation Depth(m.b.g.l)													18	27
Riser Pipe material													PVC	PVC
Riser Pipe Diameter(mm)													32	32
Pump Rod Material													Stainless steel	Stainless steel
Pump Rod Diameter(mm)													12	12

Depth to Bedrock(m b.g.l)	0	0	0	0	33	0	0	0	0	0	0	42	24
Overall Geological Setting													
Lithology Depth1												1	3
Lithology Depth2												6	15
Lithology Depth3												18	24
Lithology Depth4												42	66
Lithology Depth5												52	
Lithology Depth6													
Lithology Depth7													
Lithology Description1												BLACK TOP SOIL	CLAY SOIL
Lithology Description2												BROWN HARD CLAY	LATERITIC CLAY
Lithology Description3												SAND	WEATHERED CLAY FORMATION
Lithology Description4												WEATHERED GRANITE	FRACTURED HARD AMPHOBOLITE
Lithology Description5												FRESH GRANITE	

Lithology Description6													
Lithology Description7													
DepthToWaterStrike1												27	24
EstimatedYield1												5	0.3
AquiferType1												Fractured Bedrock	Other
OtherAquifer1													INTERFACE
DepthToWaterStrike2													
EstimatedYield2													
AquiferType2													
OtherAquifer2													
DepthToWaterStrike3													
EstimatedYield3													
AquiferType3													
OtherAquifer3													
DepthToWaterStrike4													

EstimatedYield4													
AquiferType4													
OtherAquifer4													
DepthToWaterStrike5													
EstimatedYield5													
AquiferType5													
OtherAquifer5													
Table Height(m a.g.l)												0.5	
Length of Drilling Rods(m)												3	
Length of Drill Bit(m)												0.5	
Measuring Point(m a.g.l)												0.5	0.7
Pump Installation Depth(m.b.MP)												50	42
Static Water Level(m.b.MP)												10.78	17.88
Discharge(m3/hr) Step1													
Discharge(m3/hr) Step2													

Discharge(m3/hr) Step3													
Discharge(m3/hr) Step4													
Discharge(m3/hr) Step5													
Step Test Drawdown(m b.g.l)												3.53	4.41
Step Test Duration(min)												180	180
Step Test Recovery(%)												0.9887	0.9252
Constant Test Pump Installation Depth(m b.M.P)													
Constant Test Static Water Level(m b.g.l)													
Constant Test Dynamic Water Level(m b.g.l)													
Constant Test Discharge(m b.g.l)													
Constant Test Duration(min)													
Constant Test Recovery(%)													
Depth(m)1													
BackfillMaterial1													

Depth(m)2													
BackfillMaterial2													
Depth(m)3													
BackfillMaterial3													
Depth(m)4													
BackfillMaterial4													
Depth(m)5													
BackfillMaterial5													
Transmissivity(m2/day)													
Specific Capacity(m3/hr/m)												0.2857	1
Water Quality Certificate Issued by												NWSC	NWSC
Sample Number												K639//2018	K064/14/C
Serial Number												ES/RF/2018/235	INV/2014/38-2
Bi-Carbonates												278.16	130
Calcium												46.4	0

Chloride													0	4.5
Color(apparent)													6	0
Conductivity													403	340
Fluoride													0	0.25
Magnesium													8.64	9.6
Manganese													0	0.006
Nitrate													0	0.02
PH													6.91	6.69
Sodium													0	0
Sulphates													3	7
Sulphide													0	0
Total Alkalinity													228	130
Total Dissolved Solids													257.92	173
Total Hardness													152	140
Total Iron													0.016	0.13

Total Suspended Solids													0	0
Turbidity													0.62	0.1

## APPENDIX C: Slope stability analysis\_slip surfaces tables

### 1. INITIAL CONDITIONS

#### a. Unconsolidated Undrained

X	Y	PWP	Base Normal Stress	Frictional Strength	Cohesive Strength	Suction Strength	Column Base Material	
Column 1	62.50000 m	304.98116 m	0 kPa	48.88412 kPa	12.251635 kPa	37.04 kPa	0 kPa	New Material
Column 2	87.50000 m	267.93947 m	0 kPa	305.60876 kPa	76.593524 kPa	37.04 kPa	0 kPa	New Material
Column 3	110.26786 m	238.62252 m	572.85821 kPa	737.30238 kPa	41.214 kPa	37.04 kPa	0 kPa	New Material
Column 4	130.80357 m	215.26554 m	708.47343 kPa	919.58921 kPa	52.911121 kPa	37.04 kPa	0 kPa	New Material
Column 5	151.33929 m	194.18328 m	821.78046 kPa	1,072.6306 kPa	62.869588 kPa	37.04 kPa	0 kPa	New Material
Column 6	171.87500 m	175.04977 m	915.9761 kPa	1,203.6947 kPa	72.109787 kPa	37.04 kPa	0 kPa	New Material
Column 7	192.41071 m	157.62148 m	993.44857 kPa	1,318.3363 kPa	81.425341 kPa	37.04 kPa	0 kPa	New Material
Column 8	212.94643 m	141.71099 m	1,056.0361 kPa	1,420.8452 kPa	91.430684 kPa	37.04 kPa	0 kPa	New Material
Column 9	233.48214 m	127.17060 m	1,105.187 kPa	1,514.5046 kPa	102.58565 kPa	37.04 kPa	0 kPa	New Material

Column 10	254.01786 m	113.88173 m	1,142.0642 kPa	1,601.731 kPa	115.2045 kPa	37.04 kPa	0 kPa	New Material
Column 11	274.55357 m	101.74779 m	1,167.6151 kPa	1,684.136 kPa	129.45362 kPa	37.04 kPa	0 kPa	New Material
Column 12	295.08929 m	90.68907 m	1,182.6212 kPa	1,762.5336 kPa	145.34117 kPa	37.04 kPa	0 kPa	New Material
Column 13	315.62500 m	80.63926 m	1,187.733 kPa	1,836.9126 kPa	162.70134 kPa	37.04 kPa	0 kPa	New Material
Column 14	336.16071 m	71.54275 m	1,183.4958 kPa	1,906.3933 kPa	181.17696 kPa	37.04 kPa	0 kPa	New Material
Column 15	356.69643 m	63.35268 m	1,170.3691 kPa	1,969.1909 kPa	200.20558 kPa	37.04 kPa	0 kPa	New Material
Column 16	377.23214 m	56.02949 m	1,148.741 kPa	2,022.615 kPa	219.01562 kPa	37.04 kPa	0 kPa	New Material
Column 17	397.76786 m	49.53970 m	1,118.9396 kPa	2,063.1363 kPa	236.64032 kPa	37.04 kPa	0 kPa	New Material
Column 18	418.30357 m	43.85511 m	1,081.2417 kPa	2,086.5501 kPa	251.95651 kPa	37.04 kPa	0 kPa	New Material
Column 19	438.83929 m	38.95204 m	1,035.8794 kPa	2,088.2548 kPa	263.7527 kPa	37.04 kPa	0 kPa	New Material
Column 20	459.37500 m	34.81080 m	983.04588 kPa	2,063.6449 kPa	270.8263 kPa	37.04 kPa	0 kPa	New Material
Column 21	479.91071 m	31.41528 m	922.89899 kPa	2,008.5918 kPa	272.10294 kPa	37.04 kPa	0 kPa	New Material
Column 22	500.44643 m	28.75262 m	855.56497 kPa	1,919.9574 kPa	266.76449 kPa	37.04 kPa	0 kPa	New Material
Column 23	520.98214 m	26.81294 m	781.14078 kPa	1,796.0659 kPa	254.3667 kPa	37.04 kPa	0 kPa	New Material

Column 24	541.51786 m	25.58913 m	699.69594 kPa	1,637.0482 kPa	234.92492 kPa	37.04 kPa	0 kPa	New Material
Column 25	562.05357 m	25.07678 m	611.27385 kPa	1,444.9807 kPa	208.94869 kPa	37.04 kPa	0 kPa	New Material
Column 26	582.58929 m	25.27405 m	515.89255 kPa	1,223.7705 kPa	177.41267 kPa	37.04 kPa	0 kPa	New Material
Column 27	603.12500 m	26.18164 m	413.54512 kPa	978.77957 kPa	141.66249 kPa	37.04 kPa	0 kPa	New Material
Column 28	623.66071 m	27.80282 m	304.19947 kPa	716.23324 kPa	103.26641 kPa	37.04 kPa	0 kPa	New Material
Column 29	644.19643 m	30.14350 m	187.79779 kPa	442.50277 kPa	63.835709 kPa	37.04 kPa	0 kPa	New Material
Column 30	664.73214 m	33.21228 m	64.255524 kPa	163.38159 kPa	24.843577 kPa	37.04 kPa	0 kPa	New Material
Column 31	675.18863 m	34.96498 m	0 kPa	23.406801 kPa	5.8663548 kPa	37.04 kPa	0 kPa	New Material

**b. Consolidated Drained**

X	Y	PWP	Base Normal Stress	Frictional Strength	Cohesive Strength	Suction Strength	Column Base Material	
Column 1	62.50000 m	305.08129 m	0 kPa	132.9303 kPa	90.33934 kPa	4 kPa	0 kPa	New Material
Column 2	87.50000 m	268.18627 m	0 kPa	402.41823 kPa	273.48315 kPa	4 kPa	0 kPa	New Material
Column 3	110.64815 m	238.50096 m	572.31979 kPa	855.15604 kPa	192.21531 kPa	4 kPa	0 kPa	New Material
Column 4	131.94444 m	214.38433 m	711.92391 kPa	1,055.0352 kPa	233.17822 kPa	4 kPa	0 kPa	New Material

Column 5	153.24074 m	192.66875 m	827.98094 kPa	1,223.6878 kPa	268.92213 kPa	4 kPa	0 kPa	New Material
Column 6	174.53704 m	173.00477 m	923.91795 kPa	1,369.2734 kPa	302.66323 kPa	4 kPa	0 kPa	New Material
Column 7	195.83333 m	155.13271 m	1,002.2815 kPa	1,498.055 kPa	336.92733 kPa	4 kPa	0 kPa	New Material
Column 8	217.12963 m	138.85360 m	1,065.0231 kPa	1,614.8841 kPa	373.68517 kPa	4 kPa	0 kPa	New Material
Column 9	238.42593 m	124.01120 m	1,113.6747 kPa	1,723.4684 kPa	414.41536 kPa	4 kPa	0 kPa	New Material
Column 10	259.72222 m	110.48053 m	1,149.4624 kPa	1,826.5006 kPa	460.11469 kPa	4 kPa	0 kPa	New Material
Column 11	281.01852 m	98.16003 m	1,173.3818 kPa	1,925.6899 kPa	511.26799 kPa	4 kPa	0 kPa	New Material
Column 12	302.31481 m	86.96619 m	1,186.2521 kPa	2,021.7251 kPa	567.78689 kPa	4 kPa	0 kPa	New Material
Column 13	323.61111 m	76.82973 m	1,188.7527 kPa	2,114.1924 kPa	628.92814 kPa	4 kPa	0 kPa	New Material
Column 14	344.90741 m	67.69272 m	1,181.4517 kPa	2,201.4747 kPa	693.20696 kPa	4 kPa	0 kPa	New Material
Column 15	366.20370 m	59.50655 m	1,164.8257 kPa	2,280.6712 kPa	758.32779 kPa	4 kPa	0 kPa	New Material
Column 16	387.50000 m	52.23032 m	1,139.2761 kPa	2,347.5817 kPa	821.16362 kPa	4 kPa	0 kPa	New Material
Column 17	408.79630 m	45.82961 m	1,105.1402 kPa	2,396.8145 kPa	877.82099 kPa	4 kPa	0 kPa	New Material
Column 18	430.09259 m	40.27558 m	1,062.7008 kPa	2,422.0699 kPa	923.82633 kPa	4 kPa	0 kPa	New Material

Column 19	451.38889 m	35.54424 m	1,012.1933 kPa	2,416.6324 kPa	954.45582 kPa	4 kPa	0 kPa	New Material
Column 20	472.68519 m	31.61585 m	953.8114 kPa	2,374.0654 kPa	965.20362 kPa	4 kPa	0 kPa	New Material
Column 21	493.98148 m	28.47450 m	887.71097 kPa	2,289.0424 kPa	952.34386 kPa	4 kPa	0 kPa	New Material
Column 22	515.27778 m	26.10776 m	814.01384 kPa	2,158.1908 kPa	913.50172 kPa	4 kPa	0 kPa	New Material
Column 23	536.57407 m	24.50647 m	732.81007 kPa	1,980.7804 kPa	848.11976 kPa	4 kPa	0 kPa	New Material
Column 24	557.87037 m	23.66447 m	644.15981 kPa	1,759.0854 kPa	757.70263 kPa	4 kPa	0 kPa	New Material
Column 25	579.16667 m	23.57859 m	548.0944 kPa	1,498.2943 kPa	645.75521 kPa	4 kPa	0 kPa	New Material
Column 26	600.46296 m	24.24848 m	444.61704 kPa	1,205.9378 kPa	517.39304 kPa	4 kPa	0 kPa	New Material
Column 27	621.75926 m	25.67670 m	333.7028 kPa	890.92249 kPa	378.6861 kPa	4 kPa	0 kPa	New Material
Column 28	643.05556 m	27.86870 m	215.29819 kPa	562.37332 kPa	235.87202 kPa	4 kPa	0 kPa	New Material
Column 29	664.35185 m	30.83295 m	89.320064 kPa	228.54279 kPa	94.615669 kPa	4 kPa	0 kPa	New Material
Column 30	681.64148 m	33.75470 m	0 kPa	33.899029 kPa	23.037756 kPa	4 kPa	0 kPa	New Material

## 2. STEADY STATE CONDITIONS

### Unconsolidated Undrained

X	Y	PWP	Base Normal Stress	Frictional Strength	Cohesive Strength	Suction Strength	Column Base Material	
Column 1	40.13337 m	309.25599 m	0 kPa	113.25283 kPa	28.384111 kPa	37.04 kPa	0 kPa	New Material
Column 2	62.50000 m	276.11190 m	0 kPa	428.88464 kPa	107.48968 kPa	37.04 kPa	0 kPa	New Material
Column 3	87.50000 m	243.50019 m	0 kPa	681.33084 kPa	170.75928 kPa	37.04 kPa	0 kPa	New Material
Column 4	111.88919 m	215.43820 m	-672.50222 kPa	892.9334 kPa	223.7924 kPa	37.04 kPa	0 kPa	New Material
Column 5	135.66758 m	191.04897 m	-453.03879 kPa	1,073.8282 kPa	269.12934 kPa	37.04 kPa	0 kPa	New Material
Column 6	159.44596 m	169.09613 m	-257.46901 kPa	1,236.145 kPa	309.81017 kPa	37.04 kPa	0 kPa	New Material
Column 7	183.22435 m	149.25411 m	-82.600082 kPa	1,384.0639 kPa	346.88251 kPa	37.04 kPa	0 kPa	New Material
Column 8	206.17686 m	131.84449 m	69.099351 kPa	1,524.2969 kPa	364.71046 kPa	37.04 kPa	0 kPa	New Material
Column 9	228.30350 m	116.57448 m	200.5006 kPa	1,652.1602 kPa	363.82375 kPa	37.04 kPa	0 kPa	New Material
Column 10	250.43013 m	102.63555 m	318.84784 kPa	1,764.0365 kPa	362.20196 kPa	37.04 kPa	0 kPa	New Material
Column 11	272.55677 m	89.92724 m	425.12648 kPa	1,861.9382 kPa	360.10248 kPa	37.04 kPa	0 kPa	New Material

Column 12	294.68341 m	78.36660 m	520.14987 kPa	1,947.03 kPa	357.61337 kPa	37.04 kPa	0 kPa	New Material
Column 13	316.81004 m	67.88457 m	604.59533 kPa	2,019.7114 kPa	354.665 kPa	37.04 kPa	0 kPa	New Material
Column 14	338.93668 m	58.42327 m	679.0306 kPa	2,079.6739 kPa	351.03772 kPa	37.04 kPa	0 kPa	New Material
Column 15	362.50000 m	49.44738 m	715.52722 kPa	2,129.2049 kPa	354.30448 kPa	37.04 kPa	0 kPa	New Material
Column 16	387.50000 m	41.03920 m	713.27834 kPa	2,166.2511 kPa	364.15287 kPa	37.04 kPa	0 kPa	New Material
Column 17	412.50000 m	33.76772 m	699.8818 kPa	2,182.3837 kPa	371.55364 kPa	37.04 kPa	0 kPa	New Material
Column 18	437.50000 m	27.59274 m	675.73187 kPa	2,172.9827 kPa	375.25011 kPa	37.04 kPa	0 kPa	New Material
Column 19	462.50000 m	22.48160 m	639.56501 kPa	2,133.2494 kPa	374.35626 kPa	37.04 kPa	0 kPa	New Material
Column 20	487.50000 m	18.40824 m	591.63675 kPa	2,058.4053 kPa	367.61044 kPa	37.04 kPa	0 kPa	New Material
Column 21	512.50000 m	15.35252 m	518.19675 kPa	1,946.1456 kPa	357.88122 kPa	37.04 kPa	0 kPa	New Material
Column 22	537.50000 m	13.29965 m	419.38995 kPa	1,793.7587 kPa	344.45264 kPa	37.04 kPa	0 kPa	New Material
Column 23	562.50000 m	12.23987 m	359.01104 kPa	1,591.6026 kPa	308.91958 kPa	37.04 kPa	0 kPa	New Material
Column 24	587.50000 m	12.16818 m	337.10898 kPa	1,342.044 kPa	251.86293 kPa	37.04 kPa	0 kPa	New Material
Column 25	612.50000 m	13.08424 m	302.16356 kPa	1,057.8357 kPa	189.39114 kPa	37.04 kPa	0 kPa	New Material

Column 26	637.50000 m	14.99237 m	254.13248 kPa	745.83333 kPa	123.23305 kPa	37.04 kPa	0 kPa	New Material
Column 27	652.98789 m	16.55710 m	222.01195 kPa	543.26833 kPa	80.515227 kPa	37.04 kPa	0 kPa	New Material
Column 28	665.48789 m	18.26345 m	196.42453 kPa	417.47003 kPa	55.399767 kPa	37.04 kPa	0 kPa	New Material
Column 29	687.50000 m	21.82606 m	145.89573 kPa	265.95288 kPa	30.089454 kPa	37.04 kPa	0 kPa	New Material
Column 30	713.47880 m	27.02207 m	86.085204 kPa	139.56044 kPa	13.402289 kPa	37.04 kPa	0 kPa	New Material

### 3. TRASIENT CONDITIONS

#### a. Unconsolidated Undrained

X	Y	PWP	Base Normal Stress	Frictional Strength	Cohesive Strength	Suction Strength	Column Base Material	
Column 1	62.50000 m	304.90329 m	0 kPa	87.346714 kPa	21.891364 kPa	37.04 kPa	0 kPa	New Material
Column 2	87.50000 m	267.69628 m	0 kPa	380.18201 kPa	95.283525 kPa	37.04 kPa	0 kPa	New Material
Column 3	110.76003 m	237.65637 m	-737.24281 kPa	614.1128 kPa	153.91268 kPa	37.04 kPa	0 kPa	New Material
Column 4	132.28008 m	213.13655 m	-499.10693 kPa	802.34986 kPa	201.0898 kPa	37.04 kPa	0 kPa	New Material
Column 5	153.80014 m	191.08472 m	-285.17457 kPa	970.72324 kPa	243.28856 kPa	37.04 kPa	0 kPa	New Material
Column 6	175.32019 m	171.13639 m	-91.871238 kPa	1,123.142 kPa	281.48868 kPa	37.04 kPa	0 kPa	New Material

Column 7	196.32521 m	153.41665 m	79.632078 kPa	1,273.5753 kPa	299.2333 kPa	37.04 kPa	0 kPa	New Material
Column 8	216.81518 m	137.65095 m	232.02787 kPa	1,416.1684 kPa	296.7765 kPa	37.04 kPa	0 kPa	New Material
Column 9	237.30515 m	123.22344 m	371.30001 kPa	1,539.4567 kPa	292.77054 kPa	37.04 kPa	0 kPa	New Material
Column 10	257.79513 m	110.02076 m	498.56025 kPa	1,646.0932 kPa	287.60169 kPa	37.04 kPa	0 kPa	New Material
Column 11	278.28510 m	97.95019 m	614.71791 kPa	1,737.9237 kPa	281.50467 kPa	37.04 kPa	0 kPa	New Material
Column 12	298.77507 m	86.93500 m	720.52538 kPa	1,816.1 kPa	274.57957 kPa	37.04 kPa	0 kPa	New Material
Column 13	319.26504 m	76.91116 m	816.61077 kPa	1,881.1599 kPa	266.80376 kPa	37.04 kPa	0 kPa	New Material
Column 14	339.75501 m	67.82482 m	903.50208 kPa	1,933.0903 kPa	258.04166 kPa	37.04 kPa	0 kPa	New Material
Column 15	361.43467 m	59.20742 m	972.48256 kPa	1,972.7025 kPa	250.68119 kPa	37.04 kPa	0 kPa	New Material
Column 16	384.30402 m	51.12087 m	1,022.9449 kPa	1,997.7978 kPa	244.32355 kPa	37.04 kPa	0 kPa	New Material
Column 17	407.17336 m	44.05084 m	1,063.4384 kPa	2,003.491 kPa	235.6017 kPa	37.04 kPa	0 kPa	New Material
Column 18	434.30402 m	37.03549 m	1,098.0213 kPa	2,038.9 kPa	235.80875 kPa	37.04 kPa	0 kPa	New Material
Column 19	462.50000 m	30.96215 m	1,107.7654 kPa	2,074.6306 kPa	242.32164 kPa	37.04 kPa	0 kPa	New Material
Column 20	487.50000 m	26.81499 m	1,088.3933 kPa	2,052.189 kPa	241.55234 kPa	37.04 kPa	0 kPa	New Material

Column 21	512.50000 m	23.73953 m	1,055.3996 kPa	1,988.0453 kPa	233.74532 kPa	37.04 kPa	0 kPa	New Material
Column 22	537.50000 m	21.71930 m	1,008.9462 kPa	1,878.9322 kPa	218.04118 kPa	37.04 kPa	0 kPa	New Material
Column 23	562.50000 m	20.74364 m	944.68974 kPa	1,718.8343 kPa	194.02081 kPa	37.04 kPa	0 kPa	New Material
Column 24	587.50000 m	20.80748 m	862.68027 kPa	1,509.3088 kPa	162.06198 kPa	37.04 kPa	0 kPa	New Material
Column 25	612.50000 m	21.91115 m	768.89678 kPa	1,260.8746 kPa	123.30248 kPa	37.04 kPa	0 kPa	New Material
Column 26	637.50000 m	24.06040 m	663.28276 kPa	979.31538 kPa	79.206015 kPa	37.04 kPa	0 kPa	New Material
Column 27	662.50000 m	27.26657 m	579.68127 kPa	705.79819 kPa	31.60819 kPa	37.04 kPa	0 kPa	New Material
Column 28	677.46479 m	29.56783 m	545.27223 kPa	564.88573 kPa	4.9156535 kPa	37.04 kPa	0 kPa	New Material

b. Consolidated Drained

X	Y	PWP	Base Normal Stress	Frictional Strength	Cohesive Strength	Suction Strength	Column Base Material
Column 1	62.50000 m	312.94495 m	0 kPa	83.689564 kPa	56.875369 kPa	4 kPa	0 kPa New Material
Column 2	87.50000 m	289.61519 m	0 kPa	246.67837 kPa	167.64245 kPa	4 kPa	0 kPa New Material
Column 3	110.32789 m	269.56603 m	-1,050.1341 kPa	380.85009 kPa	258.82545 kPa	4 kPa	0 kPa New Material
Column 4	130.98367 m	252.47241 m	-884.73326 kPa	490.56198 kPa	333.38558 kPa	4 kPa	0 kPa New Material

Column 5	151.63945 m	236.26169 m	-727.99115 kPa	591.2374 kPa	401.80452 kPa	4 kPa	0 kPa	New Material
Column 6	172.29523 m	220.88205 m	-579.39939 kPa	683.85673 kPa	464.74855 kPa	4 kPa	0 kPa	New Material
Column 7	192.95101 m	206.28800 m	-438.51194 kPa	769.13324 kPa	522.70241 kPa	4 kPa	0 kPa	New Material
Column 8	213.60679 m	192.43941 m	-304.93522 kPa	847.51902 kPa	575.97333 kPa	4 kPa	0 kPa	New Material
Column 9	234.26257 m	179.30069 m	-178.3202 kPa	919.21002 kPa	624.69448 kPa	4 kPa	0 kPa	New Material
Column 10	254.91835 m	166.84015 m	-58.356027 kPa	984.15158 kPa	668.82872 kPa	4 kPa	0 kPa	New Material
Column 11	275.84046 m	154.88536 m	56.619395 kPa	1,046.9519 kPa	673.0293 kPa	4 kPa	0 kPa	New Material
Column 12	297.02890 m	143.42659 m	166.70145 kPa	1,103.3546 kPa	636.54885 kPa	4 kPa	0 kPa	New Material
Column 13	318.21734 m	132.59995 m	270.58429 kPa	1,147.0055 kPa	595.61525 kPa	4 kPa	0 kPa	New Material
Column 14	339.40578 m	122.38328 m	368.48504 kPa	1,178.4759 kPa	550.46922 kPa	4 kPa	0 kPa	New Material
Column 15	361.43467 m	112.39849 m	450.83773 kPa	1,198.3263 kPa	507.99272 kPa	4 kPa	0 kPa	New Material
Column 16	384.30402 m	102.67328 m	517.37043 kPa	1,206.2748 kPa	468.17895 kPa	4 kPa	0 kPa	New Material
Column 17	407.17336 m	93.59343 m	577.57424 kPa	1,201.3286 kPa	423.903 kPa	4 kPa	0 kPa	New Material
Column 18	426.45603 m	86.38506 m	623.94781 kPa	1,215.4525 kPa	401.9862 kPa	4 kPa	0 kPa	New Material

Column 19	442.15201 m	80.87342 m	658.20496 kPa	1,252.6569 kPa	403.9891 kPa	4 kPa	0 kPa	New Material
Column 20	462.50000 m	74.20350 m	683.69745 kPa	1,275.2028 kPa	401.98662 kPa	4 kPa	0 kPa	New Material
Column 21	487.50000 m	66.58067 m	698.41116 kPa	1,275.8896 kPa	392.45395 kPa	4 kPa	0 kPa	New Material
Column 22	512.50000 m	59.64717 m	703.25336 kPa	1,252.6448 kPa	373.366 kPa	4 kPa	0 kPa	New Material
Column 23	537.50000 m	53.38861 m	698.36517 kPa	1,203.8997 kPa	343.56092 kPa	4 kPa	0 kPa	New Material
Column 24	562.50000 m	47.79234 m	679.42314 kPa	1,124.261 kPa	302.31147 kPa	4 kPa	0 kPa	New Material
Column 25	587.50000 m	42.84732 m	646.53558 kPa	1,014.1267 kPa	249.81463 kPa	4 kPa	0 kPa	New Material
Column 26	612.50000 m	38.54399 m	605.77845 kPa	881.13103 kPa	187.12942 kPa	4 kPa	0 kPa	New Material
Column 27	637.50000 m	34.87420 m	557.23179 kPa	727.3249 kPa	115.59516 kPa	4 kPa	0 kPa	New Material
Column 28	661.87866 m	31.89165 m	534.81478 kPa	592.20538 kPa	39.002611 kPa	4 kPa	0 kPa	New Material

## APPENDIX C: Pictures



Site visit and sample collection in  
SHIKURUWE VILLAGE



Specific gravity test



Falling head permeability test



Sample preparation of Triaxial test specimen

2

**DETERMINATION OF LIQUID LIMIT & PLASTIC LIMIT**  
BS 1377-2:1990

**Project:** HORIZONTAL SUBDRAINAGE SYSTEM APPROACH TOWARDS LANDSLIDE HAZARD MITIGATION

**STUDENT:** MAMFA MAYALA and AHABWE MARTHA

**Sample Location:** SHIRURUWE VILLAGE

**Sample Reference:** 165.1      **Testing Date:** 25/Jan/25

**Sample Depth (m):** 1m      **Technician:** BAKAKI MICHAEL

**Sampling Date:** 1/20/2025      **Client Reference:** TP03

TEST NO.	LIQUID LIMIT				PLASTIC LIMIT		Average
	1	2	3	4	1	2	
Initial dial gauge reading mm	0.0	0.0	0.0	0.0	0.0	0.0	
Final dial gauge reading mm	15.60	15.60	18.10	20.90	20.90	24.33	
Average penetration mm	15.6	15.6	18.1	21.0	24.3		
Container No.	44	166	70	BNS	AI	74	69
Mass of wet soil + container (a)	28.17	28.85	29.07	29.43	28.07	29.04	30.45
Mass of dry soil + container (b)	23.90	22.81	23.91	23.67	23.72	23.75	24.42
Mass of container (c)	13.84	11.64	13.71	12.28	13.51	13.64	13.77
Mass of moisture (d = a-b)	4.21	6.04	5.16	5.76	5.35	5.28	6.03
Mass of dry soil (e = b-c)	10.02	11.17	10.20	11.38	10.21	10.12	10.65
Moisture content (w = 100X(d)/e)	42.02	54.07	50.59	50.62	52.40	52.17	56.62
Average Moisture content	48.0	50.6	52.3	56.6			50.1

$y = 1.0307x - 35.986$   
 $R^2 = 0.9799$

**Natural moisture content** \_\_\_\_\_ %

**Sample Preparation**

a) as received \_\_\_\_\_ °C

b) air dried \_\_\_\_\_ °C

c) washed on 0.425 mm \_\_\_\_\_ °C

d) oven dried 105-110 \_\_\_\_\_ °C

e) unknown \_\_\_\_\_ °C

Proportion passing 0.425 mm \_\_\_\_\_ %

**Liquid limit:**

LL \_\_\_\_\_ %

PL \_\_\_\_\_ %

PI \_\_\_\_\_ %

**LINEAR SHRINKAGE**

Initial length  $L_0$  mm      140 mm      Oven-dried length  $L_1$  mm      127.5 mm

Linear shrinkage,  $LS = 100 \times (1 - L_1/L_0)$  %      9.1 %      Shrinkage Product,  $SP = LS \times \% < 0.425 \mu m$       0

**Checked by:** \_\_\_\_\_      **Approved by:** \_\_\_\_\_

Laboratory Engineer      Senior Laboratory Engineer

1

**DETERMINATION OF LIQUID LIMIT & PLASTIC LIMIT**  
BS 1377-2:1990

**Project:** HORIZONTAL SUBDRAINAGE SYSTEM APPROACH TOWARDS LANDSLIDE HAZARD MITIGATION

**STUDENT:** MAMFA MAYALA and AHABWE MARTHA

**Sample Location:** SHIRURUWE VILLAGE

**Sample Reference:** 165.2      **Testing Date:** 25/Jan/25

**Sample Depth (m):** 1m      **Technician:** BAKAKI MICHAEL

**Sampling Date:** 1/20/2025      **Client Reference:** TP03

TEST NO.	LIQUID LIMIT				PLASTIC LIMIT		Average
	1	2	3	4	1	2	
Initial dial gauge reading mm	0.0	0.0	0.0	0.0	0.0	0.0	
Final dial gauge reading mm	15.55	15.05	18.15	18.15	20.75	24.98	
Average penetration mm	15.6	15.2	18.2	20.8	24.9		
Container No.	69	AV	990	TN	23	67	154
Mass of wet soil + container (a)	30.53	30.54	31.83	31.62	32.94	32.80	34.07
Mass of dry soil + container (b)	25.21	24.85	25.87	25.55	26.27	26.24	26.95
Mass of container (c)	13.78	12.62	13.08	13.08	13.23	13.08	12.90
Mass of moisture (d = a-b)	5.32	5.69	6.12	6.07	6.67	6.82	7.94
Mass of dry soil (e = b-c)	11.43	12.33	12.72	12.46	12.94	13.16	13.75
Moisture content (w = 100X(d)/e)	46.46	46.15	48.11	48.72	51.56	50.30	57.24
Average Moisture content	46.3	48.4	50.9	56.7			50.1

$y = 0.8762x - 24.815$   
 $R^2 = 0.9828$

**Natural moisture content** \_\_\_\_\_ %

**Sample Preparation**

a) as received \_\_\_\_\_ °C

b) air dried \_\_\_\_\_ °C

c) washed on 0.425 mm \_\_\_\_\_ °C

d) oven dried 105-110 \_\_\_\_\_ °C

e) unknown \_\_\_\_\_ °C

Proportion passing 0.425 mm \_\_\_\_\_ %

**Liquid limit:**

LL \_\_\_\_\_ %

PL \_\_\_\_\_ %

PI \_\_\_\_\_ %

**LINEAR SHRINKAGE**

Initial length  $L_0$  mm      140 mm      Oven-dried length  $L_1$  mm      127.5 mm

Linear shrinkage,  $LS = 100 \times (1 - L_1/L_0)$  %      9.1 %      Shrinkage Product,  $SP = LS \times \% < 0.425 \mu m$       0

**Checked by:** \_\_\_\_\_      **Approved by:** \_\_\_\_\_

Laboratory Engineer      Senior Laboratory Engineer

Atterberg Limit test for pit 1

FORM/ISO/06 ISSUE 02

**GETLAB LTD**  
YOUR RELIABLE ENGINEERING LABORATORY

**DETERMINATION OF LIQUID LIMIT & PLASTIC LIMIT**  
BS 1377-2:1990

Project: HORIZONTAL SUBDRAINAGE SYSTEM APPROACH TOWARDS LANDSLIDE HAZARD MITIGATION

STUDENT: MAMFA MAYALA and AHABWE MARTHA

Sample Location: SHIRURWE Village  
Sample Reference: 164.1  
Sample Depth (m): 1m  
Sampling Date: 1/20/2025  
Testing Date: 25/JAN/25  
Technician: BAKAKI MICHAEL  
Client Reference: TPO2

TEST NO.	LIQUID LIMIT				PLASTIC LIMIT		Average			
	1	2	3	4	1	2				
Initial dial gauge reading mm	0.0	0.0	0.0	0.0	0.0	0.0				
Final dial gauge reading mm	19.89	19.89	19.89	19.89	20.83	20.83	20.86			
Average penetration mm	19.9	19.7	20.4	20.4						
Container No.	T7	AO	190	106	BH6	SX	119	AT	MY	BH18
Mass of wet soil + container (a)	28.62	28.09	29.15	28.94	29.37	28.53	30.17	30.50	24.34	24.32
Mass of dry soil + container (b)	23.67	23.40	23.80	24.19	24.27	24.37	24.34	24.89	21.97	21.82
Mass of container (c)	12.78	12.26	12.61	12.91	13.40	13.61	13.36	13.80	13.17	13.46
Mass of moisture (d = a-b)	4.95	4.69	5.19	5.35	5.10	5.16	5.83	5.62	2.37	2.50
Mass of dry soil (e = b-c)	10.91	10.23	11.05	11.28	10.79	10.76	11.08	11.09	8.80	8.36
Moisture content (w = 100X(d)/e)	45.37	44.97	46.97	47.43	47.27	47.96	49.92	50.72	26.93	29.90
Average Moisture content	45.2	47.2	47.6	47.6	50.3				28.4	

Natural moisture content: \_\_\_\_\_ %

Sample Preparation:  
a) as received \_\_\_\_\_ °C  
b) air dried \_\_\_\_\_ °C  
c) washed on 0.425 mm \_\_\_\_\_ °C  
d) oven dried 105-110 \_\_\_\_\_ °C  
e) unknown \_\_\_\_\_ °C

Proportion passing 0.425 mm: \_\_\_\_\_ %

Liquid limit: LL \_\_\_\_\_ %

Plastic limit: PL \_\_\_\_\_ %

Plastic Index: PI \_\_\_\_\_ %

Liquid Limit: LL **47.6** %

Plastic Limit: PL **28.4** %

Plastic Index: PI **19.2** %

LINEAR SHRINKAGE

Initial length L<sub>0</sub> mm: 140 mm      Oven-dried length L<sub>d</sub> mm: 127.5 mm

Linear shrinkage, LS = 100X(L<sub>0</sub>-L<sub>d</sub>)/L<sub>0</sub> %: 0.1 %      Shrinkage Product, SP=LSX %<425 μm: 0

Checked by: \_\_\_\_\_ Approved by: \_\_\_\_\_

Laboratory Engineer: \_\_\_\_\_ Senior Laboratory Engineer: \_\_\_\_\_

FORM/ISO/06 ISSUE 02

**GETLAB LTD**  
YOUR RELIABLE ENGINEERING LABORATORY

**DETERMINATION OF LIQUID LIMIT & PLASTIC LIMIT**  
BS 1377-2:1990

Project: HORIZONTAL SUBDRAINAGE SYSTEM APPROACH TOWARDS LANDSLIDE HAZARD MITIGATION

STUDENT: MAMFA MAYALA and AHABWE MARTHA

Sample Location: SHIRURWE Village  
Sample Reference: 164.3  
Sample Depth (m): 1m  
Sampling Date: 1/20/2025  
Testing Date: 25/JAN/25  
Technician: BAKAKI MICHAEL  
Client Reference: TPO2

TEST NO.	LIQUID LIMIT				PLASTIC LIMIT		Average			
	1	2	3	4	1	2				
Initial dial gauge reading mm	0.0	0.0	0.0	0.0	0.0	0.0				
Final dial gauge reading mm	15.87	15.87	16.73	16.73	22.84	20.84	24.00			
Average penetration mm	16.0	16.7	20.8	20.8						
Container No.	194	162	301	112	374	89	401	180	B9	86
Mass of wet soil + container (a)	28.19	28.03	29.72	29.10	29.63	29.15	30.59	30.60	23.63	23.60
Mass of dry soil + container (b)	23.32	23.40	24.26	23.89	23.68	24.89	24.55	25.30	21.30	21.28
Mass of container (c)	12.42	13.29	12.65	12.79	11.69	13.41	13.46	12.87	12.68	13.54
Mass of moisture (d = a-b)	4.87	4.63	5.46	5.21	5.94	5.17	6.70	6.05	2.33	2.32
Mass of dry soil (e = b-c)	10.90	10.11	11.61	11.10	12.00	10.57	11.43	11.88	8.62	7.74
Moisture content (w = 100X(d)/e)	44.68	45.80	47.03	46.94	49.50	48.91	49.87	51.01	27.03	29.97
Average Moisture content	45.2	47.0	47.0	49.2	50.4				28.5	

Natural moisture content: \_\_\_\_\_ %

Sample Preparation:  
a) as received \_\_\_\_\_ °C  
b) air dried \_\_\_\_\_ °C  
c) washed on 0.425 mm \_\_\_\_\_ °C  
d) oven dried 105-110 \_\_\_\_\_ °C  
e) unknown \_\_\_\_\_ °C

Proportion passing 0.425 mm: \_\_\_\_\_ %

Liquid limit: LL \_\_\_\_\_ %

Plastic limit: PL \_\_\_\_\_ %

Plastic Index: PI \_\_\_\_\_ %

Liquid Limit: LL **48.0** %

Plastic Limit: PL **28.5** %

Plastic Index: PI **19.5** %

LINEAR SHRINKAGE

Initial length L<sub>0</sub> mm: 140 mm      Oven-dried length L<sub>d</sub> mm: 127.5 mm

Linear shrinkage, LS = 100X(L<sub>0</sub>-L<sub>d</sub>)/L<sub>0</sub> %: 0.1 %      Shrinkage Product, SP=LSX %<425 μm: 0

Checked by: \_\_\_\_\_ Approved by: \_\_\_\_\_

Laboratory Engineer: \_\_\_\_\_ Senior Laboratory Engineer: \_\_\_\_\_

FORM/ISO/06 ISSUE 02

**GETLAB LTD**  
YOUR RELIABLE ENGINEERING LABORATORY

**DETERMINATION OF LIQUID LIMIT & PLASTIC LIMIT**  
BS 1377-2:1990

Project: HORIZONTAL SUBDRAINAGE SYSTEM APPROACH TOWARDS LANDSLIDE HAZARD MITIGATION

STUDENT: MAMFA MAYALA and AHABWE MARTHA

Sample Location: SHIRURWE Village  
Sample Reference: 164.2-1  
Sample Depth (m): 1m  
Sampling Date: 1/20/2025  
Testing Date: 25/JAN/25  
Technician: BAKAKI MICHAEL  
Client Reference: TPO2

TEST NO.	LIQUID LIMIT				PLASTIC LIMIT		Average			
	1	2	3	4	1	2				
Initial dial gauge reading mm	0.0	0.0	0.0	0.0	0.0	0.0				
Final dial gauge reading mm	15.65	15.85	17.98	17.98	20.38	20.38	24.28			
Average penetration mm	15.5	16.0	20.4	20.4						
Container No.	P4	50	142	193	54	156	121	88	621	BM10
Mass of wet soil + container (a)	29.78	29.37	29.86	28.42	29.70	29.85	31.19	31.17	23.50	23.50
Mass of dry soil + container (b)	24.67	24.56	24.79	23.70	24.33	24.62	25.64	25.04	21.16	21.29
Mass of container (c)	12.87	13.54	13.57	13.28	12.75	13.12	12.50	12.66	13.39	12.99
Mass of moisture (d = a-b)	5.08	4.81	5.07	4.72	5.37	5.23	6.06	6.13	2.34	2.21
Mass of dry soil (e = b-c)	11.79	11.02	11.22	10.42	11.58	11.50	12.91	12.38	7.77	8.30
Moisture content (w = 100X(d)/e)	43.42	43.65	45.19	45.35	48.37	45.48	48.53	49.67	30.12	28.63
Average Moisture content	43.5	45.2	45.8	45.8	48.9				28.4	

Natural moisture content: \_\_\_\_\_ %

Sample Preparation:  
a) as received \_\_\_\_\_ °C  
b) air dried \_\_\_\_\_ °C  
c) washed on 0.425 mm \_\_\_\_\_ °C  
d) oven dried 105-110 \_\_\_\_\_ °C  
e) unknown \_\_\_\_\_ °C

Proportion passing 0.425 mm: \_\_\_\_\_ %

Liquid limit: LL \_\_\_\_\_ %

Plastic limit: PL \_\_\_\_\_ %

Plastic Index: PI \_\_\_\_\_ %

Liquid Limit: LL **46.2** %

Plastic Limit: PL **28.4** %

Plastic Index: PI **17.6** %

LINEAR SHRINKAGE

Initial length L<sub>0</sub> mm: 140 mm      Oven-dried length L<sub>d</sub> mm: 127.5 mm

Linear shrinkage, LS = 100X(L<sub>0</sub>-L<sub>d</sub>)/L<sub>0</sub> %: 0.1 %      Shrinkage Product, SP=LSX %<425 μm: 0

Checked by: \_\_\_\_\_ Approved by: \_\_\_\_\_

Laboratory Engineer: \_\_\_\_\_ Senior Laboratory Engineer: \_\_\_\_\_

Atterberg Limit test for pit 2



FORM/SO/06 7 ISSUE 02

### GETLAB LTD YOUR RELIABLE ENGINEERING LABORATORY

**DETERMINATION OF LIQUID LIMIT & PLASTIC LIMIT**  
BS 1377-2:1990

Project: HORIZONTAL SUBDRAINAGE SYSTEM APPROACH TOWARDS LANDSLIDE HAZARD MITIGATION

STUDENT: MAMFA MAYALA and AHABWE MARTHA

Sample Location: SHIKURUWE Village  
Sample Reference: 163.2  
Sample Depth (m): 1m  
Testing Date: 25/JAN/25  
Technician: BAKAKI MICHAEL  
Client Reference: TPO1

TEST NO.	LIQUID LIMIT				PLASTIC LIMIT		Average
	1	2	3	4	1	2	
Initial dial gauge reading mm	0.0	0.0	0.0	0.0	0.0	0.0	0.0
Final dial gauge reading mm	15.03	15.03	16.76	16.76	21.07	21.07	24.26
Average penetration mm	15.0	15.0	16.88	16.88	21.1	21.1	24.2
Container No.	BL 35	BH3	21	26	BM2	X65	192
Mass of wet soil + container (a)	26.28	26.69	29.60	29.82	28.03	28.71	32.22
Mass of dry soil + container (b)	23.70	24.29	24.52	24.68	23.89	23.64	26.67
Mass of container (c)	12.61	13.68	12.78	13.57	12.60	13.14	13.56
Mass of moisture (d = a-b)	4.58	4.44	5.08	4.96	5.04	4.87	6.33
Mass of dry soil (e = b-c)	11.09	10.57	11.73	11.29	11.29	10.70	12.61
Moisture content (w = 100X(d)/e)	41.30	42.81	43.31	43.93	44.64	45.51	48.63
Average Moisture content	41.7	43.6	43.6	45.1	45.4	47.4	27.4

Graph showing Cone Penetration (mm) on the y-axis (14 to 26) and Moisture Content (%) on the x-axis (41 to 48). The data points form a straight line with the equation  $y = 1.5789x - 50.450$  and  $R^2 = 0.9919$ .

Natural moisture content: \_\_\_\_\_ %

Sample Preparation:

- a) as received \_\_\_\_\_ °C
- b) air dried \_\_\_\_\_ °C
- c) washed on 0.425 mm \_\_\_\_\_ °C
- d) oven dried 105-110 \_\_\_\_\_ °C
- e) unknown \_\_\_\_\_ °C

Proportion passing 0.425 mm: \_\_\_\_\_ %

Liquid limit: LL \_\_\_\_\_ %

Plastic limit: PL \_\_\_\_\_ %

Plastic Index: PI \_\_\_\_\_ %

LINEAR SHRINKAGE

Initial length  $L_0$ , mm: 140 mm    Oven-dried length  $L_1$ , mm: 127.5 mm

Linear shrinkage,  $LS = 100 \times (1 - L_1/L_0)$  %: 9.1 %    Shrinkage Product,  $SP = LS \times L_0$  mm: 0

Checked by: [Signature]    Approved by: [Signature]

Laboratory Engineer: [Signature]    Senior Laboratory Engineer: [Signature]

**GETLAB LTD**  
Geotechnical Engineering & Technology Laboratory Ltd  
P.O. Box 10066, Kampala

FORM/SO/06 6 ISSUE 02

### GETLAB LTD YOUR RELIABLE ENGINEERING LABORATORY

**DETERMINATION OF LIQUID LIMIT & PLASTIC LIMIT**  
BS 1377-2:1990

Project: HORIZONTAL SUBDRAINAGE SYSTEM APPROACH TOWARDS LANDSLIDE HAZARD MITIGATION

STUDENT: MAMFA MAYALA and AHABWE MARTHA

Sample Location: SHIKURUWE Village  
Sample Reference: 163.3  
Sample Depth (m): 1m  
Testing Date: 25/JAN/25  
Technician: BAKAKI MICHAEL  
Client Reference: TPO1

TEST NO.	LIQUID LIMIT				PLASTIC LIMIT		Average
	1	2	3	4	1	2	
Initial dial gauge reading mm	0.0	0.0	0.0	0.0	0.0	0.0	0.0
Final dial gauge reading mm	15.82	15.82	18.44	18.44	20.88	20.88	24.85
Average penetration mm	15.8	15.8	18.4	18.4	20.9	20.9	24.9
Container No.	563	56	M8	57	194	34	554
Mass of wet soil + container (a)	23.63	23.81	25.95	26.67	25.95	25.85	31.33
Mass of dry soil + container (b)	20.35	20.43	22.07	21.92	20.65	20.53	25.73
Mass of container (c)	13.35	12.97	13.50	13.49	11.86	13.19	13.49
Mass of moisture (d = a-b)	3.13	3.44	3.82	3.75	5.72	5.37	6.07
Mass of dry soil (e = b-c)	7.16	7.88	8.57	8.43	11.59	11.34	12.24
Moisture content (w = 100X(d)/e)	43.78	43.77	45.71	44.48	47.78	47.35	51.22
Average Moisture content	43.8	43.8	45.1	44.6	47.6	47.6	27.2

Graph showing Cone Penetration (mm) on the y-axis (14 to 26) and Moisture Content (%) on the x-axis (43 to 53). The data points form a straight line with the equation  $y = 1.1714x - 34.954$  and  $R^2 = 0.9867$ .

Natural moisture content: \_\_\_\_\_ %

Sample Preparation:

- a) as received \_\_\_\_\_ °C
- b) air dried \_\_\_\_\_ °C
- c) washed on 0.425 mm \_\_\_\_\_ °C
- d) oven dried 105-110 \_\_\_\_\_ °C
- e) unknown \_\_\_\_\_ °C

Proportion passing 0.425 mm: \_\_\_\_\_ %

Liquid limit: LL \_\_\_\_\_ %

Plastic limit: PL \_\_\_\_\_ %

Plastic Index: PI \_\_\_\_\_ %

LINEAR SHRINKAGE

Initial length  $L_0$ , mm: 140 mm    Oven-dried length  $L_1$ , mm: 127.5 mm

Linear shrinkage,  $LS = 100 \times (1 - L_1/L_0)$  %: 9.1 %    Shrinkage Product,  $SP = LS \times L_0$  mm: 0

Checked by: [Signature]    Approved by: [Signature]

Laboratory Engineer: [Signature]    Senior Laboratory Engineer: [Signature]

**GETLAB LTD**  
Geotechnical Engineering & Technology Laboratory Ltd  
P.O. Box 10066, Kampala

FORM/SO/06 8 ISSUE 02

### GETLAB LTD YOUR RELIABLE ENGINEERING LABORATORY

**DETERMINATION OF LIQUID LIMIT & PLASTIC LIMIT**  
BS 1377-2:1990

Project: HORIZONTAL SUBDRAINAGE SYSTEM APPROACH TOWARDS LANDSLIDE HAZARD MITIGATION

STUDENT: MAMFA MAYALA and AHABWE MARTHA

Sample Location: SHIKURUWE Village  
Sample Reference: 163.1  
Sample Depth (m): 1m  
Testing Date: 25/JAN/25  
Technician: BAKAKI MICHAEL  
Client Reference: TPO1

TEST NO.	LIQUID LIMIT				PLASTIC LIMIT		Average
	1	2	3	4	1	2	
Initial dial gauge reading mm	0.0	0.0	0.0	0.0	0.0	0.0	0.0
Final dial gauge reading mm	15.33	15.33	18.83	18.83	20.63	20.63	24.41
Average penetration mm	15.3	15.3	18.8	18.8	20.6	20.6	24.4
Container No.	98	183	BH1	87	BY	33	180
Mass of wet soil + container (a)	28.02	28.16	29.54	29.80	29.81	29.20	32.14
Mass of dry soil + container (b)	23.70	23.64	24.34	25.09	24.40	24.21	26.28
Mass of container (c)	13.46	12.78	12.39	13.96	12.68	13.63	13.24
Mass of moisture (d = a-b)	4.32	4.54	5.20	4.81	5.35	5.08	6.11
Mass of dry soil (e = b-c)	10.24	10.86	11.95	11.13	11.80	11.13	12.64
Moisture content (w = 100X(d)/e)	42.27	41.80	43.51	42.83	45.08	44.83	48.75
Average Moisture content	42.0	43.2	43.2	45.0	45.6	45.6	28.4

Graph showing Cone Penetration (mm) on the y-axis (14 to 26) and Moisture Content (%) on the x-axis (42 to 47). The data points form a straight line with the equation  $y = 1.8407x - 61.58$  and  $R^2 = 0.9660$ .

Natural moisture content: \_\_\_\_\_ %

Sample Preparation:

- a) as received \_\_\_\_\_ °C
- b) air dried \_\_\_\_\_ °C
- c) washed on 0.425 mm \_\_\_\_\_ °C
- d) oven dried 105-110 \_\_\_\_\_ °C
- e) unknown \_\_\_\_\_ °C

Proportion passing 0.425 mm: \_\_\_\_\_ %

Liquid limit: LL \_\_\_\_\_ %

Plastic limit: PL \_\_\_\_\_ %

Plastic Index: PI \_\_\_\_\_ %

LINEAR SHRINKAGE

Initial length  $L_0$ , mm: 140 mm    Oven-dried length  $L_1$ , mm: 127.5 mm

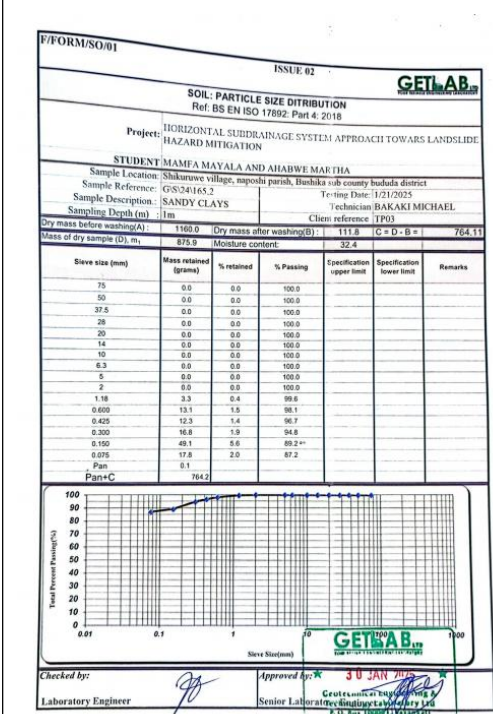
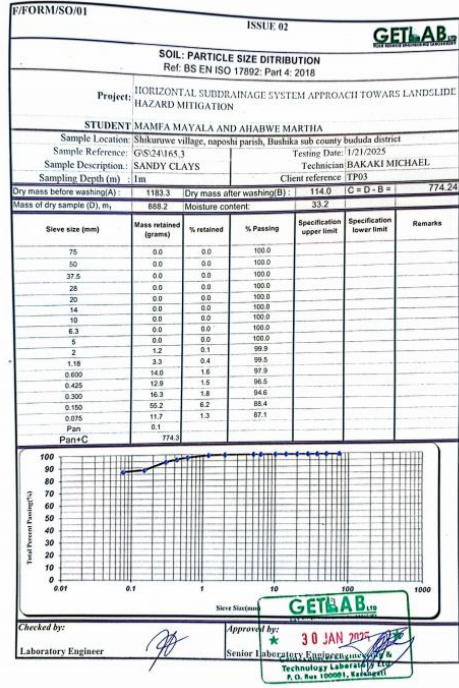
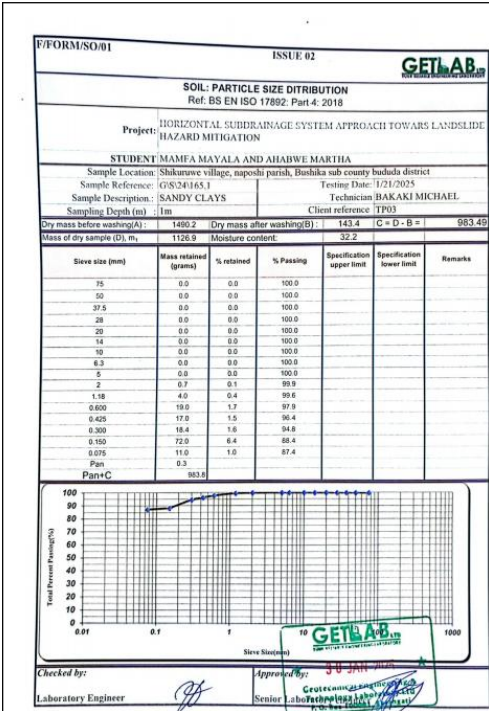
Linear shrinkage,  $LS = 100 \times (1 - L_1/L_0)$  %: 9.1 %    Shrinkage Product,  $SP = LS \times L_0$  mm: 0

Checked by: [Signature]    Approved by: [Signature]

Laboratory Engineer: [Signature]    Senior Laboratory Engineer: [Signature]

**GETLAB LTD**  
Geotechnical Engineering & Technology Laboratory Ltd  
P.O. Box 10066, Kampala

Atterberg test for pit 3



Particle size distribution for pit 1

F/FORM/SO/01 ISSUE 02 **GETLAB**  
**SOIL: PARTICLE SIZE DISTRIBUTION**  
 Ref: BS EN ISO 17892: Part 4: 2018

Project: HORIZONTAL SUBDRAINAGE SYSTEM APPROACH TOWARDS LANDSLIDE HAZARD MITIGATION

STUDENT: MAMFA MAYALA AND AHABWE MARTHA

Sample Location: Shikurwe village, naposhi parish, Bushika sub county bududa district  
 Sample Reference: GS/24/164.1 Testing Date: 1/21/2025  
 Sample Description: SANDY CLAYS Technician: BAKAKI MICHAEL  
 Sampling Depth (m): 1m Client reference: TP02

Dry mass before washing(A): 1484.2 Dry mass after washing(B): 158.9 C = D - B = 967.02  
 Mass of dry sample (D), m: 1126.8 Moisture content: 31.7

Sieve size (mm)	Mass retained (grams)	% retained	% Passing	Specification upper limit	Specification lower limit	Remarks
75	0.0	0.0	100.0			
50	0.0	0.0	100.0			
37.5	0.0	0.0	100.0			
28	0.0	0.0	100.0			
20	0.0	0.0	100.0			
14	0.0	0.0	100.0			
10	3.7	0.3	99.7			
6.3	0.0	0.0	99.7			
4	2.1	0.2	99.7			
2	1.2	0.1	99.8			
1.18	3.9	0.3	99.2			
0.600	18.0	1.6	97.6			
0.425	17.8	1.6	96.9			
0.300	21.6	1.9	94.1			
0.150	78.4	6.7	87.4			
0.075	18.1	1.4	88.0			
Pan	9.2					
Pan+C	96.1					

Checked by: [Signature] Approved by: [Signature] 30 JAN 2025  
 Laboratory Engineer Senior Laboratory Engineer  
**GETLAB**  
 Geotechnical Laboratory Ltd  
 P. O. Box 100801, Kampala

F/FORM/SO/01 ISSUE 02 **GETLAB**  
**SOIL: PARTICLE SIZE DISTRIBUTION**  
 Ref: BS EN ISO 17892: Part 4: 2018

Project: HORIZONTAL SUBDRAINAGE SYSTEM APPROACH TOWARDS LANDSLIDE HAZARD MITIGATION

STUDENT: MAMFA MAYALA AND AHABWE MARTHA

Sample Location: Shikurwe village, naposhi parish, Bushika sub county bududa district  
 Sample Reference: GS/24/164.3 Testing Date: 1/21/2025  
 Sample Description: SANDY CLAYS Technician: BAKAKI MICHAEL  
 Sampling Depth (m): 1m Client reference: TP02

Dry mass before washing(A): 1355.2 Dry mass after washing(B): 141.9 C = D - B = 904.28  
 Mass of dry sample (D), m: 1046.2 Moisture content: 29.5

Sieve size (mm)	Mass retained (grams)	% retained	% Passing	Specification upper limit	Specification lower limit	Remarks
75	0.0	0.0	100.0			
50	0.0	0.0	100.0			
37.5	0.0	0.0	100.0			
28	0.0	0.0	100.0			
20	0.0	0.0	100.0			
14	0.0	0.0	100.0			
10	0.0	0.0	100.0			
6.3	0.9	0.1	99.9			
5	0.0	0.0	99.9			
2	0.5	0.0	99.9			
1.18	2.9	0.4	99.5			
0.600	17.6	1.7	97.8			
0.425	15.8	1.5	96.3			
0.300	19.4	1.9	94.4			
0.150	71.9	6.9	87.6			
0.075	12.1	1.2	85.4			
Pan	0.1					
Pan+C	904.4					

Checked by: [Signature] Approved by: [Signature] 30 JAN 2025  
 Laboratory Engineer Senior Laboratory Engineer  
**GETLAB**  
 Geotechnical Laboratory Ltd  
 P. O. Box 100801, Kampala

F/FORM/SO/01 ISSUE 02 **GETLAB**  
**SOIL: PARTICLE SIZE DISTRIBUTION**  
 Ref: BS EN ISO 17892: Part 4: 2018

Project: HORIZONTAL SUBDRAINAGE SYSTEM APPROACH TOWARDS LANDSLIDE HAZARD MITIGATION

STUDENT: MAMFA MAYALA AND AHABWE MARTHA

Sample Location: Shikurwe village, naposhi parish, Bushika sub county bududa district  
 Sample Reference: GS/24/164.2 Testing Date: 1/21/2025  
 Sample Description: SANDY CLAYS Technician: BAKAKI MICHAEL  
 Sampling Depth (m): 1m Client reference: TP02

Dry mass before washing(A): 1358.4 Dry mass after washing(B): 134.6 C = D - B = 898.88  
 Mass of dry sample (D), m: 1033.5 Moisture content: 31.2

Sieve size (mm)	Mass retained (grams)	% retained	% Passing	Specification upper limit	Specification lower limit	Remarks
75	0.0	0.0	100.0			
50	0.0	0.0	100.0			
37.5	0.0	0.0	100.0			
28	0.0	0.0	100.0			
20	0.0	0.0	100.0			
14	0.0	0.0	100.0			
10	0.0	0.0	100.0			
6.3	0.9	0.0	100.0			
5	0.0	0.0	100.0			
2	0.4	0.0	99.9			
1.18	3.7	0.4	99.5			
0.600	16.5	1.5	98.1			
0.425	16.4	1.5	96.8			
0.300	18.2	1.8	94.8			
0.150	64.4	6.2	88.5			
0.075	15.9	1.5	87.0			
Pan	0.1					
Pan+C	899.0					

Checked by: [Signature] Approved by: [Signature] 30 JAN 2025  
 Laboratory Engineer Senior Laboratory Engineer  
**GETLAB**  
 Geotechnical Laboratory Ltd  
 P. O. Box 100801, Kampala

Particle size distribution for pit 2

F/FORM/SO/01 ISSUE 02 **GETLAB**  
**SOIL: PARTICLE SIZE DISTRIBUTION**  
 Ref: BS EN ISO 17892: Part 4: 2018

Project: HORIZONTAL SUBDRAINAGE SYSTEM APPROACH TOWARDS LANDSLIDE HAZARD MITIGATION

STUDENT: MAMFA MAYALA AND AHABWE MARTHA

Sample Location: Shikuruwe village, naposhi parish, Bushika sub county bududa district  
 Sample Reference: G/S/24/163.1 Testing Date: 1/21/2025  
 Sample Description: SANDY CLAYS Technician: BAKAKI MICHAEL  
 Sampling Depth (m): 1m Client reference: TP01

Dry mass before washing(A): 1601.1 Dry mass after washing(B): 171.5 C = D - B = 1099.58

Mass of dry sample (D), m<sub>s</sub>: 1271.1 Moisture content: 26.0

Sieve size (mm)	Mass retained (grams)	% retained	% Passing	Specification upper limit	Specification lower limit	Remarks
75	0.0	0.0	100.0			
50	0.0	0.0	100.0			
37.5	0.0	0.0	100.0			
28	0.0	0.0	100.0			
20	0.0	0.0	100.0			
14	0.0	0.0	100.0			
10	0.0	0.0	100.0			
6.3	0.0	0.0	100.0			
5	0.0	0.0	100.0			
2	1.6	0.1	99.9			
1.18	5.4	0.4	99.4			
0.850	21.3	1.7	97.8			
0.425	19.3	1.5	98.2			
0.300	24.2	1.9	94.3			
0.150	78.4	6.2	88.2			
0.075	21.3	1.7	88.5			
Pan	0.2					
Pan+C	1099.8					

Checked by: [Signature] Approved by: [Signature] 30 JAN 2025  
 Laboratory Engineer Senior laboratory engineer  
 Geotechnical Engineering & Technology Laboratory Ltd  
 P. O. Box 150001, Kampala

F/FORM/SO/01 ISSUE 02 **GETLAB**  
**SOIL: PARTICLE SIZE DISTRIBUTION**  
 Ref: BS EN ISO 17892: Part 4: 2018

Project: HORIZONTAL SUBDRAINAGE SYSTEM APPROACH TOWARDS LANDSLIDE HAZARD MITIGATION

STUDENT: MAMFA MAYALA AND AHABWE MARTHA

Sample Location: Shikuruwe village, naposhi parish, Bushika sub county bududa district  
 Sample Reference: G/S/24/163.3 Testing Date: 1/21/2025  
 Sample Description: SANDY CLAYS Technician: BAKAKI MICHAEL  
 Sampling Depth (m): 1m Client reference: TP01

Dry mass before washing(A): 1538.8 Dry mass after washing(B): 165.4 C = D - B = 1047.70

Mass of dry sample (D), m<sub>s</sub>: 1213.1 Moisture content: 26.7

Sieve size (mm)	Mass retained (grams)	% retained	% Passing	Specification upper limit	Specification lower limit	Remarks
75	0.0	0.0	100.0			
50	0.0	0.0	100.0			
37.5	0.0	0.0	100.0			
28	0.0	0.0	100.0			
20	0.0	0.0	100.0			
14	0.0	0.0	100.0			
10	0.0	0.0	100.0			
6.3	0.0	0.0	100.0			
5	0.0	0.0	100.0			
2	1.6	0.1	99.9			
1.18	5.3	0.4	99.4			
0.850	22.2	1.8	97.8			
0.425	19.4	1.6	98.0			
0.300	21.7	1.8	94.2			
0.150	78.0	6.4	87.8			
0.075	18.6	1.4	88.4			
Pan	0.1					
Pan+C	1047.8					

Checked by: [Signature] Approved by: [Signature] 30 JAN 2025  
 Laboratory Engineer Senior laboratory engineer  
 Geotechnical Engineering & Technology Laboratory Ltd  
 P. O. Box 150001, Kampala

F/FORM/SO/01 ISSUE 02 **GETLAB**  
**SOIL: PARTICLE SIZE DISTRIBUTION**  
 Ref: BS EN ISO 17892: Part 4: 2018

Project: HORIZONTAL SUBDRAINAGE SYSTEM APPROACH TOWARDS LANDSLIDE HAZARD MITIGATION

STUDENT: MAMFA MAYALA AND AHABWE MARTHA

Sample Location: Shikuruwe village, naposhi parish, Bushika sub county bududa district  
 Sample Reference: G/S/24/163.2 Testing Date: 1/21/2025  
 Sample Description: SANDY CLAYS Technician: BAKAKI MICHAEL  
 Sampling Depth (m): 1m Client reference: TP01

Dry mass before washing(A): 1423.9 Dry mass after washing(B): 146.5 C = D - B = 976.56

Mass of dry sample (D), m<sub>s</sub>: 1123.1 Moisture content: 26.8

Sieve size (mm)	Mass retained (grams)	% retained	% Passing	Specification upper limit	Specification lower limit	Remarks
75	0.0	0.0	100.0			
50	0.0	0.0	100.0			
37.5	0.0	0.0	100.0			
28	0.0	0.0	100.0			
20	0.0	0.0	100.0			
14	0.0	0.0	100.0			
10	0.0	0.0	100.0			
6.3	0.0	0.0	100.0			
5	0.0	0.0	100.0			
2	0.9	0.1	99.9			
1.18	4.9	0.4	99.5			
0.850	19.7	1.8	97.7			
0.425	17.1	1.5	98.2			
0.300	18.8	1.7	94.5			
0.150	71.4	6.4	88.2			
0.075	13.5	1.2	87.0			
Pan	0.1					
Pan+C	976.7					

Checked by: [Signature] Approved by: [Signature] 30 JAN 2025  
 Laboratory Engineer Senior laboratory engineer  
 Geotechnical Engineering & Technology Laboratory Ltd  
 P. O. Box 150001, Kampala

Particle size distribution for pit 1

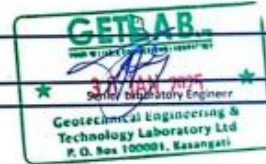
**SOIL: PARTICLE DENSITY (USING A PYKNOMETER)**  
 Ref: BS EN ISO 17892-3:2018

Project Name:	HORIZONTAL SUBDRAINAGE SYSTEM APPROACH TOWARDS LANDSLIDE HAZARD					
Student:	AHABWE MARTHA AND CYNTHIA MAYALA					
Technician:	BAKAWI MICHAEL					
Testing Date:	10/5/2024					
Sample Reference:	G/S/25/183.1	G/S/25/183.2	G/S/25/183.3	G/S/25/183.4	G/S/25/183.5	G/S/25/183.6
Pyknometer No:	C	L	T	S	B	Q
Mass of bottle (g) $M_1$	111.9	111.5	123.9	122.4	100.8	118.8
Mass of bottle + soil (g) $M_2$	501.7	161.5	173.7	172.7	151	169
Mass of bottle + soil water (g) $M_3$	412.4	412.9	417.8	413.5	399.7	405.4
Mass of bottle + water (g) $M_4$	381	381.5	388.1	383.8	359	378.1
Specific Gravity, $G_s$	2.65	2.85	2.49	2.44	2.58	2.53

Sample Reference:	G/S/25/164.1	G/S/25/164.2	G/S/25/164.3
Pyknometer No:	L	M	35
Mass of bottle (g) $M_1$	113.3	110.5	105.4
Mass of bottle + soil (g) $M_2$	163.2	180.2	153.2
Mass of bottle + soil water (g) $M_3$	418.2	406.6	397
Mass of bottle + water (g) $M_4$	385.5	385.5	363.8
Specific Gravity, $G_s$	2.50	2.67	2.66

Tested by: *[Signature]* Checked by: \_\_\_\_\_  
 Laboratory Engineer



Specific gravity test for pit 1,2,and 3

# CHC ANALYSIS UG LIMITED WORK SHEET



Report No : C250265

Document No.CHC-WS-028

## DETERMINATION OF PERMEABILITY OF SOIL (FALLING HEAD)

Test method: BS EN ISO 17892-11:2019

Project:		N/A									
Project location					Sample depth (m)		N/A				
Lab number		C250265001			Trial Pit Number		N/A				
Sample Description		Soil									
Preparation method		Prepared in accordance with BS 1377-1-2016									
Test Records											
DETAILS OF THE SPECIMEN				Wet Weight of the sample +Ring		323		Initial Moisture content (%)		35.8	
Specimen Diameter (D) cm		6.00		Dry Weight of the sample +Ring		265.0		Final Moisture content (%)		35.6	
Specimen Height (L) cm		4.00		Bulky Density (kg/m <sup>3</sup> )		1938		Void Ratio e		0.89	
Specimen area (A) cm <sup>2</sup>		28.3		Dry Density (kg/m <sup>3</sup> )		1402					
Water Temperature (T) °C		24.5		Specific Gravity		2.65		Degree of saturation		106	
Stand Pipe Area a (cm <sup>2</sup> )		0.33									
Hydraulic gradient		1.25									
MDD (kg/m <sup>3</sup> )		1355		Compaction(%)				103			
Serial No.	Lab No.	Start Time/Date	End Time/Date	Change in Time(sec) Δt	Discharge Q (ml)	Δh1(cm)	Δh2 (cm)	k(m/s)	Average		
1	C250265001	1:27pm (28/1/2025)	3:27pm (28/1/2025)	7200	1.659	90.0	85.0	3.73E-09	2.44E-09		
		3:27pm (28/1/2025)	9:29am (29/1/2025)	64920	8.030	85.0	60.8	2.42E-09			
		9:29am (29/1/2025)	1:01pm (29/1/2025)	12720	0.630	60.8	58.9	1.17E-09			

Technician:Barbrah

Checked Titus

Date: 29/01/2025

Falling Head permeability test for pit 1



## CHC ANALYSIS UG LIMITED WORK SHEET



Report No : C25026S

Document No.CHC-WS-028

### DETERMINATION OF PERMEABILITY OF SOIL (FALLING HEAD)

Test method: BS EN ISO 17892-11:2019

Project:		N/A									
Project location				Sample depth (m)		N/A					
Lab number		C25026S002		Trial Pit Number		N/A					
Sample Description		Soil									
Preparation method		Prepared in accordance with BS 1377-1-2016									
Test Records											
DETAILS OF THE SPECIMEN				Wet Weight of the sample +Ring		321		Initial Moisture content (%)		37.0	
Specimen Diameter (D) cm		6.00		Dry Weight of the sample +Ring		263.2		Final Moisture content (%)		35.8	
Specimen Height (L) cm		4.00		Bulky Density (kg/m <sup>3</sup> )		1928		Void Ratio e		0.91	
Specimen area (A) cm <sup>2</sup>		28.3		Dry Density (kg/m <sup>3</sup> )		1386					
Water Temperature (T) °C		24.5		Specific Gravity		2.65		Degree of saturation		104	
Stand Pipe Area a (cm <sup>2</sup> )		0.33		Hydraulic gradient		6.15					
MDD (kg/m <sup>3</sup> )		1325		Compaction(%)				105			
Serial No.	Lab No.	Start Time/Date	End Time/Date	Change in Time(sec) Δt	Discharge Q (ml)	Δht1(cm)	Δht2 (cm)	k(m/s)	Average		
1	C25026S002	1:41pm (28/1/2025)	1:52pm (28/1/2025)	660	8.163	90.5	65.9	2.26E-07	1.58E-07		
		1:52pm (28/1/2025)	2:34pm (28/1/2025)	2520	15.131	65.9	20.3	2.19E-07			
		2:37pm (28/1/2025)	2:56pm (28/1/2025)	1140	9.955	90.5	60.5	1.66E-07			
		2:58pm (28/1/2025)	4:02pm (28/1/2025)	3840	12.610	60.5	22.5	1.21E-07			
		4:03pm (28/1/2025)	4:25pm (28/1/2025)	1320	8.661	90.5	64.5	1.21E-07			
		4:25pm (28/1/2025)	5:31pm (28/1/2025)	3960	11.913	64.5	28.6	9.64E-08			

Technician:Barbrah

Checked Titus

Date: 29/01/2025

Falling Head Permeability test for pit 2



## CHC ANALYSIS UG LIMITED WORK SHEET



Report No : C25026S

Document No.CHC-WS-028

### DETERMINATION OF PERMEABILITY OF SOIL (FALLING HEAD)

Test method: BS EN ISO 17892-11:2019

Project:		N/A							
Project location				Sample depth (m)		N/A			
Lab number		C25026S003		Trial Pit Number		N/A			
Sample Description		Soil							
Preparation method		Prepared in accordance with BS 1377-1-2016							
Test Records									
DETAILS OF THE SPECIMEN		Wet Weight of the sample +Ring		324		Initial Moisture content (%)		34.4	
Specimen Diameter (D) cm		6.00		Dry Weight of the sample +Ring		265.9		Final Moisture content (%)	
Specimen Height (L) cm		4.00		Bulk Density (kg/m <sup>3</sup> )		1935		Void Ratio e	
Specimen area (A) cm <sup>2</sup>		28.3		Dry Density (kg/m <sup>3</sup> )		1410		0.88	
Water Temperature (T) °C		24.5		Specific Gravity		2.65		Degree of saturation	
Stand Pipe Area a (cm <sup>2</sup> )		0.33		5.50				105	
Hydraulic gradient									
MDD (kg/m <sup>3</sup> )		1385		Compaction(%)				102	
Serial No.	Lab No.	Start Time/Date	End Time/Date	Change inTime(sec) Δt	Discharge Q (ml)	Δht1(cm)	Δht2 (cm)	k(m/s)	Average
1	C25026S003	1:37pm (28/1/2025)	1:43pm (28/1/2025)	360	7.30	90.0	68.0	3.66E-07	1.51E-07
		1:43pm (28/1/2025)	2:35pm (28/1/2025)	3120	15.30	68.0	21.9	1.70E-07	
		2:38pm (28/1/2025)	2:57pm (28/1/2025)	1140	8.50	91.0	65.4	1.36E-07	
		2:58pm (28/1/2025)	4:02pm (28/1/2025)	3840	12.34	65.4	28.2	1.03E-07	
		4:03pm (28/1/2025)	4:30pm (28/1/2025)	1620	7.47	91.0	68.5	8.23E-08	
		4:30pm (28/1/2025)	5:31pm (28/1/2025)	3660	7.30	68.5	46.5	4.97E-08	

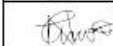


Technician:Barbrah

Checked Titus

Date: 29/01/2025

Falling Head Permeability test fort pit 3



DETERMINATION OF THE UNDRAINED STRENGTH IN TRIAXIAL COMPRESSION								
Tested in accordance to BS: 1377:1990: Part 7: Clause 8								
TEST REPORT								
Project Location	Shikuruwe village, naposho parish, Bushika sub county badada district							
Client	MAMFA MAYALA AND AHABWE MATHA	Sample Depth	1.0					
BH/TP Location	TP01	Sample Type	U-Sample					
Sample Description	SANDY CLAYS	Sampled by	W.M					
Tested by	BAKAKI MICHAEL OWEN	Sampling Date	N.A					
Checked by	Lab Engineer	Test Date	Tuesday, January 21, 2025					
DETERMINATION OF MOISTURE CONTENT								
CONTAINER NO.	Mass of Wet Soil + Container	Mass of Dry Soil + Container	Mass of Container	Mass of Moisture	Mass of Dry Soil	Moisture Content	Average	
ALL	239.9	186.7	39.3	53.3	147.4	36.1	36.3	
ROO	225.2	177.3	46.0	47.9	131.3	36.5		
SPECIMEN DETAILS								
		Specimen 1		Specimen 2		Specimen 3		Average
Height [mm]	76	Mass (g)	190.9	Mass (g)	190.9	Mass (g)	190.9	190.9
Diameter [Do]	38	Volume (cm <sup>3</sup> )	86.2	Volume (cm <sup>3</sup> )	86.2	Volume (cm <sup>3</sup> )	86.2	86.2
Initial Length [Lo]	76	Bulk Density (Mg/m <sup>3</sup> )	2.307	Bulk Density (Mg/m <sup>3</sup> )	2.307	Bulk Density (Mg/m <sup>3</sup> )	2.307	2.307
Area [Ao]	1134.6	Unit Weight (KN/m <sup>3</sup> )	22.6	Unit Weight (KN/m <sup>3</sup> )	22.6	Unit Weight (KN/m <sup>3</sup> )	22.6	22.63
Rate of Strain $\epsilon$ , (%/min)	2	Dry Density (Mg/m <sup>3</sup> )	1.692	Dry Density (Mg/m <sup>3</sup> )	1.692	Dry Density (Mg/m <sup>3</sup> )	1.692	1.692
SPECIMEN 1								
Force	$\epsilon$	$\Delta L$	$\Delta L/L$	$\epsilon$	$1-\epsilon$	Area	$\sigma_1-\sigma_3$	$\epsilon$
N	mm	mm	mm	mm	mm	mm <sup>2</sup>	Kpa	%
0	0.0	0.0	0.0000	0.0000	1.000	1134.6	0.0	0.0
150	1.4	1.4	0.0184	0.0184	0.982	1155.9	129.8	1.8
162	3.3	1.9	0.0250	0.0434	0.957	1186.1	136.6	4.3
165	5.1	1.8	0.0237	0.0671	0.933	1216.2	135.7	6.7
167	6.6	1.5	0.0197	0.0868	0.913	1242.5	134.4	8.7
171	8.2	1.6	0.0211	0.1079	0.892	1271.8	134.5	10.8
175	9.8	1.6	0.0211	0.1289	0.871	1302.5	134.4	12.9
182	11.5	1.7	0.0224	0.1513	0.849	1336.9	136.1	15.1
185	13.1	1.6	0.0211	0.1724	0.828	1370.9	135.0	17.2
190	14.6	1.5	0.0197	0.1921	0.808	1404.4	135.3	19.2
195	16.7	2.1	0.0276	0.2197	0.780	1454.1	134.1	22.0
SPECIMEN 2								
Force	Displacement	$\Delta L$	$\Delta L/L$	$\epsilon$	$1-\epsilon$	Area	$\sigma_1-\sigma_3$	$\epsilon$
N	mm	mm	mm	mm	mm	mm <sup>2</sup>	Kpa	%
0	0.0	0.0	0.0000	0.0000	1.000	1134.6	0.0	0.0
185	1.6	1.6	0.0211	0.0211	0.979	1159.0	159.6	2.1
230	3.3	1.9	0.0250	0.0461	0.954	1189.3	193.4	4.6
242	5.1	1.8	0.0237	0.0697	0.930	1219.6	198.4	7.0
247	6.6	1.5	0.0197	0.0895	0.911	1246.1	198.2	8.9
249	8.5	1.9	0.0250	0.1145	0.886	1281.2	194.3	11.4
251	10.2	2.0	0.0263	0.1408	0.859	1320.5	190.1	14.1
252	11.5	1.7	0.0224	0.1632	0.837	1355.8	185.9	16.3
253	13.4	1.9	0.0250	0.1882	0.812	1397.5	181.0	18.8
254	14.6	1.5	0.0197	0.2079	0.792	1432.3	177.3	20.8
255	16.6	2.0	0.0263	0.2342	0.766	1481.6	172.1	23.4
SPECIMEN 3								
Force	Displacement	$\Delta L$	$\Delta L/L$	$\epsilon$	$1-\epsilon$	Area	$\sigma_1-\sigma_3$	$\epsilon$
N	mm	mm	mm	mm	mm	mm <sup>2</sup>	Kpa	%
0	0.0	0.0	0.0000	0.0000	1.000	1134.6	0.0	0.0
221	1.7	1.7	0.0224	0.0224	0.978	1160.5	190.4	2.2
320	3.5	2.1	0.0276	0.0500	0.950	1194.3	267.9	5.0
345	5.3	2.0	0.0263	0.0763	0.924	1228.3	280.9	7.6
353	6.6	1.5	0.0197	0.0961	0.904	1255.1	281.2	9.6
356	8.6	2.0	0.0263	0.1224	0.878	1292.8	275.4	12.2
359	10.2	2.0	0.0263	0.1487	0.851	1332.7	269.4	14.9
361	11.5	1.7	0.0224	0.1711	0.829	1368.7	263.8	17.1
363	13.4	1.9	0.0250	0.1961	0.804	1411.3	257.2	19.6
365	15.1	2.0	0.0263	0.2224	0.778	1459.0	250.2	22.2
368	16.8	2.2	0.0289	0.2513	0.749	1515.4	242.8	25.1
Prepared by:				Lab Technician				
Approved by:				Lab Engineer				
								

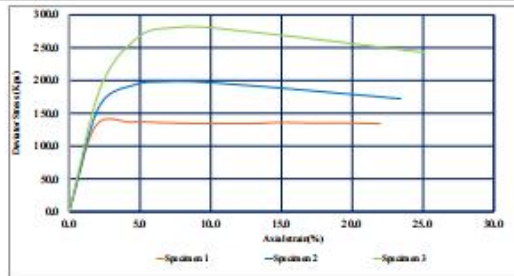
**DETERMINATION OF THE UNDRAINED STRENGTH IN TRIAXIAL COMPRESSION**  
Tested in accordance to BS: 1377:1990: Part 7: Clause 8  
**TEST REPORT**

Project Location	Shikunwe village, raposhi parish, Bushika sub county bududa district		
Client	MAMFA MAYALA AND AHABWE MARTHA	Sample Depth	L.O
BH/TP Location	TP01	Sample Type	U-Sample
Sample Description	SANDY CLAYS	Sampled by	W.M
Tested by	BAKAKI MICHAEL OWEN	Sampling Date	N.A
Checked by	Lab Engineer	Test Date	Tuesday, January 21, 2025

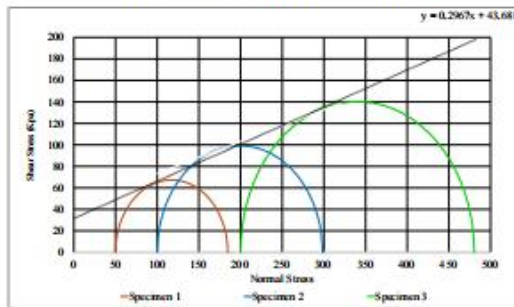
**CONDITIONS AT FAILURE**

STRESSES	Specimen 1	Specimen 2	Specimen 3	Specimen 1	Specimen 2	Specimen 3
Cell pressure (Kpa)	50	100	200			
Corr. Deviator Stress (Kpa)	136.6	198.4	281.2			
Shear strength (Kpa)	68.3	99.2	140.6			
The Cell Confining Pressures of 50Kpa, 100kpa & 200 Kpa have been used while conducting the Test						
EFFECTIVE STRESS ( $\sigma_v$ )		22.63	(Kpa)			
Mode of failure				Barrelling	Barrelling	Barrelling

**DEVIATOR STRESS(Kpa) AGAINST AXIAL STRAIN (%)**



**SHEAR STRESS(Kpa) AGAINST NORMAL STRESS(Kpa)**



**UNDRAINED PARAMETERS**

C	43.7
$\phi$	16.5

**COMMENT**

No Comment

Prepared by:  
Lab Technician



Approved by:  
Lab Engineer

Triaxial Test for pit 1

DETERMINATION OF THE UNDRAINED STRENGTH IN TRIAXIAL COMPRESSION  
Tested in accordance to BS: 1377:1990: Part 7: Clause 8

TEST REPORT

Project Location	Shikuruwe village, napothi parish, Bushika sub county badada district		
Client	MAMFA MAYALA AND AHABWE MARTHA	Sample Depth	1.0
BH/TP Location	TP02	Sample Type	U-Sample
Sample Description	SANDY CLAYS	Sampled by	W.M
Tested by	BAKAKI MICHAEL	Sampling Date	N/A
Checked by	Lab Engineer	Test Date	Tuesday, January 21, 2025

DETERMINATION OF MOISTURE CONTENT

CONTAINER NO.	Mass of Wet Soil + Container	Mass of Dry Soil + Container	Mass of Container	Mass of Moisture	Mass of Dry Soil	Moisture Content	Average
BT	249.7	212.2	61.4	37.5	150.8	24.9	24.7
A54	242.4	205.6	55.2	36.8	150.4	24.5	

SPECIMEN DETAILS		Specimen 1		Specimen 2		Specimen 3		Average
Height [mm]	76	Mass (g)	200.4	Mass (g)	200.4	Mass (g)	200.4	200.4
Diameter [Do]	30	Volume (cm <sup>3</sup> )	86.2	Volume (cm <sup>3</sup> )	86.2	Volume (cm <sup>3</sup> )	86.2	86.2
Initial Length [Lo]	76	Bulk Density (Mg/m <sup>3</sup> )	2.324	Bulk Density (Mg/m <sup>3</sup> )	2.324	Bulk Density (Mg/m <sup>3</sup> )	2.324	2.324
Area [Ao]	1134.6	Unit Weight (KN/m <sup>3</sup> )	22.8	Unit Weight (KN/m <sup>3</sup> )	22.8	Unit Weight (KN/m <sup>3</sup> )	22.8	22.80
Rate of Strain $\epsilon$ , (%/min)	2	Dry Density (Mg/m <sup>3</sup> )	1.864	Dry Density (Mg/m <sup>3</sup> )	1.864	Dry Density (Mg/m <sup>3</sup> )	1.864	1.864

SPECIMEN 1

Force	t	$\Delta L$	$\Delta L/L$	$\epsilon$	1- $\epsilon$	Area	$\sigma_1 - \sigma_3$	$\epsilon$
N	mm	mm	mm	mm	mm	mm <sup>2</sup>	Kpa	%
0	0.0	0.0	0.0000	0.0000	1.000	1134.6	0.0	0.0
84	1.4	1.4	0.0184	0.0184	0.982	1155.9	72.7	1.8
102	3.3	1.9	0.0250	0.0434	0.957	1186.1	86.0	4.3
126	5.1	1.8	0.0237	0.0671	0.933	1216.2	103.6	6.7
141	6.6	1.5	0.0197	0.0868	0.913	1242.5	113.5	8.7
152	8.2	1.6	0.0211	0.1079	0.892	1271.8	119.5	10.8
155	9.7	1.5	0.0197	0.1276	0.872	1300.6	119.2	12.8
156	11.6	1.9	0.0250	0.1526	0.847	1338.9	116.5	15.3
156	13.2	1.6	0.0211	0.1737	0.826	1373.0	113.6	17.4
156	14.8	1.6	0.0211	0.1947	0.805	1408.9	110.7	19.5
156	16.3	1.5	0.0197	0.2145	0.786	1444.3	108.0	21.4

SPECIMEN 2

Force	Displacement	$\Delta L$	$\Delta L/L$	$\epsilon$	1- $\epsilon$	Area	$\sigma_1 - \sigma_3$	$\epsilon$
N	mm	mm	mm	mm	mm	mm <sup>2</sup>	Kpa	%
0	0.0	0.0	0.0000	0.0000	1.000	1134.6	0.0	0.0
106	1.8	1.8	0.0237	0.0237	0.976	1162.1	91.2	2.4
151	3.5	2.1	0.0276	0.0513	0.949	1195.9	126.3	5.1
168	5.2	1.9	0.0250	0.0763	0.924	1228.3	136.8	7.6
177	6.6	1.5	0.0197	0.0961	0.904	1255.1	141.0	9.6
198	8.4	1.8	0.0237	0.1197	0.880	1288.9	153.6	12.0
210	10.2	2.0	0.0263	0.1461	0.854	1328.6	158.1	14.6
226	11.6	1.9	0.0250	0.1711	0.829	1368.7	165.1	17.1
240	13.5	1.9	0.0250	0.1961	0.804	1411.3	170.1	19.6
254	14.8	1.6	0.0211	0.2171	0.783	1449.2	175.3	21.7
255	16.3	1.5	0.0197	0.2368	0.763	1486.7	171.5	23.7

SPECIMEN 3

Force	Displacement	$\Delta L$	$\Delta L/L$	$\epsilon$	1- $\epsilon$	Area	$\sigma_1 - \sigma_3$	$\epsilon$
N	mm	mm	mm	mm	mm	mm <sup>2</sup>	Kpa	%
0	0.0	0.0	0.0000	0.0000	1.000	1134.6	0.0	0.0
131	2.0	2.0	0.0263	0.0263	0.974	1165.2	112.4	2.6
220	3.4	2.0	0.0263	0.0526	0.947	1197.6	183.7	5.3
254	5.2	1.9	0.0250	0.0776	0.922	1230.1	206.5	7.8
282	6.8	1.7	0.0224	0.1000	0.900	1260.6	223.7	10.0
285	8.5	1.9	0.0250	0.1250	0.875	1296.7	219.8	12.5
294	10.2	2.0	0.0263	0.1513	0.849	1336.9	219.9	15.1
296	11.6	1.9	0.0250	0.1763	0.824	1377.4	214.9	17.6
298	13.4	1.8	0.0237	0.2000	0.800	1418.2	210.1	20.0
296	14.9	1.7	0.0224	0.2224	0.778	1459.0	202.9	22.2
300	16.5	1.7	0.0224	0.2447	0.755	1502.2	199.7	24.5

Prepared by:   
Lab Technician

Approved by:   
Lab Engineer



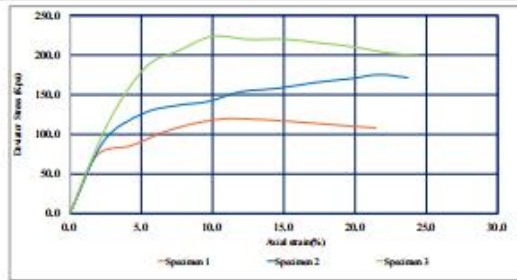
**DETERMINATION OF THE UNDRAINED STRENGTH IN TRIAXIAL COMPRESSION**  
 Tested in accordance to BS: 1377:1990: Part 7: Clause 8  
**TEST REPORT**

Project Location	Shikurwe village, raposhi parish, Bushika sub county bududa district		
Client	MAMFA MAYALA AND AHABWE MARTHA	Sample Depth	1.0
BH/TP Location	TP02	Sample Type	U-Sample
Sample Description	SANDY CLAYS	Sampled by	W.M
Tested by	BAKAKI MICHAEL	Sampling Date	NA
Checked by	Lab Engineer	Test Date	Tuesday, January 21, 2025

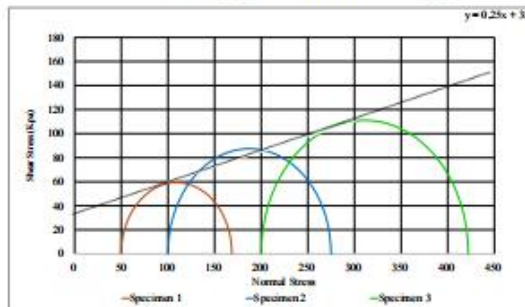
**CONDITIONS AT FAILURE**

STRESSES	Specimen 1	Specimen 2	Specimen 3	Specimen 1	Specimen 2	Specimen 3
Cell pressure (Kpa)	50	100	200			
Corr. Deviator Stress (Kpa)	119.5	175.3	223.7			
Shear strength (Kpa)	59.8	87.6	111.8			
The Cell Confining Pressures of 50Kpa, 100kpa & 200Kpa have been used while conducting the Test						
EFFECTIVE STRESS ( $\sigma_v$ )		22.80	(Kpa)	Barelling		
<i>Mode of failure</i>				Barelling		

**DEVIATOR STRESS(Kpa) AGAINST AXIAL STRAIN (%)**



**SHEAR STRESS(Kpa) AGAINST NORMAL STRESS(Kpa)**



**UNDRAINED PARAMETERS**

C	35.0
$\phi$	14.0

**COMMENT**

No Comment

Prepared by:  
 Lab Technician



Approved by:  
 Lab Engineer

*[Signature]*

Triaxial Test for pit 2



DETERMINATION OF THE UNDRAINED STRENGTH IN TRIAXIAL COMPRESSION

Tested in accordance to BS: 1377:1990: Part 7: Clause 8

TEST REPORT

Project Location	Shikunwe village, naposhi parish, Bushika sub county bududa district		
Client	MAMFA MAYALA AND AHABWE MARTHA	Sample Depth	1.0
BH/TP Location	TPO3	Sample Type	U-Sample
Sample Description	Sandy clays	Sampled by	W.M
Tested by	BAKAKI MICHAEL OWEN	Sampling Date	N.A
Checked by	Lab Engineer	Test Date	Tuesday, January 21, 2025

DETERMINATION OF MOISTURE CONTENT

CONTAINER NO.	Mass of Wet Soil + Container	Mass of Dry Soil + Container	Mass of Container	Mass of Moisture	Mass of Dry Soil	Moisture Content	Average
IUE	225.5	192.0	54.4	33.5	137.6	24.3	23.7
AE	268.6	229.2	58.6	39.4	170.6	23.1	

SPECIMEN DETAILS		Specimen 1		Specimen 2		Specimen 3		Average
Height [mm]	76	Mass (g)	210.5	Mass (g)	210.5	Mass (g)	210.5	210.5
Diameter [Do]	38	Volume (cm <sup>3</sup> )	86.2	Volume (cm <sup>3</sup> )	86.2	Volume (cm <sup>3</sup> )	86.2	86.2
Initial Length [Lo]	76	Bulk Density (Mg/m <sup>3</sup> )	2.441		2.441	Bulk Density (Mg/m <sup>3</sup> )	2.441	2.441
Area [Ao]	1134.6	Unit Weight (KN/m <sup>3</sup> )	23.9	Unit Weight (KN/m <sup>3</sup> )	23.9	Unit Weight (KN/m <sup>3</sup> )	23.9	23.95
Rate of Strain ε, (%/min)	2	Dry Density (Mg/m <sup>3</sup> )	1.973	Dry Density (Mg/m <sup>3</sup> )	1.973	Dry Density (Mg/m <sup>3</sup> )	1.973	1.973

SPECIMEN 1

Force	Displacement	ΔL	ΔL/L	ε	l-e	Area	σ <sub>1</sub> -σ <sub>3</sub>	ε
N	mm	mm	mm	mm	mm	mm <sup>2</sup>	Kpa	%
0	0.0	0.0	0.0000	0.0000	1.000	1134.6	0.0	0.0
75	1.3	1.3	0.0171	0.0171	0.983	1154.3	65.0	1.7
88	3.3	2.0	0.0263	0.0434	0.957	1186.1	74.2	4.3
106	5.1	1.8	0.0237	0.0671	0.933	1216.2	87.2	6.7
116	6.6	1.5	0.0197	0.0868	0.913	1242.5	93.4	8.7
124	8.5	1.9	0.0250	0.1118	0.888	1277.4	97.1	11.2
133	10.1	1.6	0.0211	0.1329	0.867	1308.5	101.6	13.3
136	11.6	1.5	0.0197	0.1526	0.847	1338.9	101.6	15.3
143	13.1	1.5	0.0197	0.1724	0.828	1370.9	104.3	17.2
146	14.8	1.7	0.0224	0.1947	0.805	1408.9	103.6	19.5
153	16.5	1.7	0.0224	0.2171	0.783	1449.2	105.6	21.7

SPECIMEN 2

Force	Displacement	ΔL	ΔL/L	ε	l-e	Area	σ <sub>1</sub> -σ <sub>3</sub>	ε
N	mm	mm	mm	mm	mm	mm <sup>2</sup>	Kpa	%
0	0.0	0.0	0.0000	0.0000	1.000	1134.6	0.0	0.0
106	1.5	1.5	0.0197	0.0197	0.980	1157.4	91.6	2.0
127	3.3	2.0	0.0263	0.0461	0.954	1189.3	106.8	4.6
141	5.1	1.8	0.0237	0.0697	0.930	1219.6	115.6	7.0
151	6.7	1.6	0.0211	0.0908	0.909	1247.9	121.0	9.1
155	8.6	2.0	0.0263	0.1171	0.883	1285.1	120.6	11.7
158	10.2	1.7	0.0224	0.1395	0.861	1318.5	119.8	13.9
160	11.5	1.4	0.0184	0.1579	0.842	1347.3	118.8	15.8
166	13.4	1.8	0.0237	0.1816	0.818	1386.3	119.7	18.2
171	14.6	1.5	0.0197	0.2013	0.799	1420.6	120.4	20.1
178	16.8	2.0	0.0263	0.2276	0.772	1469.0	121.2	22.8

SPECIMEN 3

Force	Displacement	ΔL	ΔL/L	ε	l-e	Area	σ <sub>1</sub> -σ <sub>3</sub>	ε
N	mm	mm	mm	mm	mm	mm <sup>2</sup>	Kpa	%
0	0.0	0.0	0.0000	0.0000	1.000	1134.6	0.0	0.0
172	1.8	1.8	0.0230	0.0230	0.977	1161.3	148.1	2.3
173	3.4	2.1	0.0276	0.0507	0.949	1195.1	144.8	5.1
192	5.3	2.0	0.0263	0.0770	0.923	1229.2	156.2	7.7
212	6.5	1.4	0.0184	0.0954	0.905	1254.2	169.0	9.5
217	8.5	1.9	0.0250	0.1204	0.880	1289.9	168.2	12.0
223	10.3	1.8	0.0237	0.1441	0.856	1325.6	168.2	14.4
226	10.7	0.6	0.0079	0.1520	0.848	1337.9	168.9	15.2
232	12.3	0.7	0.0092	0.1612	0.839	1352.6	171.5	16.1
236	15.0	1.9	0.0250	0.1862	0.814	1394.1	169.3	18.6
241	16.7	1.9	0.0250	0.2112	0.789	1438.3	167.6	21.1

Prepared by:  
 Lab technician






Approved by:  
 Lab engineer

**DETERMINATION OF THE UNDRAINED STRENGTH IN TRIAXIAL COMPRESSION**  
 Tested in accordance to BS: 1377:1990: Part 7: Clause 8

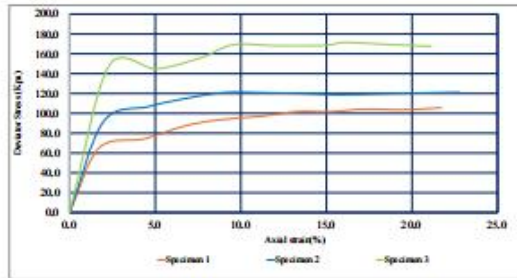
**TEST REPORT**

Project Location	Shikamuwe village, naposhi parish, Bushuka sub county bu danda district		
Client	MAMFA MAYALA AND AHABWE MARTHA	Sample Depth	L0
BH/TIP Location	TPO3	Sample Type	U-Sample
Sample Description	Sandy clays	Sampled by	W.M
Tested by	BAKAKI MICHAEL OWEN	Sampling Date	N/A
Checked by	Lab Engineer	Test Date	Tuesday, January 21, 2025

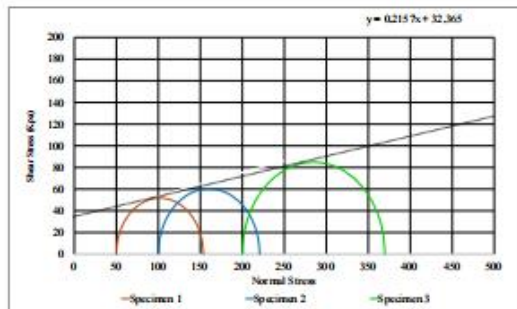
**CONDITIONS AT FAILURE**

STRESSES	Specimen 1	Specimen 2	Specimen 3	Specimen 1	Specimen 2	Specimen 3
Cell pressure (Kpa)	50	100	200			
Corr. Deviator Stress (Kpa)	105.6	121.2	171.5			
Shear strength (Kpa)	52.8	60.6	85.8			
The Cell Confining Pressures of 50Kpa, 100kpa & 200Kpa have been used while conducting the Test						
EFFECTIVE STRESS ( $\sigma_v$ )		23.95	(Kpa)			
<b>Mode of failure</b>				Barrelling	Barrelling	Barrelling

**DEVIATOR STRESS(Kpa) AGAINST AXIAL STRAIN (%)**



**SHEAR STRESS(Kpa) AGAINST NORMAL STRESS(%)**



**UNDRAINED PARAMETERS**

C	32.4
$\phi$	12.2

**COMMENT**

No Comment

Prepared by:  
Lab technician

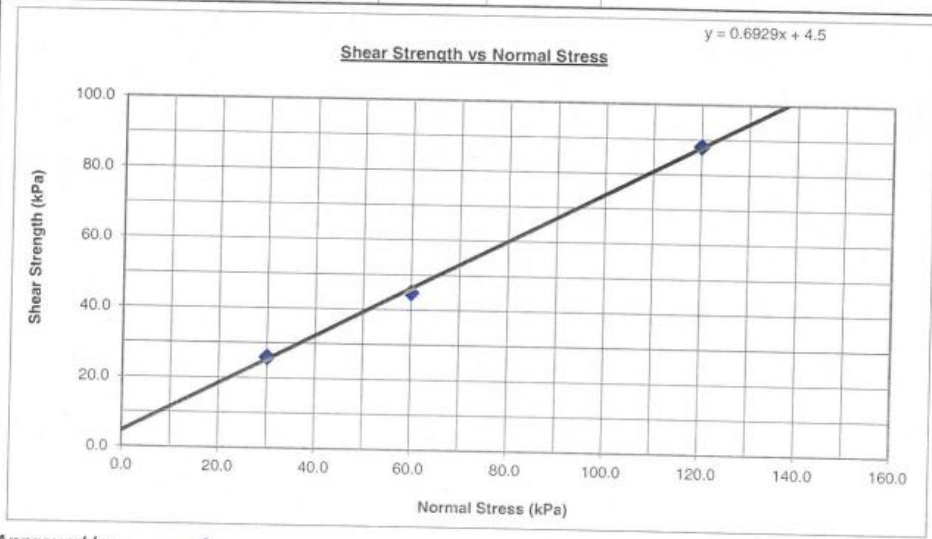


Approved by:  
Lab engineer

Triaxial test for pit 3

**DIRECT SHEAR BOX TEST OF SOILS (BS EN ISO 17892-7:2017)**

Project: HORIZONTAL SUBDRAINAGE SYSTEM APPROACH TOWARDS LANDSLIDE HAZARD MITIGATION					
Client: MAMFA MAYALA AND AHABWE MARTHA					
Location: Pit 01, Sample 2				Date Tested: 27/02/25	
Depth (m): 1.00					
Bulk Density	Normal Stress	Shear Strength	Cohesion	Angle of Internal Friction	Soil Description
$\gamma_b$ Mg/m <sup>3</sup>	$\bar{\sigma}_n$ kPa	$\tau_s$ kPa	C kPa	$\phi$ (Degree)	
1.96	30.0	26.0	4.5	34.7	Moist loose reddish brown sandy clays
	60.0	45.0			
	120.0	88.0			



Approved by:  
*[Signature]*  
Laboratory Engineer

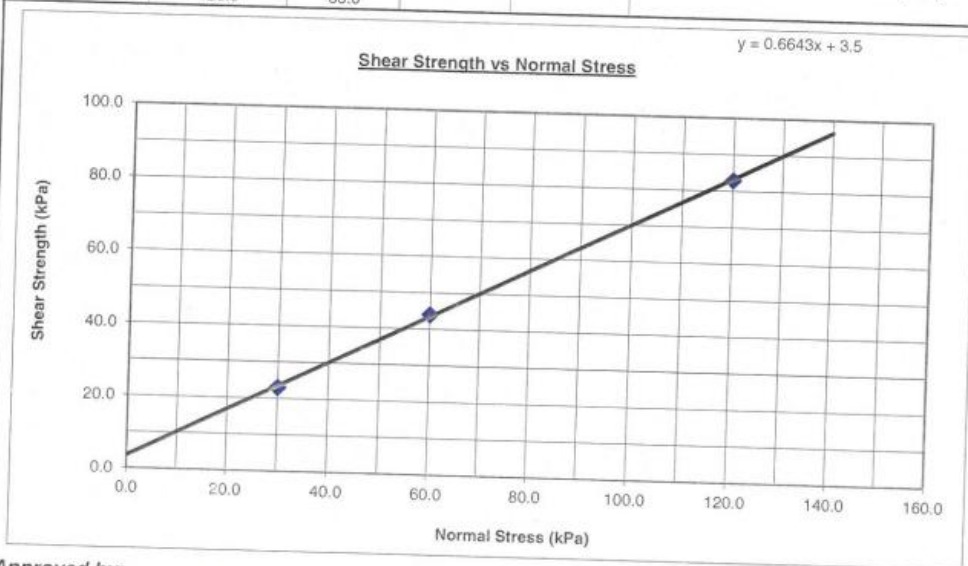
**GETLAB LTD**  
Senior Laboratory Engineer  
★ 04 MAR 2025 ★  
Geotechnical Engineering & Technology Laboratory Ltd  
P. O. Box 100001, Kasangati

Direct Shear box test for pit 1

**DIRECT SHEAR BOX TEST OF SOILS (BS EN ISO 17892-7:2017)**

Project:	HORIZONTAL SUBDRAINAGE SYSTEM APPROACH TOWARDS LANDSLIDE HAZARD MITIGATION		
Client:	MAMFA MAYALA AND AHABWE MARTHA		
Location:	Pit 01, Sample 1	Date Tested:	27/02/25
Depth (m):	1.00		

Bulk Density	Normal Stress	Shear Strength	Cohesion	Angle of Internal Friction	Soil Description
$\gamma_b$ Mg/m <sup>3</sup>	$\sigma_n$ kPa	$\tau_s$ kPa	C kPa	$\phi$ (Degree)	
1.93	30.0	23.0	3.5	33.6	Moist loose reddish brown sandy clays
	60.0	44.0			
	120.0	83.0			



Approved by:

Laboratory Engineer *[Signature]*

**GETLAB LTD**  
Senior Laboratory Engineer

★ 07 MAR 2025 ★

Geotechnical Engineering & Technology Laboratory Ltd  
P. O. Box 100001, Kasangati

Direct Shear box test for Pit 2